Universidade de Aveiro

Secção Autónoma de Ciências da Saúde

2013

Rafaela Cerdeira Silva

Identificação de biomarcadores de Alzheimer por FTIR – estudo piloto

Identification of Alzheimer biomarkers by FTIR – a pilot study

Universidade de Aveiro

Secção Autónoma de Ciências da Saúde

2013

Rafaela Cerdeira Silva

Identificação de biomarcadores de Alzheimer por FTIR – estudo piloto

Identification of Alzheimer biomarkers by FTIR – a pilot study

Tese apresentada à Universidade de Aveiro para cumprimento dos requisitos necessários à obtenção do grau de Mestre em Biomedicina Molecular, realizada sob a orientação científica da Doutora Carla Alexandra Pina da Cruz Nunes, Professora Auxiliar Convidada da Secção Autónoma de Ciências da Saúde da Universidade de Aveiro

Para aos meus pais que tornaram possível toda a minha conduta académica e que sempre se dedicaram em proporcionar-me a estabilidade e o conforto essenciais para a minha vida e para ao meu namorado pelo seu companheirismo, otimismo e confiança.

" Eu não tenho filosofia: tenho sentidos...
Se falo na Natureza não é porque saiba o que ela é,
Mas porque a amo, e amo-a por isso,
Porque quem ama nunca sabe o que ama
Nem sabe por que ama, nem o que é amar...

Amar é a eterna inocência,
E a única inocência não pensar... "

(Alberto Caeiro)

o júri

presidente

Professora Doutora Odete Abreu Beirão da Cruz e Silva
professora Auxiliar com Agregação da Secção Autónoma de Ciências da Saúde, Universidade de Aveiro

Professora Doutora Ivonne Delgadillo Giraldo
professora Associada com Agregação do Departamento de Química, Universidade de Aveiro

Professora Doutora Carla Alexandra Pina da Cruz Nunes
professora Auxiliar Convidada da Secção Autónoma de Ciências da Saúde, Universidade de Aveiro

Professora Doutora Ana Gabriela da Silva Cavaleiro Henriques
professora Auxiliar Convidada da Secção Autónoma de Ciências da Saúde, Universidade de Aveiro

.

agradecimentos

Um agradecimento muito especial à Professora Doutora Alexandra Nunes por todo o seu apoio, dedicação e confiança que teve neste projeto. Agradeço todos os bons conselhos e momentos de boa disposição.

À Professora Doutora Ana Gabriela Henriques, um obrigada muito especial pela sua coorientação, apoio e sugestões.

À Professora Doutora Odete da Cruz e Silva e à Doutora Ilka Martins pelas sugestões e por terem facultado as amostras e informações essenciais para este trabalho.

Ao Departamento de Química e ao Grupo de Química dos Produtos Naturais e Alimentares (Pest-C / QUI / UI0062 / 2011) da Universidade de Aveiro, em especial à Professora Doutora Ivonne Delgadillo pela disponibilização do FTIR.

Ao Centro de Biologia Celular (Pest-OE/SAU/UI0482/2011) da Universidade de Aveiro, obrigada pelo material disponibilizado.

Ao JPND BIOMARKAPD - Biomarkers for Alzheimer's disease and Parkinson's disease (Projeto FCT).

À Professora Doutora Margarida Fardilha, à Joana Vieira, à Liliana, obrigada pela vossa disponibilidade. À Joana Oliveira, obrigada pela participação no processamento das amostras. A todos os pacientes, obrigada por se terem voluntariado para este estudo.

À Inês, obrigada por teres estado sempre presente em todos as etapas deste trabalho e pelos bons momentos de descontração. À Luísa e à Catarina, obrigada pela vossa companhia ao longo de todo o meu percurso académico. A todos os meus colegas de mestrado, obrigada pelo apoio.

Aos meus pais, obrigada pelo esforço, dedicação e amor que me ajudaram a definir e a realizar os meus objetivos ao longo de toda a vida. Mãe, obrigada pelo teu aconchego e por estares sempre do meu lado. Pai, obrigada por seres tão determinado, por olhares para mim com orgulho. Obrigada por acreditarem em mim. Adoro-vos.

Ao Zé, obrigada por fazeres parte da minha vida e por toda a confiança que tens em mim, adoro-te.

Aos meus irmãos João Pedro e Vanda, obrigada pela vossa amizade, obrigada por me transmitirem a vossa força e por me ajudarem a corrigir os meus erros. À Maria e ao Simão, obrigada pelos vossos sorrisos e por crescerem perto de mim.

À toda a minha família e amigos, obrigada por acreditarem em mim e por me fazerem sorrir. Obrigada avô Trindade por olhares por mim.

A Deus, por nunca me ter desamparado e por olhar sempre por mim.

palavras-chave

Doença de Alzheimer, espectroscopia de infravermelho, biomarcadores, plasma e soro, análise multivariada.

resumo

A absorção de radiação na região espectral do infravermelho médio fornece informações detalhadas sobre a composição química das amostras biológicas. A maioria das espécies moleculares absorve a luz infravermelha, que dá origem a padrões espectrais característicos na luz transmitida. As condições patológicas estão associadas a perturbações do metabolismo, que se refletem em alterações homeostáticas dos componentes moleculares das células e dos tecidos. O potencial clínico da espectroscopia de infravermelho por transformada de Fourier (FTIR) para detetar tais mudanças e o seu uso como uma ferramenta de diagnóstico tem recebido cada vez mais atenção. Esta técnica permite a identificação de sinais associados à demência, a um nível bioquímico, e auxilia na identificação de biomarcadores específicos.

Esta dissertação é um estudo exploratório que pretendeu testar a capacidade da espectroscopia FTIR para discriminar amostras de indivíduos controlo de amostras de possíveis doentes de Alzheimer, e identificar sinais espectroscópicos correspondentes a grupos funcionais de biomarcadores presentes no soro e no plasma relativos à doença.

As amostras de sangue foram colhidas e os voluntários do estudo foram submetidos à avaliação cognitiva através do Mini Exame do Estado Mental (MEEM) e da Escala de Avaliação Clínica da Demência (CDR). Informações clínicas relevantes também foram recolhidas. As amostras dos possíveis doentes de Alzheimer, assim como as amostras dos controlos pareados com a mesma idade e sexo foram analisadas por FTIR. Os espectros na gama de 4000-900 cm^{-1} foram submetidos à análise em componentes principais (ACP).

Com o diagrama das coordenadas fatoriais (*scores*) do PCA foi possível discriminar os espectros das amostras de possíveis doentes de Alzheimer dos espectros das amostras dos controlos. O diagrama das contribuições fatoriais (*loadings*) permitiu a identificação de sinais espectroscópicos associados a grupos funcionais de biomarcadores envolvidos na discriminação entre amostras de doentes e controlos.

Futuramente, após a recolha de todos os sinais espectroscópicos correspondentes aos biomarcadores de AD e de definir o (s) biomarcadores responsável (eis) pela identificação espectroscópica de AD, será possível desenvolver um modelo de classificação multivariada.

keywords

Alzheimer’s disease, infrared spectroscopy, biomarkers, plasma and serum, multivariate analysis.

abstract

The absorption of radiation in the mid-infrared spectral region provides detailed information on the chemical composition of biological samples. Most molecular species absorbs infrared light, giving rise to distinctive spectral patterns in transmitted light. The pathological conditions are associated with metabolic disorders that are reflected in homeostatic changes of molecular components of cells and tissues. The clinical potential of Fourier Transform Infrared (FTIR) spectroscopy to detect such changes and its use as a diagnostic tool has received increasing attention. This technique allows the identification of signals associated with dementia at a biochemical level, and helps to identify specific biomarkers.

This dissertation is an exploratory study, which aimed to test the ability of FTIR to discriminate between control and Alzheimer’s Disease (AD) samples and to identify spectroscopic signals spectroscopic signals corresponding to functional groups of biomarkers present in serum and plasma of the disease.

Blood samples were collected and volunteers of the study were submitted to cognitive evaluation through Mini Mental State Examination (MMSE) and Clinical Dementia Rating (CDR). Relevant clinical information was also collected. Samples of putative Alzheimer's patients, as well as samples of the controls matched by age and sex were analyzed by FTIR. Spectra in the range 4000-900 cm^{-1} were submitted to Principal Component Analysis (PCA).

With the diagram of the factorial coordinates (*scores*) of the PCA was possible to discriminate the sample spectra of putative Alzheimer's patients, of the sample spectra of controls. The diagram of the factorial contributions (*loadings*) allowed the identification of spectroscopic signals associated with functional groups of biomarkers involved in discrimination between samples from patients and controls.

In future, after matching all spectroscopic signals of the corresponding AD biomarkers and gathering biomarker (s) responsible for the spectroscopic identification of AD will be possible to develop a model of multivariate classification.

Index

CHAPTER 1 ..... **1**

I. EPIDEMIOLOGY OF ALZHEIMER'S DISEASE 3
II. PATHOLOGY OF AD 3
1. Hallmarks of AD *4*
1.1. Neurofibrillary tangles (NFTs) 4
1.2. Senile Plaques (SPs) 5
1.3. Other neuropathological lesions in AD 7
2. Genetics of AD *8*
2.1. Familial AD 8
2.2. Sporadic AD 8
3. Pathogenesis of AD *9*
3.1. Aβ Genesis 9
3.2. The amyloid cascade hypothesis 10
3.3. Oxidative stress 11
3.4. Signaling alteration 13
3.5. Vascular risk factors 13
III. THERAPEUTIC STRATEGIES FOR AD 15
IV. DIAGNOSIS OF AD 16
1. Current guidelines *16*
2. Typical clinical pattern of dementia related conditions *16*
3. Clinical evaluation *18*
3.1. Neuropsychological tests 18
3.2. Neuroimaging 19
4. Genetic tests *20*
5. Alzheimer's disease diagnosis in Portugal *20*
V. BIOMARKERS AS DIAGNOSTIC TOOLS FOR AD 21
1. CSF biomarkers *23*
2. Fluid biomarkers to detect Alzheimer's disease under investigation *25*
2.1. CSF biomarkers 25
2.2. Blood biomarkers 25
2.3. Biomarkers of other biological fluids 26
3. Strategies for novel biomarkers discovery in neurological disease *27*
3.1. A focus on metabolomics techniques 27
3.2. The potential of the FTIR as clinical tool 28
VI. SIGNIFICANCE OF THE STUDY 30

CHAPTER 2 ..... **33**

I. METHOD OVERVIEW AND EXPERIMENTAL CONDITIONS OPTIMIZATION 35
1. General considerations on infrared spectroscopy *35*
1.1. Vibrations of molecules 36
1.2. FTIR equipment 38
1.3. Mid-infrared spectroscopy applied in biological samples 41
2. Method optimization *43*
2.1. Sample preparation 43
2.2. MIR spectral acquisition 44
3. Results *44*
3.1. Drying Kinetics of serum and plasma 44

3.2. Comparison of different methods to minimized water signals of plasma and serum samples 47
4. Conclusion 49

CHAPTER 3 51

I. METHODS OF STUDY 53
1. Study group 53
2. Blood samples collection and preparation 54
3. Biospectroscopy procedure 54
3.1. MIR spectral acquisition 54
3.2. Data multivariate analysis 55
II. RESULTS AND DISCUSSION 57
1. Spectral analysis 57
1.1. Results 57
1.2. Discussion 60
2. Multivariate analysis 62
2.1. Results 63
2.2. Discussion 67
III. CONCLUSION 73
IV. LIMITATIONS AND FUTURE REMARKS 74

BIBLIOGRAPHY 75

Figures Index

Figure 1. Spatiotemporal pattern of neurofibrillary degeneration.. 5
Figure 2. Spatiotemporal pattern of amyloid plaque deposition. 6
Figure 3. Neurofibrillary tangles and Aβ plaques in temporal cortex of patients with Alzheimer's disease. 7
Figure 4. The two pathways of APP proteolysis..... 10
Figure 5. The amyloid cascade hypothesis. 11
Figure 6. Illustrative model of the ordering of biomarkers of AD relative to stages in the clinical onset and progression of AD. 23
Figure 7. The IR regions of the electromagnetic spectrum..... 36
Figure 8. Examples of vibrational modes of stretching and bending. 37
Figure 9. The optical diagram of a typical Michelson interferometer. 39
Figure 10. The process of collecting an infrared spectrum in an FTIR spectrometer. 40
Figure 11. Golden Gate ATR™ accessory. 41
Figure 12. ATR spectra acquired during the drying process (film preparation) of a serum sample. 45
Figure 13. ATR spectra acquired during the drying process (film preparation) of a plasma sample..... 45
Figure 14. PCA scores (a) and loadings (b) of 16 spectra of one sample obtained by dry kinetics..... 47
Figure 15. Comparison of the effect of 3 different methods to minimize water signals of a serum sample. 48
Figure 16. Comparison of the effect of 3 different methods to minimize water signals of a plasma sample. ... 48
Figure 17. Most frequently applied multivariate data-analysis techniques in combination with MIR spectroscopic methods. 56
Figure 18. Spectra of all serum samples of putative AD patients and controls, obtained after drying kinetics 58
Figure 19. Spectra of all plasma samples of putative AD patients and controls, obtained after drying kinetics. 58
Figure 20. 4000-600 and 1800-800 cm^{-1} regions of the FTIR spectra of serum and plasma samples. 59
Figure 21. PCA scores (Aa) and loadings (Ab) of serum samples (3600-3000 cm^{-1} range)..... 64
Figure 22. PCA scores (Ba) and loadings (Bb) of plasma samples (3600-3000 cm^{-1} range)..... 64
Figure 23. PCA scores (Aa) and loadings (Ab) of serum samples (1800-900 cm^{-1} range)..... 64
Figure 24. PCA scores (Ba) and loadings (Bb) of plasma samples (1800-900 cm-1 range)..... 65
Figure 25. PCA Scores (Aa) and loadings (Ab) of serum samples (1200-900 cm^{-1} range). 65
Figure 26. PCA Scores (Ba) and loadings (Bb) of plasma samples (1200-900 cm^{-1} range). 66
Figure 27. PCA scores (Aa) and loadings (Ab) of serum samples, without D1, D4 and D6 (1200-900 cm^{-1} range). 71
Figure 28. PCA scores (Ba) and loadings (Bb) of plasma samples, without D1, D4 and D6 (1200-900 cm^{-1} range). 71
Figure 29. PCA Scores (Aa) and loadings (Ab) of serum samples, without D2 (1200-900 cm^{-1} range). 72
Figure 30. PCA Scores (Ba) and loadings (Bb) of plasma samples, without D2 (1200-900 cm^{-1} range)..... 72

Tables Index

Table 1. Approved medications by the U.S. Food and Drug Administration to treat Alzheimer's disease. 15
Table 2. Neuropathological characteristics and symptoms of the most common dementia related conditions. 17
Table 3. Imaging approach in Alzheimer's disease. 20
Table 4. Currently accepted biomarkers for the diagnosis of Alzheimer's disease..... 22
Table 5. Characterization of study subjects according to MMSE and CDR scores. 54
Table 6. Spectral regions according to some metabolic characteristics related with Alzheimer's pathology. 57
Table 7. Spectral assignments of plasma and serum samples. 60
Table 8. MIR bands between 1200 and 900 cm^{-1} range identified in PCA loadings. 67

Abbreviations

A	Absorbance
AD	Alzheimer’s disease
ADAM	A disintegrin and metalloproteinase
ADAS-Cog	Alzheimer's disease assessment scale-cognitive subscale
ADDLs	Amyloid-beta derived diffusible ligands
ADL	Activities of daily living scale
ADRDA	Alzheimer’s disease and related disorders association
AGEs	Advanced glycation end-products
AICD	Amyloid precursor protein intracellular domain
ANNS	Artificial neural networks
ApoE	Apolipoprotein E
ApoE ε4	Apoe ε4 allele
APH-1	Anterior pharynx defective
APP	Amyloid precursor protein
ATR	Attenuated total reflection
Aβ	Amyloid-β
BACE	Beta-site app-cleaving enzyme
CA	Cluster analysis
CAA	Cerebral amyloid angiopathy
CATCH	Critically attained threshold of cerebral hypoperfusion
CDR	Clinical dementia rating
CFH	Complement factor H
CIBIC-plus	Clinician interview based impression of change plus caregiver input
CSF	Cerebrospinal fluid
CT	Computed tomography
C83	Membrane-anchored α-carboxy terminal fragment
C99	Membrane-anchored β-carboxy terminal fragment
DLB	Dementia with Lewy bodies
DM	Diabetes Mellitus
DN	Dystrophic neuritis
ELISA	Enzyme-linked immunosorbent assay
EOFAD	Early-onset familial Alzhemer’s disease
ER	Endoplasmic reticulum
FIR	Far infrared region
FMRI	Functional MRI
FTD	Frontotemporal dementia
FTIR	Fourier Transform Infrared spectroscopy
GC	Gas chromatography
GDS	Geriatric depression scale
GVD	Granulovacuolar degeneration
HPLC	High performance liquid chromatography
IDE	Insulin degrading enzyme
IGF-I	Insulin-like growth factor I
IR	Infrared
LDA	Linear discriminant analysis
LOAD	Latter-onset sporadic cases of Alzheimer’s disease
MCI	Mild cognitive impairment

MIR	Mid Infrared region
MMSE	Mini-mental state examination
MoCA	Montreal cognitive assessment
MRI	Magnetic resonance imaging
MRS	Magnetic resonance spectroscopy
MS	Mass spectrometry
NCSTN	Nicastrin
NIR	Near Infrared region
NFTs	Neurofibrillary tangles
NINCDS	National institute of neurological and communicative disorders and stroke
NTP	Neural thread protein
PCA	Principal components analysis
PCR	Principal components regression
PCs	Principal components
PDD	Parkinson's disease dementia
PEN	Presenilin enhancer
PET	Positron emission tomography
PHFs	Paired helical filaments
PLS	Partial least squares regression
PLS-DA	Partial least-squares discriminant analysis
PS	Presenilin protein
PSEN	Presenilin gene
P-Tau	Phospho-tau
ROS	Reactive oxygen species
SIMCA	Soft independent modeling of class analogy
SNR	Signal-to-noise ratio
SNV	Standard Normal Variate
SPECT	Single-photon emission computed tomography
SPs	Senile plaques
T-Tau	Total tau
VaD	Vascular dementia
α2M	A2-macroglobulin
8-OHdG	8-hydroxy-2'deoxyguanosine
8-OHG	8-hydroxyguanosine
%T	Transmittance

Chapters overview

Chapter 1

This chapter gives an overview of Alzheimer's disease, its diagnosis methodologies and the most studied biomarkers. It also presents the FTIR technique as a tool to investigate new biomarkers.

Chapter 2

This chapter gives an overview of FTIR principles and it aims to discuss the intense water contribution in mid-infrared spectrum of serum and plasma samples, providing an optimized experimental methodology to overcome this problem.

Chapter 3

This chapter presents the results on the application of FT-IR spectroscopy to the plasma and serum samples of putative Alzheimer’s patients, and controls matched by age and sex, in order to identify spectral differences that help discriminate between the two groups.

Chapter 1

I. Epidemiology of Alzheimer's disease

Dementia is one of the major causes of disability in later life. It accounts for 11.9% of the years lived with disability due to a non communicable disease. It is the leading cause of dependency and disability among older people (1,2).

Alzheimer's disease is the most common form of dementia and possibly contributes to 60–70% of cases of dementia. Other major contributors include vascular dementia (VaD) contributing with 20% of the cases, dementia with Lewy bodies (DLB) with a frequency of 30-40%, frontotemporal dementia (FTD) explaining 3%-10% of demented individuals and dementia in Parkinson's disease (PDD), whose frequency is lower (1–3). Mixed pathologies are also very common, particularly for AD and VaD, and AD and DLB (2). Mild Cognitive Impairment (MCI) is a pre-demented state highly associated with progression to AD or other dementia.

There are approximately 35.6 million people living with dementia worldwide today. This number is likely to double by 2030, and triplicate by 2050. In addition, Alzheimer's is becoming a more common cause of death (1). About 2% to 10% of all dementia cases start before the age of 65, and the likelihood of developing dementia roughly doubles every five years (2). Due to women's longer life expectancy, it is difficult distinguish the risk to develop AD between women and men (1). The total worldwide costs estimated for dementia were US$ 604 billion in 2010 (2).

In Portugal it is estimated that there are around 153,000 people with dementia, among them 90,000 with AD (4). At the moment, because of the economic crisis, dementia is not one of the political priorities (5). As consequence, both the general population and health professionals have scarce information, and the latter are not sensitive for early diagnosis, devaluating often the symptoms and interpreting them as part of the normal aging process. This lack of awareness leads to a more pronounced progression of symptoms because patients do not receive appropriate care in good time (6).

Given the global impact of disease, Alzheimer's disease is recognized as a priority, and a special attentions to the needs for improve early diagnosis was declared by European Parliament (6).

II. Pathology of AD

The outcome of Alzheimer's disease is dementia that typically begins as a progressive loss of episodic memory. Subsequently, a possible disconnection between cortical areas occurs due to

progressive deterioration in cognitive and adaptive functioning, leading to the next characteristic symptoms of dementia such as impairment of thinking, orientation and language, and other dementia-related symptoms (7).

1. Hallmarks of AD

Although the brain of an Alzheimer's disease patient shows a typical symmetric pattern of cortical atrophy mainly at the medial temporal lobes that can be recognized early in the clinical course of the disease by MRI scan, so far, the definitive diagnosis of AD is only made *post mortem* through the histological examination of the brain (8).

Although other neuropathological lesions are encountered in AD cases, the two primary cardinal lesions associated with Alzheimer's disease are the senile plaques (SPs) and the neurofibrillary tangles (NFTs) (7). Thus, demented individuals who do not have plaques and tangles does not qualify for a diagnosis of AD, but the simple presence of plaques and tangles do not distinguish demented from nondemented individuals since brains of aged nondemented individuals frequently contain plaques and tangles (9). Instead, fundamental characteristics that define the neuropathological entity of AD are the spatiotemporal pattern of deposition of both SPs and NFTs (7).

1.1. Neurofibrillary tangles (NFTs)

Neurofibrillary tangles (NFTs) are considered to be a major pathological hallmark of Alzheimer's disease. However, presence of NFTs *per se* is not sufficient to diagnose AD since it may also be encountered in association with many other chronic neurological diseases (8).

Neurofibrillary tangles are developed within the pyramidal neuronal soma, and then extend into the neuronal processes. Apparently, NFTs are primarily made of paired helical filaments (PHFs) that are fibrils of approximately 10 nm in diameter that form pairs with a helical tridimensional conformation. However, other structures may also constitute the NFTs such as fibrils with appearance of straight filaments (8).

The primary constituent of the neurofibrillary tangles is the microtubule-associated protein tau abnormally phosphorylated (P-tau) at very specific protein sites (8). Tau protein is involved in cytoskeletal functions and has a critical role in microtubule stabilization and in the efficiency of the synapse (10). Therefore, contribution of tau to AD pathology is mainly due to its loss of function, as well as gain of toxic function such as aggregation and deposition as neurofibrillary

tangles (11). In addition to tau protein, other protein constituents are associated with the neurofibrillary tangle, such as ubiquitin**,** cholinesterases and beta-amyloid (Aβ) (8).

Remarkably, NFTs have a stereotypical spatiotemporal progression that correlates with both the degree of dementia and the duration of illness (8). Briefly, the neurofibrillary degeneration starts in the allocortex of the medial temporal lobe (entorhinal cortex and hippocampus) leading to loss of memory and then spreads to the associative isocortex leading to disconnection between cortical areas. The primary sensory, motor, and visual areas are relatively spared (Figure 1) (8,12).

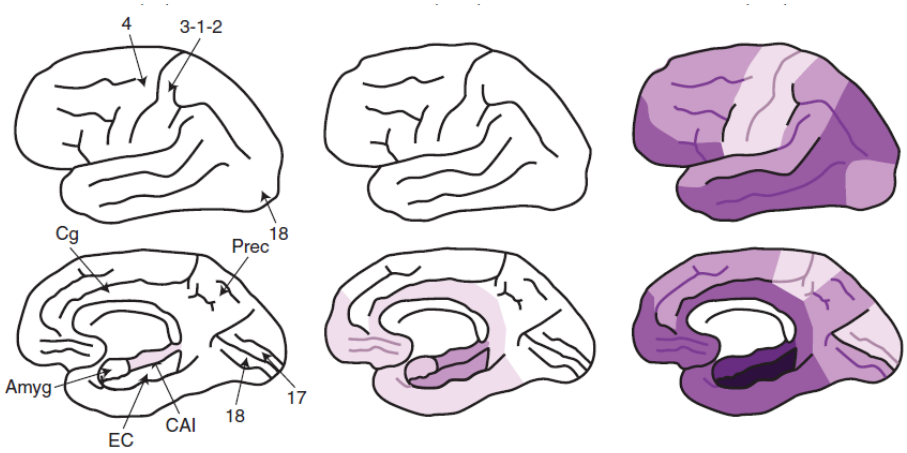

Figure 1. Spatiotemporal pattern of neurofibrillary degeneration. Shading indicates the distribution of NFTs with darker colors representing increasing densities. Amyg: Amygdala; EC: Entorhinal cortex; CA1: Cornus ammonis 1 hippocampal subfield; Cg: Cingulate cortex; Prec: Precuneus; 4 = Primary motor cortex; 3-1-2 = Primary sensory cortex; 17 = Primary visual cortex; 18 = Associative visual córtex; Adapted from (8).

1.2. Senile Plaques (SPs)

The other cardinal pathological lesion encountered in patients suffering from Alzheimer's disease is the neuritic or senile plaque (SP).

SPs are constituted by extracellular deposits of enlarged axons, synaptic terminals and dendrites, associated with insoluble Aβ peptide in the parenchyma of the brain (8).

SPs result from the abnormal extracellular accumulation and deposition of the Aβ. Moreover, several forms of Aβ-containing plaques may be present in the brains of aged individuals and AD patients. Among them, diffuse or immature plaques that consist of Aβ in a non-aggregated form, free of any neuritic involvement, are often in brains of elderly healthy. On the other hand, dense-

core plaques which are consequence of the neurite dystrophy that occurs due to Aβ deposits, are characteristics of brains of AD patients (8,13).

Ultra-structurally, the dense-core plaques are comprised of a central mass of extracelullar filaments that radially extend toward the periphery. In periphery, filaments intermingle with neuronal, astrocytic, and microglial processes. The neuronal processes, known as dystrophic neuritis (DN), often contain PHFs, abnormal mitochondria and dense bodies of apparent mitochondrial and lysosomal origin (8).

Topographically, the amyloid deposits accumulate first in isocortical areas, followed by limbic and allocortical structures, and, in a later stage, by subcortical structures including basal ganglia, selected nuclei in diencephalon and brainstem, and the cerebellar cortex (Figure 2) (8)**.** Likewise NFTs, among the isocortical areas, primary sensory, motor, and visual areas tend to be less affected as compared to association multimodal areas (12).

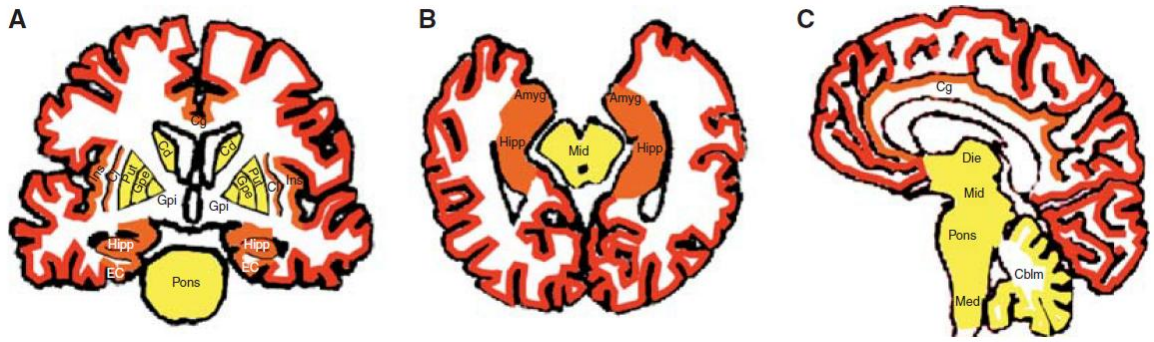

Figure 2. Spatiotemporal pattern of amyloid plaque deposition. Coronal (A), axial (B), and sagittal (C) views of the brain. Areas in red are the first areas of deposition, the second affected areas are in orange and last areas are represented in yellow. Amyg: Amygdala; EC: Entorhinal cortex; Hipp: Hippocampus; Cg: Cingulate cortex; Cd: Caudate nucleus; Put: Putamen; Gpe: Globus pallidus externus; Gpi: Globus pallidus internus; Cl: Claustrum; Ins: Insular cortex; Die: Diencephalon; Mid: Midbrain; Med: Medulla oblongata; Cblm: Cerebellum; Adapted from (8,14).

Clinical-autopsy correlation studies demonstrate a much tighter correlation between neurofibrillary pathology and cognitive impairment than between amyloid pathology and cognitive impairment (8). Thereby, Aβ pathology is thought to develop first during the long preclinical phase, whereas the neurodegenerative pathology, including NFTs formation and neuronal or synapse loss, accelerates slightly before the appearance of the symptomatic phase of AD (15).

NFTs and SPs are detected with staining techniques or with specific antibodies directed against hyper-phosphorylated tau to detect NFTs and against Aβ to detect SPs. Since DNs often contains PHFs, antibodies directed against P-tau can be used to detect SPs (Figure 3) (16).

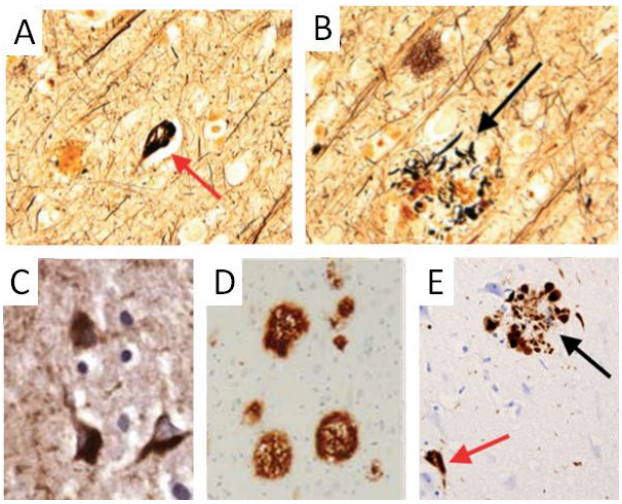

Figure 3. Neurofibrillary tangles and Aβ plaques in temporal cortex of patients with Alzheimer's disease. Use of modified Bielschowski stain to visualize neurofibrillary tangles (A) and neuritic plaques (B); Immunohistochemical preparation using antibodies directed against tau tangles (C) and Aβ plaques (D); Antibody directed against neurofibrillary tangles (red arrow) also detects dystrophic neuritis (black arrow) (E). Adapted from (8,16).

1.3. Other neuropathological lesions in AD

Since Aβ peptide also tends to deposit in the walls of the cerebral cortical blood vessels, cerebral amyloid angiopathy (CAA) is another feature possibly present in AD brain that may lead to spontaneous vascular rupture, and bleeding (16). Granulovacuolar degeneration (GVD) and Hirano bodies are two poorly understood lesions present in the cytoplasm of hippocampal pyramidal neurons of AD patients. While GVD have a possible role in tangle formation and in the apoptosis, Hirano bodies have unknown significance (8)**.** Other lesions are reactive astrocytes and activated microglial cells that are trigged either by Aβ as by neurofibrillary degeneration (8).

Indeed, the main pathological substrates of cortical atrophy are loss of neurons and of neuron-to-neuron communications (synapses) that constitute the major morphological counterparts to cognitive loss in Alzheimer's disease, with a better correlation with cognitive deficits than number of NFTs (8,16).

2. Genetics of AD

AD is genetic and clinically heterogeneous and is usually classified according to its age of onset. Therefore, early-onset AD (<5% of cases) occurs before 65 years and is often the familial form associated with an inheritance autosomal dominant pattern, and late-onset AD (>95% of cases) occurs in subjects over 65 years of age and is more frequently of sporadic origin (17).

2.1. Familial AD

To date, three genes have been identified whose mutations cause the early-onset familial AD (EOFAD) with full penetrance. These genes are the amyloid precursor protein (APP) gene in chromosome 21 (with ~10-15% of EOFAD cases), the presenilin 1 (PSEN1) gene in chromosome 14 (with ~20-15% of EOFAD), and the presenilin 2 (PSEN2) gene in chromosome 1 (more rarely affected)(17,18). APP is a larger transmembrane protein maybe implicated in synapse formation, neural plasticity and iron export (19–21), whose amyloid metabolism originates the Aβ peptide. Presenilin (PS) is the major component of the γ-secretase, an enzymatic complex that performs the second cleavage of APP (22).

2.2. Sporadic AD

Contrary to familial AD, in most sporadic AD cases, with a complex etiology, genetic factors act as predisposing agents which taken alone are not often enough to develop the disease. Thus, to exert their pathogenic effect, specific genes probably interact with environmental risk factors such as head trauma, social engagement and diet, or with other pathologic conditions including cardiovascular disease and MCI, or with physiologic risk conditions such as advanced age (1).

Apoliprotein E (ApoE) is the major lipoprotein throughout the brain expressed by astrocytes, under physiologic conditions, or by neurons, under stress (10). This apoliprotein participates in the distribution and metabolism of cholesterol and triglycerides. Among its isoforms, the ε4 allele of the apolipoprotein E (ApoE ε4) is the major genetic risk factor for both early-onset AD and late-onset sporadic cases (LOAD) (23). ApoE ε4 allele strongly affects deposition of Aβ to form senile plaques and also contributes to AD pathogenesis by Aβ-independent mechanisms such as synaptic plasticity, cholesterol homeostasis, neurovascular functions, and neuroinflammation (23).

Comparing with ApoE ε4 non carriers with a frequency of 20% to develop AD, in subjects heterozygous the frequency of Alzheimer's disease is about 47% and in homozygous is about 91%.

Furthermore, the clinical onset with an earlier age is dramatically increased in a gene dose-dependent manner (23).

Only less than 50% of sporadic AD cases are carriers of the ApoE ε4 allele. Therefore, other susceptibility genes related with Aβ metabolism, tau phosphorylation or synaptic transmission must be involved in the pathogenesis of the sporadic cases of the disease (17).

3. Pathogenesis of AD

Although the exact etiology and pathogenesis of AD still remains obscure, it is believed that several factors interact and are overlapped pathways that increase the capacity of injury in specific brain regions and circuits involved in memory and language (hippocampus and cerebral cortex), resulting in a progressive cognitive deficit.

The preeminent hypothesis of AD pathogenesis is based on the amyloid cascade hypothesis, in which Aβ is the key player (24). In addition, other interveners have some weight in neuronal loss and progression of damage and cognitive decline, including oxidative stress, lysosomal dysfunction, signaling pathways alteration and vascular risk factors (10,25). Neurotransmitters such as glutamate, acetylcholine, dopamine, and serotonin are also dysfunctional (10,25) and are the main targets to current therapeutic strategies.

3.1. Aβ Genesis

Aβ peptide is a proteolytic cleavage final product of APP, which in turn can undergo proteolytic processing by one of two pathways (Figure 4).

Most of APP is processed through the non-amyloidogenic pathway. In the later, APP suffers its first cleavage by α-secretase (ADAM 9, 10 or 17) yielding the membrane-anchored α-carboxy terminal fragment (C83) and the ectodomain sAPPα that may have neuroprotective roles. Then, C83 is cleaved by γ-secretase releasing P3 peptide and APP intracellular domain (AICD), which prevents the generation and release of the Aβ peptide. On the other hand, APP molecules that are not cleaved by the non-amyloidogenic pathway follow the amyloidogenic pathway and become a substrate for the β-secretase (BACE1), releasing the sAPPβ and membrane-anchored β-carboxy terminal fragment (C99). C99 is subsequently cleaved 38–43 amino acids from the amino terminus to release Aβ by the γ-secretase complex, comprising presenilin 1 (PS-1) or 2 (PS-2), nicastrin (NCSTN), presenilin enhancer 2 (PEN2) and anterior pharynx defective (APH-1) (22,26).

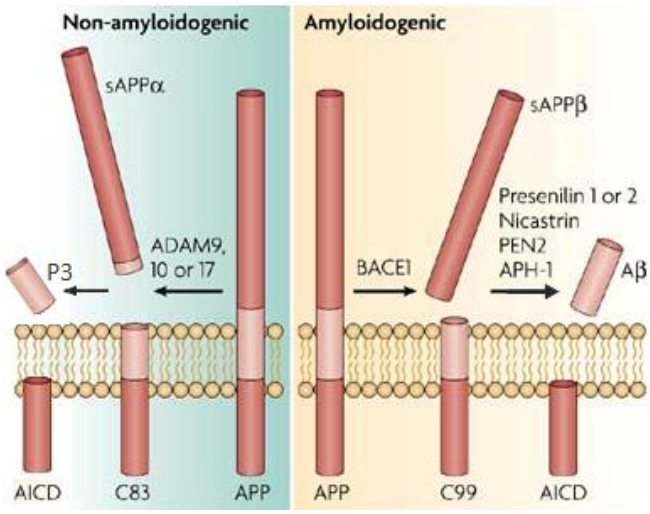

Figure 4. The two pathways of APP proteolysis. Non amyloidogenic (background blue) and amyloidogenic (background beige) pathways for APP processing. Adapted from (22,26).

Under physiological conditions, $A\beta_{1-40}$ is the most predominant peptide that can be eliminated from the brain due to its soluble features. In contrast, $A\beta_{1-42}$ is the predominant monomer in AD that is highly fibrinogenic, difficult to degrade, and with tendency to aggregate in soluble toxic oligomers called amyloid-β-derived diffusible ligands (ADDLs) (27).

3.2. The amyloid cascade hypothesis

Amyloid cascade hypothesis is the one that best explains the AD pathogenesis and suggests that $A\beta_{1-42}$ aggregation initiate the pathogenic cascade that leads to neuronal loss (Figure 5).

Accumulation of $A\beta_{1-42}$ is due to imbalance between the levels of Aβ production, aggregation and clearance (28). Thereby, its overproduction may be promoted by mutations in the APP, PSEN1 or PSEN2 genes. The ability of $A\beta_{1-42}$ monomers to aggregate is enhanced by failures in its enzymatic degradation and clearance, and, under pathological conditions, can accumulate into potentially toxic oligomers and/or plaques (24,28). In turn, oligomers can also be sequestered into plaques, also due to failures in degradation and clearance of $A\beta_{1-42}$. Oligomers may be the toxic Aβ species that contribute to de-regulation of signaling pathways, resulting in formation of PHFs of tau, which in turn are very difficult to degrade (24). PHFs accumulation directly affects intracellular transport, leading to synaptic damage accompanied by neuronal loss (24,28).

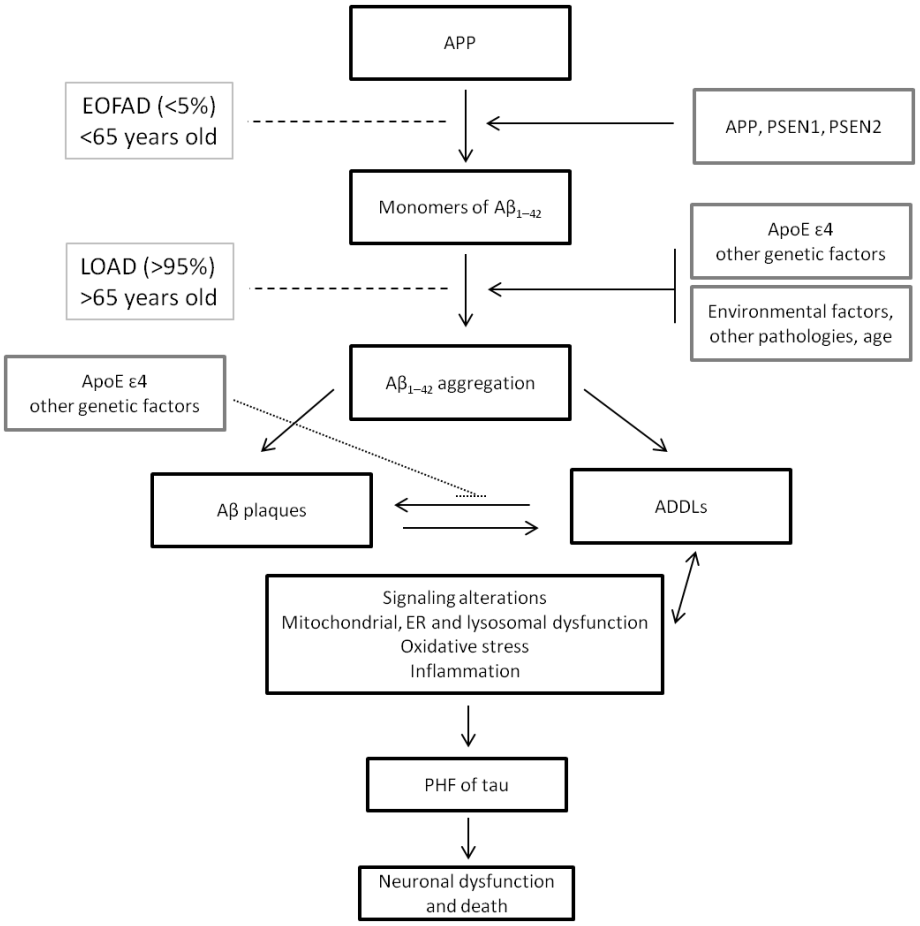

Figure 5. The amyloid cascade hypothesis. ADDLs: Amyloid-β-derived diffusible ligands. Adapted from (24,28).

3.3. Oxidative stress

Oxidative stress is other prominent pathological change in the AD brain and occurs when excessive generation of reactive oxygen species (ROS) during normal metabolic processes in the cell is unbalanced by the antioxidative defense system.

Mitochondrial oxidative phosphorylation is the major source of ROS like the hydrogen peroxide radicals (H_2O_2), hydroxyl radicals ($OH^{\cdot}$) and the superoxide radical ($O^{2-\cdot}$) that are very unstable and highly reactive. ROS increase lipid peroxidation, leading to alteration of the membrane properties of the cell such as fluidity, ion transport, enzyme activities, and protein cross-linking (22). The oxidative damage that ensues is seen in lipids, proteins, nucleic acids, and sugars, all of which are organic compounds essential for the structural and functional integrity of neurons.

Brain tissue is highly susceptible to ROS damage because neurons require high-energy support and the oxidative processes lead to dysfunction of mitochondria. Furthermore, brain tissue is rich in easily peroxidizable unsaturated fatty acids (mainly arachidonic and docosahexaenoic acids) and has a high content of iron, that is important to lipoperoxidization reactions (29).

Several studies suggest that oxidative stress is involved in Aβ fibrillization and NFT formation in AD, and in turn the Aβ also increases oxidative stress. Thereby it is created a vicious cycle of ROS generation that far exceeds the antioxidant defense system. Hence, oxidative stress is, undoubtedly, a contributing factor for neuronal death in AD (22).

3.3.1. Oxidative stress and dysfunction of the autophagy and the apoptosis

Autophagy is a homeostatic process involved in the turnover of proteins and cell organelles and has an important role in the regulation of cell destiny after stress injury. This process is a non-lethal stress response mechanism. The lysosome, an intracellular organelle completely devoted to the degradation or recycling of intra and extracellular components, is the main player of this process (22). Apoptosis is a type of programmed cell death regulated in an orderly way by a series of signal cascades. Apoptosis plays an essential role in regulating growth, development, immune response and eliminating excess or abnormal cells in organisms. However, the up-regulation of apoptotic process leads to increase of cell death and can result in neurodegeneration if occur in neuron cells (22).

In lysosomes, a failure to degrade aggregated $A\beta_{1-42}$ may contribute to intracellular accumulation of Aβ in AD (30). In addition, the intracellular $A\beta_{1-42}$ is resistant to protease degradation and stable within the neurons, this may invokes the rapid ROS generation within lysosomes and disruption of lysosomal membrane that leads to a lysosomal general dysfunction. Lysosomal dysfunction leads to accumulation of unfolded proteins that can also induce stress in endoplasmic reticulum (ER). Between other consequences, ER stress can increase γ-secretase activity that consequently enhances the Aβ secretion (22,31). In addition, ER and mitochondria are in close communication, and ER stress, occurring in AD brain, can be expanded to the mitochondria, where are triggered pathways of cell death by apoptosis (31). Some studies have also demonstrated the direct and indirect involvement of Aβ in the activation of the apoptotic pathway. The direct mechanism by which Aβ causes apoptosis is by inducing specific caspases (8 and 9) that lead to neuronal death. By the indirect mechanism, Aβ promotes membrane lipid peroxidation that also leads to apoptosis (32). In sum, lysosomal dysfunction mediated by Aβ can

lead to stress of ER and mitochondria, which in turn leads to production of more Aβ and activation of apoptosis that culminates in neurodegeneration (30).

3.4. Signaling alteration

One of the most relevant aspects for signal transduction in AD pathology is protein phosphorylation. Phosphorylation refers to the addition of a phosphate to one of the amino acid side chains of a protein by kinases and removal of the same group by phosphatases. The addition and removal of a phosphate group to the structure of the protein alters its function, and this balanced process serves multiples roles in the regulation of cell function.

However, the imbalance of protein kinases and phosphatases, contribute to abnormal activation of signaling pathways, which can be a cause or consequence of many diseases, including AD.

In the brain, phosphorylated Aβ aggregates could serve as endogenous seeds, triggering further aggregation of soluble and extracellular Aβ into plaques (33). In turn, the Aβ can lead to abnormal protein phosphorylation, and subsequent abnormal signaling cascades (34). The abnormal activation of signaling pathways may promote abnormal phosphorylation and aggregation of tau and cytoskeletal abnormalities. This might lead to synaptic failure, altered neurogenesis and apoptosis, typical of AD pathogenesis (28). Abnormal phosphorylation levels of APP have been also reported in AD (33,34), as well as other AD associated proteins such as PSs and BACE (33).

3.5. Vascular risk factors

Vascular risk factors such as hypertension, atherosclerosis, hyperlipidemia, metabolic syndrome, diabetes, obesity, ApoE ε4 and inflammation are risk factors that increase the propensity to AD and accelerate its progression (35). In turn, insulin resistance and type 2 diabetes increase the risk of cardiovascular disease and stroke that, consequently is associated with AD (36).

Vascular risk factors together with advancing age create a progressive degeneration in cerebral capillaries that may lead to a severe state of hypoperfusion – critically attained threshold of cerebral hypoperfusion (CATCH) – which in turn may lead to the cellular and subcellular pathology underlying to the manifestations of AD (10,25). In addition, it seems that Aβ peptide have a

vasoconstrictor effect that also leads to hypoperfusion that precedes onset of clinical dementia (10).

Cholesterol: The dysregulation of cholesterol homeostasis in the brain, mainly related to increased levels of cholesterol in plasma, takes a place in AD pathogenesis. Apparently, cholesterol loading increases γ-secretase activity and amyloidogenic pathway, while low intracellular cholesterol favors non-amyloidogenic pathway (25,37). ApoE is the major cholesterol carrier in the brain and the inheritance of the ApoE ε4 allele was associated with elevated cholesterol levels. Indeed, presence of the ApoE ε4 allele is associated with increased amyloid burden, decreased Aβ peptide degradation, and less effective neuronal repair mechanisms (38).

Inflammatory changes: Microglia, astrocytes and possibly neurons are involved in the inflammatory process in AD. Aβ can activate microglia which leads to an increase of pro-inflammatory cytokines such as TNF-α and IFN-γ, which in turn induce expression of nitric oxide synthase resulting in neuronal damage. Similarly, astrocytes, due to its agglomeration at sites of Aβ deposits, and neurons, by expression of higher levels of classical pathway complement and pro-inflammatory products, are able to trigger inflammatory processes (25).

Cerebral insulin resistance: AD is also considered a metabolic disease that results in progressive impairment in the brain's capacity to utilize glucose and respond to insulin stimulation (39). Cerebral insulin resistance can be due to peripheral insulin resistance, e.g. due to Diabetes Mellitus (DM) 2 type, or can be due to toxicity induced by ADDLs (39). In turn, insulin might increase extraneuronal accumulation of Aβ. This insulin effect is due to the competition between insulin and Aβ for insulin degrading enzyme (IDE) that is involved in the degradation of both of them (25).

In addition, it was shown that the expression and activity of IDE is significantly decreased in AD brains and that IDE and Aβ are deposited in neuritic plaques and vessels. This also leads to: increase of insulin resistance; insufficient degradation of insulin and Aβ; formation of Aβ oligomers; and neurodegeneration (10).

Glycation of proteins is another consequence of insulin resistance due to increased levels of sugars. Hyperglycemia promotes protein glycation and the gradual accumulation of advanced glycation end-products (AGEs) in body tissues (40). AGEs comprise molecules formed by irreversible, non-enzymatic reactions between sugars and the free amino groups of proteins, lipids and nucleic acids (41). In fact, it was found high levels of AGEs in AD brains, even in neurons

where Aβ is absent, suggesting that glycation is risk factor to AD (40). Both the occurrence of insulin resistance in AD and hyperglicemia suggest that DM 2 type might not only be involved in CATCH (42), but also in hormonal and metabolic changes that also leads to AD (39). Therefore, these conditions might be closely related (41).

III. Therapeutic strategies for AD

Currently, AD treatment cannot stop the disease, but can slow down symptoms progression in some cases. Four medications, descript in Table 1, are approved by the U.S. Food and Drug Administration to treat Alzheimer's. All four AD drugs are available to patients in Portugal and are part of the reimbursement system (43). These drugs produce improvements in cognitive and behavioral symptoms, but their role in the pathogenesis of AD is unknown.

Table 1. Approved medications by the U.S. Food and Drug Administration to treat Alzheimer's disease. Adapted from (44–47).

AD pathology	Drug name	Drug type	Clinical phase	Action mechanism
Failures in glutamate removal leads to its intracellular increase, leading to excitotoxicity, free radical production and then cell death.	**Namenda® (memantine)**	NMDA antagonist	Moderate to severe	Blocks the toxic effects associated with excess glutamate and regulates its activation
Decrease of cholinergic receptors leads to dysfunction of cholinergic signals transmission resulting in failures of signaling between neurons, free radicals toxicity and inflammation and then neurodegeneration.	**Razadyne® (galantamine)**	Cholinesterase inhibitor	Mild to moderate	Prevents the breakdown of Ach and stimulates nicotinic receptors to release more Ach in the brain
	Exelon® (rivastigmine)	Cholinesterase inhibitor	Mild to moderate	Prevents the breakdown of Ach and butyrylcholine (a brain chemical similar to Ach) in the brain
	Aricept® (donepezil)	Cholinesterase inhibitor	Mild to moderate and Moderate to severe	Prevents the breakdown of Ach in the brain

NMDA, N-methyl D-aspartate; Ach, acetylcholine

In recent years, several approaches aimed at inhibiting disease progression have advanced to clinical trials. The foci have been on reducing Aβ, by diminishing its accumulation or increasing its clearance, or by reducing tau deposition, by decreasing its synthesis or its phosphorylation.

Other complementary and/or alternative strategies currently tested to protect selective neuronal populations include gene therapy, vaccination, intra-thecal drug delivery and use of compounds bound to lipids (28). Furthermore, strategies to promote synaptic formation and

neurogenesis are also attractive options to inhibit disease progression. Among them, cellular therapies are rapidly in expanding, aiming to transplant new neurons that integrate, synapse, and recapitulate a neural network similar to that lost in disease. In addition, the complementary use of stem cells may provide environmental enrichment to support host neurons by producing neurotrophic factors, scavenging toxic factors, or creating auxiliary neural networks around affected areas (22).

IV. Diagnosis of AD

1. Current guidelines

The diagnosis of AD is usually based on criteria established in 1984 by National Institute of Neurological Disorders and Stroke–Alzheimer Disease and Related Disorders (NINCDS–ADRDA) (48). NINCDS-ADRDA criteria are based in the fact that clinical symptoms are in close correspondence with the pathologic changes of disease. However, this presupposition is not clear and is insufficient to detect dementia in a pre-dementia phase. This early detection is crucial for delay progression of dementia with appropriate therapies.

In 2011 new criteria and guidelines incorporate some changes such as incorporation of biomarkers, formalization of different stages of disease and consideration of common coexistence of AD and other neurodegenerative diseases (7). However, these criteria are currently intended mostly for research purposes due to the lack of standardization of biomarkers values (49).

According to NINCDS-ADRDA guidelines of 1984 that still remain in force, the clinical diagnosis is only probabilistic and the definite diagnostic is only possible after histologic confirmation (48).

2. Typical clinical pattern of dementia related conditions

AD diagnosis may be complicated by coexisting conditions or when symptoms and pathologies of various dementias overlap (2). Therefore, an accurate diagnosis will help patients receiving the treatment and support services appropriate for their condition and maintain the highest possible quality of life. The neuropathological characteristics and typical symptoms of AD and other common dementia related conditions are briefly describes in Table 2.

Table 2. Neuropathological characteristics and symptoms of the most common dementia related conditions.

Condition	Clinical and Imaging	Hispathologic hallmarks	Refs
MCI	◆ Impaired recent memory; ◆ General cognition is preserved; ◆ History or cognitive screening tests indicate mild memory failures; ◆ MRI shows increased atrophy of the hippocampus and the parietal and lateral temporal regions.	◆ Not completely characterized; ◆ Amnestic MCI may be a forerunner of AD	(3)
AD	◆ Loss of episodic memory; ◆ Cognitive impairment (thinking, orientation, comprehension, calculation, learning capacity, language, and judgment); ◆ Deterioration in emotional control, social behavior, or motivation ◆ MRI shows increased atrophy involving medial, basal, and lateral temporal lobes and medial and lateral parietal cortices; ◆ PET scans demonstrate glucose hypometabolism in superior/posterior temporal regions, and marked retention of PiB in the frontal, parietal, temporal, and occipital cortices.	◆ Amyloid plaques outside the neuron; ◆ Intracellular neurofibrillary tangles	(2,3,10,50)
VaD	◆ Sudden post-stroke changes in thinking and perception (confusion, disorientation, trouble speaking or understanding speech and vision loss); ◆ Cognitive and functional decline occurs gradually; ◆ History of cardiovascular risk factors are suggestive of VaD; ◆ CT or MRI scanning demonstrates areas of past infarction and perivascular ischaemia.	◆ Cerebrovascular lesions; ◆ Ischemic brain damage	(3)
DLB	◆ Fluctuating cognition, visual hallucinations and parkinsonism; ◆ Cognitive decline similar to AD, with memory impairment less prominent in early state, and apathy more remarkable; ◆ MRI shows diffuse atrophy with less hippocampus atrophy than in AD; ◆ SPECT or PET imaging shows reduced dopaminergic activity in basal ganglia.	◆ α-synuclein immunoreactive protein deposits (Lewy bodies) in neurons and glial cells.	(3,51,52)
PDD	◆ Parkinsonism, depression, psychosis and cognitive impairment; ◆ Visuospatial functions affected; ◆ Memory relatively preserved; ◆ MRI shows no significant difference in whole brain and caudate nucleus between controls; ◆ SPECT or PET imaging shows reduced dopaminergic activity in basal ganglia.	◆ Lewy bodies, amyloid plaques and neurofibrillary tangles	(53,54)
FTD	◆ Personality change and behavioural disturbance occur early and are prominent features; ◆ Impulsiveness, poor financial judgment, inappropriate social conduct and declining interest in grooming and hygiene; ◆ The age of onset is often between 50-60 years; Family history of FTD is a risk factor; ◆ MRI shows focal degeneration within the anterior frontal, temporal, and insular regions; ◆ PET or SPECT scanning show reduced brain activity in the frontal and anterior temporal regions.	◆ Microtubule-associated protein tau (FTLD-TAU) inclusions; ◆ TAR DNA-binding protein-43 (FTLD-TDP) inclusions; ◆ Fused in sarcoma protein (FTLD-FUS) inclusions	(3,55,56)
MD	◆ Vascular pathology may interact with preexisting subclinical AD, resulting in clinical dementia; ◆ The severity of cognitive impairment is correlated to the total volume of infarcts; ◆ There are no generally accepted and validated clinical and neuropathological guidelines for the diagnosis of MD; ◆ Criteria for AD and VaD are of limited value for the diagnosis of MD.	◆ Combination of AD with vascular or ischemic lesions ◆ Neuropathological evaluation needs further validation	(3,57)

MCI: Mild Cognitive Impairment; AD: Alzheimer's Disease; VaD: Vascular Dementia; DLB: Dementia with Lewy Bodies; PDD: Parkinson's disease dementia; FTD: frontotemporal dementia; MD: Mixed Dementia

The signals and symptoms of each dementia condition allow for the differential diagnosis of dementia. Diagnosis of AD and other dementias is a stepwise process that involves clinical evaluation with examination of patient history and early warning signs, as well as neuropsychological assessments that comprise performance screening, assessment of daily functioning, behavioral problems, and caregiver status. Finally, it may be required a referral to specialist clinics for more thorough assessment that may include radiological and biological analyses (1,58).

3. Clinical evaluation

The first step of clinical evaluation relies on prediagnostic tests to investigate other conditions that mimic dementia and to determine coexisting disorders. For this should be considered the history of mental and behavioral symptoms, a physical examination, and laboratory findings through blood and urine analyses, and radiologic tests such as Magnetic Resonance Imaging (MRI) or Computed Tomography (CT) to help in the identification and to rule out other potential causes of dementia (48,58,59).

The course of the disease is an individual process, however it should be noted that there are prevalent symptoms during disease progression. Even before the onset of cognitive problems, there are several warning signs that can predict those individuals at a higher risk of developing AD or other dementia. The American Alzheimer's Association lists ten key warning signs of AD, including memory loss, difficulty performing familiar tasks, problems with language, disorientation to time and place, poor or decreased judgment, problems with abstract thought, misplacing things, changes in mood or behavior, changes in personality and loss of initiative (58), while conscious remains unaltered (2). Severe dementia frequently causes such complications as immobility, swallowing disorders and malnutrition. These complications can significantly increase the risk of developing pneumonia, the most commonly identified cause of death among elderly people with Alzheimer's disease and other dementias (1).

3.1. Neuropsychological tests

To assess performance of patients some cognitive tests may be used to help in screening of AD, by discriminating patients with cognitive deficits from those without it, including the Mini-mental State Examination (MMSE), the Montreal Cognitive Assessment (MoCA), and Clock-

drawing (60,61). The MMSE has reigned as the screening test as it is quick and easy to administer and can track the overall progression of cognitive decline *per se* (58).

Activities of daily living should also be explored, and tests such as the Activities of Daily Living Scale (ADL) can determine the extent of the patient's disability and dependence on the caregiver.

More that 80% of AD patients experience some form of behavioral symptoms such as anxiety, agitation, depression, and apathy during the course of the disease. The common test to evaluate depression is the Geriatric Depression Scale (GDS) that helps to differentiate AD from depression (62).

In addition, there are some tests that intend: acquire detailed profile of cognitive deficits such as Alzheimer's Disease Assessment Scale-cognitive subscale (ADAS-Cog); evaluate staging of dementia, for example the Clinical Dementia Rating (CDR); and examine global changes such as Clinician Interview Based Impression of Change plus Caregiver Input (CIBIC-plus) (61). Due to the wide variety of neuropsychological tests, this kind of evaluation is time consuming and is not available for all concerned people (59). In an attempt to increase the accuracy of diagnosis, still exists an urge to continue developing instruments of cognitive indicators more reliable in early dementia (63).

3.2. Neuroimaging

A variety of imaging techniques are available for evaluating the structural, biochemical, and functional changes of the brain that increase the accuracy of clinical diagnosis of neurodegenerative diseases. Conventional structural neuroimaging with CT or MRI is recommended in the routine evaluation of patients with memory disorders, to exclude treatable causes such as intracranial mass or vascular dementia and to help assess the degree of atrophy (48,64). Since brain structural alterations are most evident in latter stages of disease, the diagnostic potential of these techniques in early stages of AD is limited.

There are other available imaging techniques that can also be used on suspicion of other dementia related condition. Functional imaging modalities, including single-photon emission computed tomography (SPECT) and positron emission tomography (PET), offer value in the differential diagnosis of dementia, particularly in distinguishing AD from VaD, FTD, DLB, and depression. Functional techniques also allow identifying more subtle pathologic changes earlier during the disease course than structural ones.

Functional MRI (FMRI), magnetic resonance spectroscopy (MRS), single-photon emission computed tomography (SPECT), structural magnetic resonance imaging (MRI) and positron

emission tomography (PET) are the most used in research and/or diagnosis of Alzheimer's disease and other dementia (Table 3). Since MRI and PET revealed more consistent results, they were introduced at the new criteria as biomarkers tools of AD.

Table 3. Imaging approach in Alzheimer's disease.

Technique	Alzheimer's correlation	References
Strutural MRI	◆ Atrophy involving medial, basal, and lateral temporal lobes and medial and lateral parietal cortices	(7,59)
Functional MRI	◆ Pattern of altered activation in the medial temporal lobes and parietal lobes	(22,59)
^{1}H-MRS	◆ Lower levels of NAA in the parietal gray matter and hippocampus	(22,50,59)
PET	◆ FDG–PET* scans demonstrate reduced glucose metabolism in the parietal and superior/posterior temporal regions	(50)
	◆ ^{11}C-PiB PET** has marked retention in the frontal, parietal, temporal, and occipital cortices as well as the striatum, consistent with the pattern of amyloid plaque deposition	(50,65)
SPECT	◆ Temporoparietal hypoperfusion or hypometabolism	(50)

NAA: N-acetylaspartate;
PDG-PET: fluorodeoxyglucose is a radiotracer analog of glucose*
*^{11}C-PiB**: Pittsburgh compound B is a radiotracer capable of highlighting deposits of beta-amyloid in living individuals during a PET scan*

4. Genetic tests

AD is mainly considered a sporadic pathology and, consequently, genetic screening cannot be largely utilized for its diagnosis. However, for the rare cases in which individuals have family members with early onset familial AD, genetic tests are available. These genetic screenings include testing for PSEN1, PSEN2, APP and APOE mutations, wherein PSEN1 and APOE mutations take the lead role.

However, like predictive value of APOE ε4 homozygotes is as high as for many other Mendelian diseases, the APOE genotyping has gained greater importance as predictive potential. Thereby, APOE ε4 homozygotes have high risk of developing AD, heterozygotes have modest risk, and individuals who do not carry an APOE ε4 allele have low risk of developing AD (22).

5. Alzheimer's disease diagnosis in Portugal

Similarly to other European countries, in Portugal, to assess patients with suspects of cognitive impairment or dementia, are performed clinical history evaluations, general physical examination including laboratory tests on blood (hemogram; glucose; calcium levels; serum ionogram; liver, kidney and thyroid functions; dosage of vitamin B12 and folic acid and serologic test for syphilis),

and neuropsychological tests with cognitive evaluation (MMSE and MoCA), assessment of activities of daily living (ADL) and depression rating (GDS)(43).

In addition, structural imaging test such as CT or MRI, are used in order to exclude treatable causes of cognitive decline and to provide information for a diagnosis specific etiological (43). In atypical situations or when clinical features are suggestive of other diseases, the specialist may collect CSF samples for suspected cases of neoplastic involvement, inflammation or infection of the CNS, and SPECT can be used on suspicion of DLB (43).

Genetic studies are performed if there is a family history of autosomal dominant disease or a phenotype suggestive. However, for most of the patients with sporadic Alzheimer's disease, the genetic study, mainly ApoE genotyping, is currently not recommended in clinical (43).

V. Biomarkers as diagnostic tools for AD

Since the early symptoms of the disease are shared by a variety of neuropathological disorders it is important to find markers that assist in the diagnose and that help the monitoring of the disease progression (1,22,66).

The ideal biomarker for the diagnosis of AD should be directed at its basic neuropathology and correlate with histological criteria for the diagnosis. Furthermore it should detect AD at an early asymptomatic stage and mark its presence by itself rather than a risk factor, as well as it should track severity of AD pathology at preclinical stage. In addition, the ideal biomarker should be also reliable, reproducible, non-invasive, inexpensive, and rapid. Not least, it should react upon pharmacological intervention and display high sensitivity (>80%) and specificity (>80%) for the disease as compared with related disorders (67).

Five biomarkers (Table 4) that have been widely studied, were now formally incorporated into the diagnostic criteria of AD (7). These comprise: structural brain changes visible on structural magnetic resonance imaging (MRI); molecular neuroimaging changes seen with positron emission tomography (PET); and concentration changes of $A\beta_{1-42}$ and tau in the cerebrospinal fluid (CSF) (7).

Table 4. Currently accepted biomarkers for the diagnosis of Alzheimer's disease. These biomarkers were grouped into two broad categories agreed by National Institute on Aging. Adapted from (7).

Biomarkers category	Category description	Biomarkers for AD Diagnosis
Biomarkers of Aβ accumulation	Indicative of initiating or upstream events which seem to be most dynamic before clinical symptoms	◆ Abnormal tracer retention on amyloid PET (^{11}C-PiB) imaging
		◆ Low CSF $A\beta_{1-42}$
Biomarkers of neuronal degeneration or injury	Indicative of downstream pathophysiological processes which become dynamic later	◆ Elevated CSF tau (T-tau and P-tau)
		◆ Decreased fluorodeoxyglucose uptake on PET (FDG-PET) in a specific topographic pattern involving temporoparietal cortex
		◆ Atrophy on structural MRI—again in a specific topographic pattern—involving medial, basal, and lateral temporal lobes and medial and lateral parietal cortices

The role of biomarkers differs somewhat in each of the disease phases. Figure 6 shows a hypothetical relation of the biomarkers of AD with phases of disease. In the preclinical phase (cognitively normal) begins the most of the molecular alteration observed in AD and biomarkers are used to establish the presence of the pathophysiological process, aiming a better care for AD patients. In this phase, Aβ can be measured by PET-amyloid and CSF Aβ biomarkers, and neuronal injury and degeneration are detected by CSF tau and FDG-PET biomarkers (68).

In the symptomatic predementia/MCI phase, biomarkers are used to establish the underlying etiology responsible for the clinical deficit and to assess the likelihood of disease progression. In this phase, characterized by a little recent memory impaired, can also be measured Aβ and neuronal injury and degeneration and some atrophy of the brain is detected by MRI (68).

In the dementia phase, the neuropsychological tests disclose impairment of the memory and cognition, and biomarkers are used to increase or decrease the level of certainty of the pathophysiological process underlies the dementia due to AD (68).

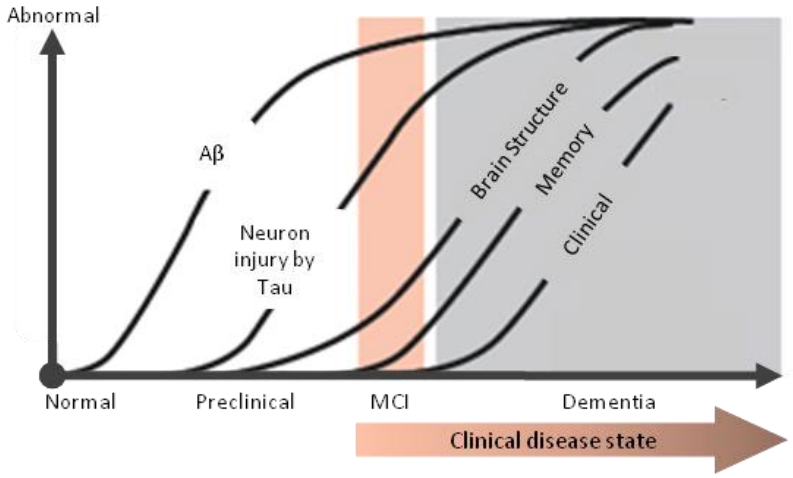

Figure 6. Illustrative model of the ordering of biomarkers of AD relative to stages in the clinical onset and progression of AD. Clinical phases are on the horizontal axis. The vertical axis relates, in function of the disease progression, the appearance of the hallmarks of disease, the morphological alterations of the brain, the memory loss and the increased general clinical dysfunction. Adapted from (68).

1. CSF biomarkers

The lumbar puncture to collect cerebrospinal fluid is an invasive procedure that hinders obtaining this fluid for analysis. However, CSF is a very useful fluid for AD diagnosis since it reflects metabolic process in the brain due to the direct contact between the brain and CSF. Furthermore, CSF biological modifications seem to appear before first modifications seen on MRI (69).

Among the high numbers of CSF brain-derived proteins undergoing investigation, three biomarkers, all soluble in CSF, were validated internationally and included in AD diagnosis criteria: low $A\beta_{1-42}$, high total Tau (T-Tau) and high phospho-Tau-181 (P-Tau) (22,59,67). This core of biomarkers reflects AD pathology, and has high diagnostic accuracy to diagnose AD in dementia and symptomatic predementia phase (59,70).

Investigating levels of key Alzheimer-related proteins in cerebrospinal fluid (CSF) is largely researched due to inconsistence of the proteins levels from institution to institution. To facilitate consistency and move this vital area forward, the American Alzheimer's Association has funded the *Alzheimer's Association QC Program for CSF Biomarkers*, wherein organizations can improve their analytic capabilities by comparing their outcomes to results at reference laboratories in the United States and Europe (54).

Aβ$_{1-42}$ peptide: In AD patients the CSF concentration of soluble $A\beta_{1-42}$ decreases, suggesting that this may be due to the preferential deposition of Aβ peptides into cerebral amyloid plaques with

lower levels diffusing to CSF (59). CSF $A\beta_{1-42}$ concentration may differentiate AD patients from controls with high sensitivity (86%) and specificity (90%). ELISA measurements indicate a range of values between 600 and 1230 pg/mL to normal subjects and between 260 and 500 pg/mL to AD patients (59,70)

Tau protein: Increase of CSF tau total (T-tau) levels is not AD specific since it is also observed in other dementia types, in which neuronal death occurs. However, CSF T-tau levels are around 150 – 450 pg/mL in normal subjects and range 300 – 1100 pg/mL in AD patients (59,70).

Phosphorilated Tau protein: CSF P-tau species might specifically mark a cerebral degenerative process because its increasing levels are correlated with cognitive decline. The most commonly used ELISA methods for P-tau in CSF use antibodies for phosphorylation at either threonine 181 ($P\text{-}tau_{181}$) or threonine 231 ($P\text{-}tau_{231}$), thus improving accuracy of biological diagnosis. $P\text{-}tau_{181}$ levels are between 30 and 50 pg/mL in normal subjects, and between 75 and 100 in AD patients (59,70).

Combination of Tau and Aβ: It has been suggested that the use of combinations of these three CSF markers could have more successfully to discriminate AD from control or other forms of dementia than an individual marker, wherein the high CSF P-tau/ $A\beta_{1-42}$ ratio possesses the higher diagnosis accuracy (71).

Although these biomarkers are recognized in Portugal, is still not used in clinical evaluation (43,72), since its standardization is hampered, implying that each centre establishes its own reference values (72).

A recent Portuguese study evaluated CSF biomarkers in AD and in pre-dementia stages, and in agreement with previous publications, confirmed that CSF biomarkers, namely the $A\beta_{1-42}$/p-Tau, are accurate tools (specificity and sensitivity above 85%) for the diagnosis of AD and may be useful in the identification of MCI patients (72). Given the invasive character of CSF collection, the investigations become restricted and, at moment, its diagnostic use in Portugal is limited. Therefore, there is a need to find more viable options in more peripheral fluids.

2. Fluid biomarkers to detect Alzheimer's disease under investigation

2.1. CSF biomarkers

Apart from $A\beta_{1-42}$, T-tau and P-tau_{181}, numerous other molecules have been investigated as biological CSF promising markers and are liable to participate on etiological dementia diagnosis. Some of them that seem to supply advantage for differential and early diagnosis include: $A\beta_{1-42}/A\beta_{1-40}$, $A\beta_{1-42}/A\beta_{1-38}$ and $A\beta_{1-42}/A\beta_{1-16}$ ratios that may give slightly higher accuracy than $A\beta_{1-42}$ alone; the high concentrations of ADDLs in AD patients compared with controls. In addition, BACE1 may also be a CSF promising marker, given that upregulation of β-secretase is an early event of AD (70,71).

Neuronal and synaptic proteins are also research targets as AD biomarkers, wherein the calcium sensor VLP1 and the synaptic protein GAP-43 have demonstrated to be high in AD patients than in controls, and neurofilaments are often in normal concentrations compared with VaD or FTD patients (70,71).

The oxidative stress AD markers in CSF include high levels of F2-isoprostanes compared to healthy controls or patients with other dementia. Possible markers of neuroinflammation include acute-phase protein α-ACT that is either increased or unchanged in CSF samples of AD patients, and cytokines (interleukins, TNFα, Interferon-γ and TGF-β) (70,71).

2.2. Blood biomarkers

Although plasma biomarkers as reliable markers for AD diagnose have met little success, some molecules have been investigated, and some of them can be used to evaluate AD prediction, progression and therapeutic monitoring. For example, high plasma levels of $A\beta_{1-42}$ were suggested to be a risk factor for developing AD, and Aβ measures are potentially used in clinical studies to therapeutic monitoring that affect APP processing. However, plasma Aβ measures are not sensitive or specific markers for diagnosis of AD (73). This is probably explained by the fact that the major plasma Aβ is derived from peripheral tissues and does not reflect brain Aβ production. Furthermore, the hydrophobic nature of Aβ makes the peptide bind to plasma proteins, which could result in epitope masking and other analytical interferences (70,71). On the other hand, quantification of platelet APP isoforms holds promise for tracking diagnosis, progression, and

treatment effects (73). Indeed, mononuclear leukocytes seem to offer a stable medium to determine β-sheet structure levels as a function of AD development (74).

Increased markers of oxidation of protein, lipid, and nucleic acid and reduced activities of antioxidant enzymes are according to neurodegeneration in AD and are also in plasma/serum. Plasma/serum antioxidants include carotene, lycopene, vitamin A, C and E, urate and bilirubin. ROS damage of protein, polyunsaturated fatty acids and nucleic acids are markers of oxidative state and was associated with AD pathology (31,73). Among stress oxidative markers, malondialdehyde (MDA), 8- hydroxy-2'-deoxyguanosine (8-OHdG) and F2-isopropanes were the most promising (59).

Reactive inflammatory responses are consequences of amyloid deposition, and AD may be associated with the immune dysregulation, detectable in plasma (73). Furthermore, two proteins present in SPs, α2-Macroglobulin (α2M) and complement factor H (CFH), and increased levels of α1 antitrypsin, α1-antichymotrypsin, and decreased levels of apolipoprotein A1 in plasma/serum were observed in AD patients compared with healthy controls. However, these differences have not yet attained the sensitivity, specificity and reproducibility to become AD biomarkers (71).

Additionally, it was found 18 signaling proteins in blood plasma that can be used to classify samples from Alzheimer's and control subjects with high accuracy and to identify patients who had MCI that progressed to AD. Further independent studies are needed to verify this combination of plasma biomarkers and their diagnostic value (75).

2.3. Biomarkers of other biological fluids

Among several biological fluids, a special attention is accorded to saliva and urine. Although urine has the obvious advantage of easy collection, is a limited source of biomarkers due to its very low protein concentrations and high salt levels (71). However, neural thread protein (NTP) levels have been consistently identified as a possible AD biomarker in urine, and its levels increase with disease severity (71). Similarly, saliva is simple to obtain and has the property that may reflect changes in CSF. Therefore, in a pilot study (76), it was suggest that saliva $A\beta_{1-42}$ levels could be considered a potential peripheral marker for detect early AD with an additional ability to discriminate AD from other types of neurodegenerative disorders.

3. Strategies for novel biomarkers discovery in neurological disease

Identification of biomarkers in neurological disease remains impeded by many obstacles. There are four basic challenges to biomarker identification in neurological disease. The first is the lack of availability of tissue at the site of pathology ante-mortem that hinders the discovering etiologically relevant genes, proteins or small molecules to diagnose the disease. The second is that clinical diagnostics are poor in information, and the state in which the disease is diagnosed is usually advanced, being the definitive diagnoses of neurodegenerative disease only achieved upon autopsy. The third challenge is the complexity and tissue heterogeneity that is more accentuated in the brain than in other organs resulting in transcriptomes, proteomes, morphological phenotypes and interactive connections widely variables within the neurons and glial cells. The fourth challenge is the paucity of model systems for functional validation in neurological diseases that hinders the confirmation of candidate biomarkers, because neurological diseases are mainly behavioral in nature, therefore it is difficult to ascertain many of the phenotypic characteristics as they occur *in vitro* or *in vivo* (animal models) (77).

Ideally, a systematic approach to biomarker identification will involve multiple "-omic" technologies to investigate the disease process at all levels. Genomics is used to identify relevant disease genes, aberrant cellular signaling pathways, and expression signatures correlated with disease. Proteomics is used to identify aberrant protein expression, post-translational modification, protein interactions, and protein profiles that are specific to a particular disorder. Finally, metabolomics is implemented to identify the presence of abnormal levels of small molecule metabolites that are specific to and indicative of an underlying disease process (67,77)

Given this, and the multiplicity of processes implicated in AD, the diagnostic accuracy of biomarkers may be improved by combining several serum or plasma markers in order to create a more robust biomarker profiling characteristic of AD (73).

3.1. A focus on metabolomics techniques

The metabolome is the sum of all low molecular weight metabolites in a biological system and metabolomics refers to its analysis. Metabolomics has begun to have a more prominent role in efforts at biomarker identification and will increasingly be applied to neurological disorders. Metabolomics is typically performed on biofluids, such as serum, urine, saliva and CSF (77).

By assessing hundreds of metabolites simultaneously, metabolomics techniques produce high-resolution biochemical snapshots showing the functional endpoints of genetic predisposition as well as the sum of all environmental influences such as nutrition and medication. This snapshot can provide an almost real-time image of the pathophysiology of an entire organism, which it is not possible obtain in genomics, proteomics or in other "-omics" (78). Specifically, due to the fact that any biochemical change must precede any morphological manifestation of the disease itself, the metabolomic approach may be very useful for early diagnosis.

Metabolomics is a multi-disciplinary science that requires analytical techniques such as chromatography, molecular spectroscopy or mass spectrometry, coupled with bioinformatics tools such as multivariate data analysis methods, to get the most out of the data.

There are three major approaches used in metabolomics studies: targeted analysis; metabolite profiling; and metabolic fingerprinting (79).

Targeted analysis is used to quantify a limited number of known/target metabolites precisely (79). Metabolite profiling restricts itself to a certain range of compounds or even to screening a pre-defined number of members of a compound class. For these two approaches, main techniques are gas chromatography (GC), high performance liquid chromatography (HPLC) and MRS, which rely on chromatographic separations, often coupled with well-developed calibrations for specific analytes (80).

Metabolic fingerprinting does not attempt to identify or precisely quantify all the metabolites in the sample. Rather, it considers a total profile, or fingerprint, as a unique pattern characterizing a snapshot of the metabolism in a particular cell line or tissue. The metabolic fingerprinting is most useful in biomarker discovery and diagnostics, namely to discover specific metabolic patterns of diseases.

Mass spectrometry (MS) and Fourier transform infrared (FTIR) spectroscopy (or other spectroscopic techniques) are usually used in fingerprinting for directly acquire spectra without any separation step such as chromatography or electrophoresis (79).

3.2. The potential of the FTIR as clinical tool

FTIR is a technique almost universal because many molecules have strong absorbances in the mid-infrared region, and is applicable for many types of samples (solids, liquids, gases and pasts. It is highly versatile, since is needed minimum sample preparation. Infrared spectra are information rich, wherein peaks positions give the information about the structure of molecules in a sample.

The intensity of peaks is related to the concentration of molecules and peak widths are sensitive to the chemical matrix of the sample (pH and hydrogen bonding).

Given that FTIR spectroscopy is a technique based on metabolomics is able to detect biochemical changes caused by pathologies, even at a very early stage of the disease. In addition, comparing with other laboratory instruments (e.g. for NMR, GC-MS or LC-MS) infrared spectrometer is relatively inexpensive (81). It gives the opportunity to analyze, in real time, small amount of sample, providing reliable and reproducible spectral data (82). Whilst it is not as specific and sensitive as other techniques of metabolomics such as GC-Tof-MS, it has been recognized as a valuable tool for metabolic fingerprinting, owning to its simplicity and ability to analyze several biomolecules simultaneously (83).

FTIR has been applied to samples of human tissue and body fluids and has shown potential to support clinical pathology, i.e. detecting and grading of disease (84,85). In this context FTIR spectroscopy proved to have potential in cancer diagnosis (86–88) such as cervical cancer (89), colorectal cancer (90), liver cancer (91), prostate cancer (92,93) and breast cancer (94). The diagnosis and evaluation of the chemotherapeutic efficacy of patients with leukemia was also achieved with this technique (95,96). Others applications include diagnosing arthritic disorders (97,98) and determination of kidney complex stones composition (99,100). Infrared spectroscopy has also proved to be a valuable tool for characterizing and differentiating microbial cells (101), proving a rapid method for identifying micro-organisms responsible for human infections (102). In addition, FT-IR has proved to be very useful to understand the mechanism of atherosclerosis development (103,104) and the diabetes diagnosis (105,106). It also can be used to the determination of the concentrations of metabolites in whole blood, plasma and urine (107–110).

With particular relevance, FTIR has been used in neurological disorders, wherein the quest for diagnosing Alzheimer's disease has a considerable role. Thereby, studies showed its potential use in the diagnosis of AD from autopsy tissue (111). More recently has been investigated its potential for early diagnosis, using biofluids such as CSF (112) and parts of blood including plasma and leukocytes (74,113). In the study with CSF, it was found a high diagnostic accuracy, corresponding to Aβ and tau protein identification. In plasma samples, it was possible to associate oxidative stress in AD groups (113) and in the mononuclear leukocytes of peripheral blood, it was found spectroscopic regions mainly associated with Aβ peptide (74).

VI. Significance of the study

Alzheimer's disease is the major cause of cognitive impairment and subsequent dementia, in the elderly. As life expectancy tends to increase, AD is becoming a greater health problem with many costs associated. Therefore, there is a need to early, simple and cost-effective diagnosis of AD in order to apply correct therapies that slowed cognitive decline. An early diagnosis, in the MCI phase, may delay the onset of Alzheimer's dementia (114).

At present, the most reliable and sensitive diagnostic techniques are invasive, hindering its clinical implementation. Blood-based tests are an appealing alternative because of its simplicity and reduced cost-effectiveness in clinical application. However, to date, the biomarkers investigated in blood of AD patients have reduced sensitivity and specificity for AD diagnosis (59).

Given the multiplicity of pathophysiologic processes involved in AD, a multi-analyte profiling approach to plasma/serum contents can yield biologically important signatures of disease to allow for diagnostic accuracy, prognosis and novel therapeutic development (73,115,116). Metabolomics showed to be a valuable tool for the identification of molecular mechanisms involved in the etiology of AD, wherein plasma was validated as a reliable biofluid for metabolic studies of brain-related disorders, resembling the profiles in CSF (115). In turn, FTIR spectroscopy is a valuable metabolic fingerprinting tool, simple and with minimal needs of sample preparation that has been shown promising results for diagnostics of many pathologic conditions (84).

Given the small sample size of this study, it is impracticable define if obtained data constitute a biologically relevant effect. Therefore, here it will be carried out an exploratory study or a pilot study. This kind of studies aims to the generation of data that suggest hypotheses for more intensive and targeted confirmatory experiments in the future (117).

Considering that plasma/serum samples are aqueous samples and that water absorbs IR radiation strongly, the spectra interpretation may be difficult due to the band overlap. Thus, a specific aim of this study is remove water signals using drying of the samples under controlled conditions by a procedure called drying kinetics. **Chapter 2** aims to present this methodology applied in plasma and serum.

Chapter 3 presents a direct analysis of serum and plasma spectra in order to exhaustively identify and assign the spectroscopic bands. Here it is also discussed the limitations of the direct spectra analysis to accurate discrimination between spectra of putative AD patients and corresponding age and sex matched controls and the key role of multivariate analysis (PCA) to this

achievement. Finally, it is intended the identification of spectroscopic signals, arising from the functional groups of possible biomarkers, involved in the discrimination of the putative AD and controls.

Therefore, the exploratory study presented here specifically aims to:

1) test the ability of FTIR to analyze plasma and serum samples, after overcoming water band overlap;
2) test the ability of FTIR together with multivariate analysis (PCA) to discriminate between non-AD and putative AD patients, using plasma and serum samples;
3) identify spectroscopic signals and assign functional groups of possible biomarkers in plasma and serum samples that discriminate non-demented controls from the putative AD patients;
4) establish conditions of spectroscopic analysis for serum and plasma samples;
5) establish the type of sample, either serum or plasma, that best distinguishes the non-demented controls from the putative AD patients.

With this exploratory study it is hoped to contribute to a future development of objective and sensitive methodology for the diagnosis of Alzheimer's disease, based on spectroscopy and multivariate analysis.

Chapter 2

I. Method overview and experimental conditions optimization

1. General considerations on infrared spectroscopy

Spectroscopy is based on the interaction between sample and electromagnetic radiation, to perform an analysis of individual chemical components including proteins, nucleic acids and metabolites, and provides detailed information about the structure and mechanism of action of molecules (81).

The type of spectroscopy depends on the interaction that different frequencies of electromagnetic radiation have with the molecules. With different radiation is possible to extract information of the energies of electronic, vibrational and rotational states, structure and symmetry of molecules as well as dynamic information. Among spectroscopic techniques, those with great utility to biomedicine include NMR, infrared, Raman, UV/Vis circular dichroism and fluorescence spectroscopy (118).

The infrared (IR) radiation of electromagnetic spectrum is invisible to the naked eye, its wavenumber range lies between 14000 and 4 cm^{-1} and is responsible for molecular vibrations. Energy frequencies higher than 14000 cm^{-1} (ultraviolet and visible light) cause electronic transitions, while energy frequencies lower than 4 cm^{-1} (microwaves) create the molecular rotations (Figure 7) (81).

The IR spectrum can be subdivided into near-infrared (NIR) region between 14000 and 4000 cm^{-1}, mid-infrared (MIR) region between 4000 and 400 cm^{-1}, and far-infrared (FIR) region between 400 and 4 cm^{-1} (81). When MIR radiation is used in infrared spectroscopy it is possible to obtain valuable information about sample chemical composition. When NIR radiation is used in spectroscopy the spectral information obtained is more difficult to interpret due to the characteristics of spectroscopic signals that are fewer and broader (81).

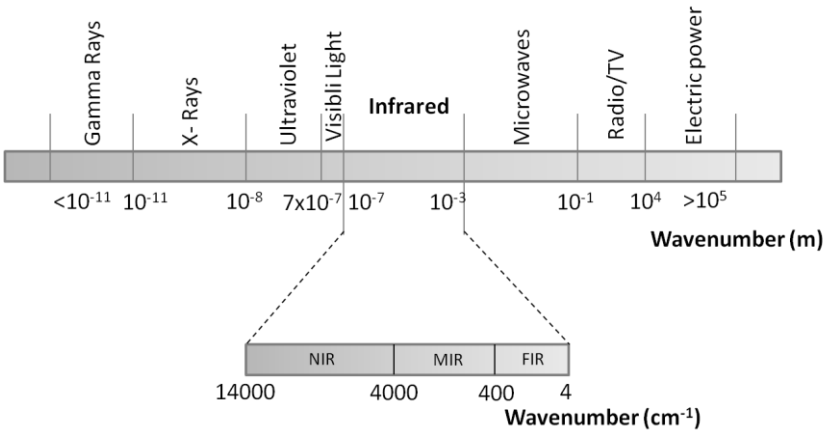

Figure 7. The IR regions of the electromagnetic spectrum. Adapted from (81,119).

1.1. Vibrations of molecules

The molecular bonds are not rigid, and do not have fixed lengths. Instead the nuclei oscillate/vibrate about their mean positions.

A molecule consisting of *n* atoms has a total of 3 *n* degrees of freedom, corresponding to the Cartesian coordinates (x, y and z) of each atom in the molecule. In a nonlinear molecule, 3 of these degrees are rotational and 3 are translational, whereas the remaining corresponds to fundamental modes of vibration. In a linear molecule, 2 degrees are rotational and 3 are translational. Therefore, the fundamental vibrations for nonlinear molecules are $3n - 6$, and $3n - 5$ for linear molecules (120). For example, H_2O molecule has three (3(3) – 6) molecular vibrations, while CO_2 has four fundamental modes of vibration (3(3) – 5).

The molecular vibrations can be classified into axial deformation (stretching) and angular deformation (bending). A vibration of axial deformation is a rhythmic movement along the axis of the molecular bond that can be symmetric or asymmetric (Figure 8). The vibrations of angular deformation correspond to rhythmical variations of molecular bonds that have an atom in common, or the movement of a group of atoms relative to the rest of the molecule with no changes in the relative positions of the atoms of those groups. The vibrations of angular deformation involve changes in bond angles in relation to an arbitrary coordinate ensemble of the molecule. Four vibrational modes of angular deformation (bend) include scissoring (symmetrical bend in-plane), rocking (asymmetrical bend in-plane), wagging (symmetrical bend out-of-plane) and twisting (asymmetrical bend out-of-plane) (Figure 8).

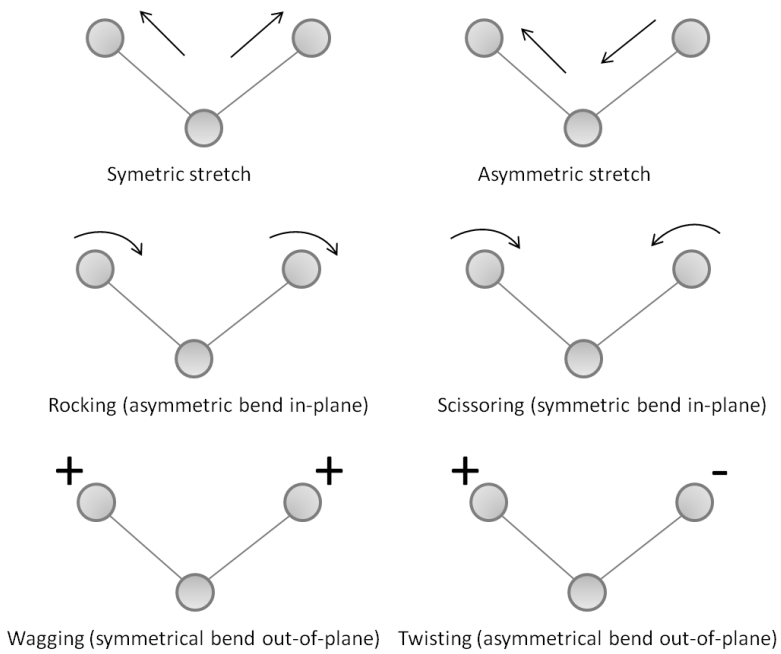

Figure 8. Examples of vibrational modes of stretching and bending. Adapted from (121).

Not all vibrations of the molecules are observed in the IR spectrum. The IR absorption process involves absorption of energy by the molecule if the vibration causes a change in the dipole moment of the molecule (120). There is a dipole moment when there is a difference in electronegativities of the bonded atoms. When the oscillating electric field, induced by the vibration of the atoms in the molecule, interacts with the radiation appears a peak in the infrared spectrum. If there is no variation, there will be no oscillating field to interact with radiation, and no radiation will be absorbed or emitted (120). Thus, while homonuclear diatomic molecules (H_2, N_2, and O_2) have no dipole moment because the two identical atoms have identical electronegativities, heteronuclear diatomic molecules (HCl, NO, and CO) have dipole moments, so they have IR active vibrations (120). Likewise, the same molecule may have vibrations that are active in IR and other inactive. For example, the symmetric stretching mode of CO_2 is inactive in IR, because this vibration does not break the symmetry of the molecule and, thus, the dipole moment remains zero. There are also molecules such as H_2O that have all its fundamental modes of vibration active in IR.

Since a molecule can have many vibrational active modes, the use of mixtures makes spectrum highly complex and difficult to analyze due to the several overlaps of bands (81). When applying FTIR to biomedical samples such as tissues or body fluids, one the major obstacles is the large

water content. Furthermore, even with no water signals, a peak may have several assignments and the same functional group may give signals at different sites of the spectrum.

1.2. FTIR equipment

A spectrometer comprises a light source, an optical system, a detector and a sample holder. Radiant energy from source is directed to the sample and a detector measures the intensity of the emergent beam.

FTIR is the predominant type of infrared spectrometer in use and have advantages and disadvantages when compared to other types of spectrometers (81).

One of the major advantages of FTIR over other spectrometers is their ability to acquire spectra with high signal-to-noise ratios (SNRs). SNR values are due to some spectrometer characteristics like: throughput, multiplex and wavenumber precision. The throughput advantage is attributable to high-intensity of infrared beam that arrives to the detector, increasing the signal level. The advantage of multiplex is related to the possibility of co-adding scans, another way of improving SNR of a spectrum. Finally, the high precision is due to the laser that acts as an internal wavenumber standard. High SNRs increase the sensitivity of the instrument, and allow quantitative accuracy, increasing the possibilities of applications (81).

Artifacts are one of the FTIRs disadvantages. There are peaks present in the spectrum that are not from the sample, some of them are caused by the atmospheric CO_2 and water vapor peaks. Fortunately, this problem can usually be overcome by removing the background contribution, this operation is successful if there are no variation in concentrations of atmospheric gas between the measurement of the background and the sample spectra (81).

FTIR spectrometers use an interferometer, usually a four arms Michelson interferometer. The top arm contains the infrared source, and a collimating mirror that collects the light from the source and makes its rays parallel. The bottom arm contains a stationary mirror, and the right arm contains a moving mirror. The left arm contains the sample and detector. At the center of the interferometer there is a beamsplitter (Figure 9) (81).

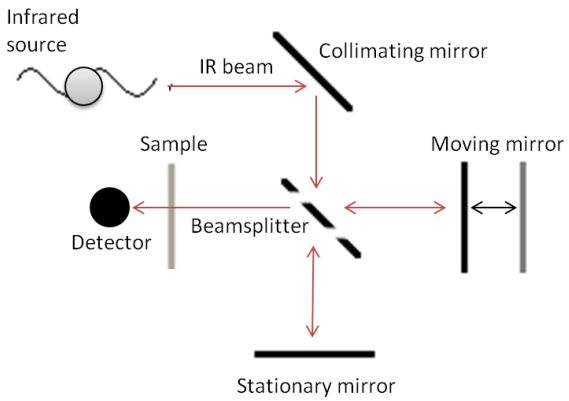

Figure 9. The optical diagram of a typical Michelson interferometer. Adapted from (81).

The beamsplitter, a semi-reflecting film, bisects the planes of two mirrors is designed to reflect 50% of the incident radiation to one of the mirrors and transmit the remaining 50% to the other mirror (81,121). After reflecting to the mirrors the two radiation beams recombine and return to the beamsplitter. The recombined radiation leaves the interferometer, interact with the sample and then reaches the detector (81).

The detector reads information about every infrared range wavenumber simultaneously. Then, the detector signal is sent to the computer and is applied the Fourier transform algorithm that converts the interferogram (IFG) into a single beam spectrum, that is a plot of arbitrary infrared intensity units versus wavenumber (81).

To produce an artefact-free transmittance spectrum, removing atmospheric effects and instrument contributions, the sample single beam spectrum must be normalized against the background spectrum of the air (Figure 10) (81). The obtained transmittance spectrum can be converted to absorbance by taking the negative $\log_{10}$ of all the data points (Figure 10) (121,122).

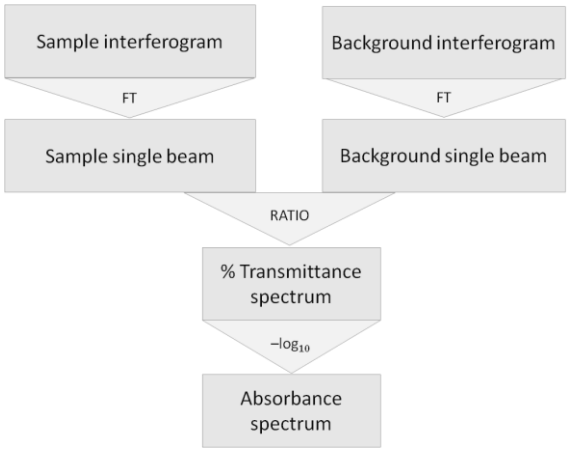

Figure 10. The process of collecting an infrared spectrum in an FTIR spectrometer. FT: Fourier Transform

1.2.1. The Golden Gate ATR™, a accessory of sample analysis

Currently IR-measurements are largely performed in Attenuated Total Reflection (ATR) mode because this technique is more versatile and simpler to use than the conventional transmission mode. Transmission technique implies that IR beam cross the whole sample, being necessary control the sample thickness and opacity. As well as liquid samples are difficult to analyze (121).

With ATR it is possible to rapidly analyze solids, liquids, powders or pastes samples. In ATR sampler the crystal is in contact with the sample, and the IR beam passes through the crystal within which it is totally internally reflected beyond the surface of the crystal into the sample in contact with the crystal (123)**.** As the sample placed on the crystal absorbs energy, the beam will be attenuated or altered. The attenuated beam reaches the detector in the IR spectrometer and the information is converter to IR spectra. The absorption (attenuation) of IR beam is proportional to chemical concentration of the sample, enabling to extract quantitative data (120).

The Golden Gate™ ATR (Figure 11) is one of the most sensitive, robust and versatile infrared accessory designed for all the high performance FT-IR spectrometers. The excellent physical characteristics of the diamond and the rugged construction of the accessory are the main advantage features. The diamond is very resistant and is responsible for the great versatility of the Golden Gate™ ATR. Indeed, it can be cleaned quite aggressively, resists to chemical attack and thus it is possible the analysis of corrosive liquids, and resists to high loads applied against a solid. The diamond also has very good thermal conductivity. This makes it ideal for ATR measurements at high or low temperatures because it can be heated or cooled rapidly. Furthermore, its thermal conductivity ensures that there are no temperature gradients across the ATR element (124)**.**

In addition, the small aperture (~2 mm) for placing the sample requires very small sample amounts, without or very little need for preparation (124).

Figure 11. Golden Gate ATR™ accessory. From (124).

1.2.2. What is shown in infrared spectrum?

Molecules absorb IR radiation due to the vibrational movements of their chemical bonds. Those movements occur at specific energy levels, after IR radiation exposure, the chemical bonds absorb IR radiation at wavenumbers correlated to their energy levels. IR spectroscopy measures this absorption and, as result, a spectrum is obtained. The peaks (spectroscopic signals) are related to specific chemical bonds of functional groups of the sample molecules (116).

The infrared spectrum is a plot of measured infrared light intensity, which may be presented in percent transmittance (*%T*) or in absorbance (*A*), versus a property of the radiation, such as a wavenumber (cm^{-1}) scale. *%T* ranges from 0 to 100% and *A* ranges from 0 to infinity, however the peaks should be less than 2 absorbance units or greater than 10% to avoid truncated peaks that can compromise the confidence of results, for both qualitative and qualitative analysis (81).

For qualitative analysis, to identify unknown peaks or perform spectral comparisons can be used both of the spectra types, *%T* or *A*. For quantitative analysis, spectra must be transformed in absorbance because absorbance is linearly proportional to concentration (81).

1.3. Mid-infrared spectroscopy applied in biological samples

Most disease diagnoses researches are focused in the mid-infrared region of the spectrum (4000 to 400 cm^{-1}) since this region contains many sharp peaks and can provide valuable chemical information (83).

Mid-infrared spectra between 1800 and 900 cm^{-1} have a large number of spectroscopic information as a result of the absorption of a large number of biochemical molecules (116). Therefore, this region may be very useful to characterize biological samples by identifying disease biomarkers. However, this kind of samples have great amount of water in their composition that absorbs great part of radiation in mid-infrared spectra. The water dilutes the solutes and, in MIR spectra, has broad and intense peaks at ranges of 3400-3200 cm^{-1} and 1700 and 1500 cm^{-1} that can mask the spectroscopic signals of the solutes, thus hindering spectral interpretation.

1.3.1. Overcome water overlapping

The presence of water in biological samples may be minimized by subtracting the spectrum of pure water from the spectrum of the sample, this arithmetic operation remove the water signals making the peaks of interest much easier to identify. However, a solute in liquid water needs to be present in a concentration higher than 0.1% to be detected/identified (81). Another strategy is using pure water in the ATR crystal during the acquisition of background single beam. When the ratio with the sample single beam is made, the water spectroscopic signals tend to disappear. An alternative to overcome this issue is promote the water evaporation and then analyze the resulting film. This approach has already been applied on serum samples and, in addition to eliminating the spectral interference of water, can provide better spectral resolution in virtue of eliminating the water/solute interactions (125).

The present study is also based on drying methodology to eliminate water contribution but under controlled conditions. All the samples are submitted to the same drying time and, to control all the process, the spectra are constantly being acquired and recorded. This procedure was called drying kinetics and has been used in other biological fluids such as amniotic liquid with great results (126). In the present work this procedure was adapted to the serum and plasma samples.

1.3.2. General considerations about blood samples

The human blood is a complex fluid matrix of plasma (with high volume of water) and cellular components (red blood cells, white blood cells and platelets). For analytical purposes it must be performed the immediate separation of plasma or serum from cells to provide analyte stability at room temperature (127).

Plasma is produced when blood with no cells is treated with an anticoagulant, serum is also the liquid fraction of whole blood but is collected after the clotting factors being allowed to act.

Thus, serum differs qualitatively from plasma because the bulk of the fibrinogen is removed by conversion into a fibrin clot together with the platelets. Varying amounts of other proteins and other molecules such as RNA (128) are removed into the fibrin clot either by specific or non-specific interactions (129). So, there are several chemical differences between serum and plasma.

Serum and plasma are usually considered to have similar compositions and properties. Both samples are composed mainly by water, by a complex matrix of low molecular-weight organic (lipids, carbohydrates, amino acids and nucleic acids) and inorganic chemicals (Na^{+}, K^{+}, Ca^{2+}, Mg^{2+}, Cl^{2+}, HCO^{3-}, HPO_4^{2-} and SO_4^{2-}), combined with other higher-molecular-weight species, including proteins (albumins, globulins, regulatory proteins and, only in plasma, fibrinogen) (130). With respect to physical characteristics, serum and plasma are usually light yellow in color, odorless, pH within the narrow range of 7.35 to 7.45 (slightly basic) and more viscous than water (131).

According to several studies the use of serum is recommended because of the higher instability of plasma analytes (127,132,133). In this study, both samples were study in order to compare the results and establish the one that presents the best results to the aim of the study.

Since water is the main constituent of both plasma and serum, requires that its presence is minimized for the analysis by FTIR. In this way it is possible gather reliable information of their dissolved constituents.

2. Method optimization

2.1. Sample preparation

In order to optimize the acquisition methodology and to overcome water signals overlap, a blood sample from an apparently healthy elderly was used. The sample used belongs to a project that was approved by the ethics committee of the Regional Health Center - Coimbra, protocol number 012 804 of April 4, 2012.

All blood samples of this project were received at the laboratory in the range of 30 minutes after its collection. Pre-processing was performed immediately.

From each sample were prepared aliquots of plasma and serum. To obtain plasma, tubes *K2 EDTA* 5 mL with gel separator were used. Then a centrifugal force of 1800*g*, during 15 minutes, at 8ºC, was applied, wherein the blood cells were separated from plasma. The obtained plasma was transferred and resuspended in a tube of 5 ml. For the present study, aliquots of 30 µL of plasma were performed that then were stored at -80ºC.

Simultaneously serum sample was prepared, tubes of 5 mL with gel separator were used, in which blood was allowed to stand approximately 30 minutes. The particularity of this kind of tubes is that contains clot activator that accelerates coagulation and removes fibrinogen. Then a centrifugal force of 2000*g*, during 15 minutes, at 8ºC was applied, and the supernatant was collected and resuspended in a tube of 5 ml. For this work, aliquots of 30 µL of serum were also stored at -80ºC.

2.2. MIR spectral acquisition

Samples of plasma/serum were thawed at room temperature and vortexed for ~8 seconds immediately before spectroscopic analysis. Spectra were acquired with a Perkin-Elmer Spectrum BX FT-IR^{TM} spectrometer in the range of 4000-900 cm^{-1}, at resolution of 8 cm^{-1} with 64 co-added scans. During acquisition, room temperature and humidity were kept at ± 25ºC and ± 37% respectively.

For spectral acquisition by drying kinetics the acquisition of background single beam was performed against air (with the empty crystal). Then, 8 µL of plasma/serum were placed on the ATR crystal (diamond crystal). In this method, the liquid is simply poured onto the crystal that should be fully covered. The drying time was achieved and established after approximately 40 minutes that correspond to the acquisition of 16 consecutive spectra.

For the arithmetic subtraction of the water spectrum it was necessary to acquire a spectrum of water, and spectra of both types of samples (plasma and serum).

Additionally two spectra (one of plasma and one of serum) were measured, using water during the acquisition of background single beam (instead the normal background against air – with the empty crystal).

3. Results

3.1. Drying Kinetics of serum and plasma

Figures 12 and 13 show typical sequences of ATR MIR spectra of serum and plasma respectively, as a function of drying time.

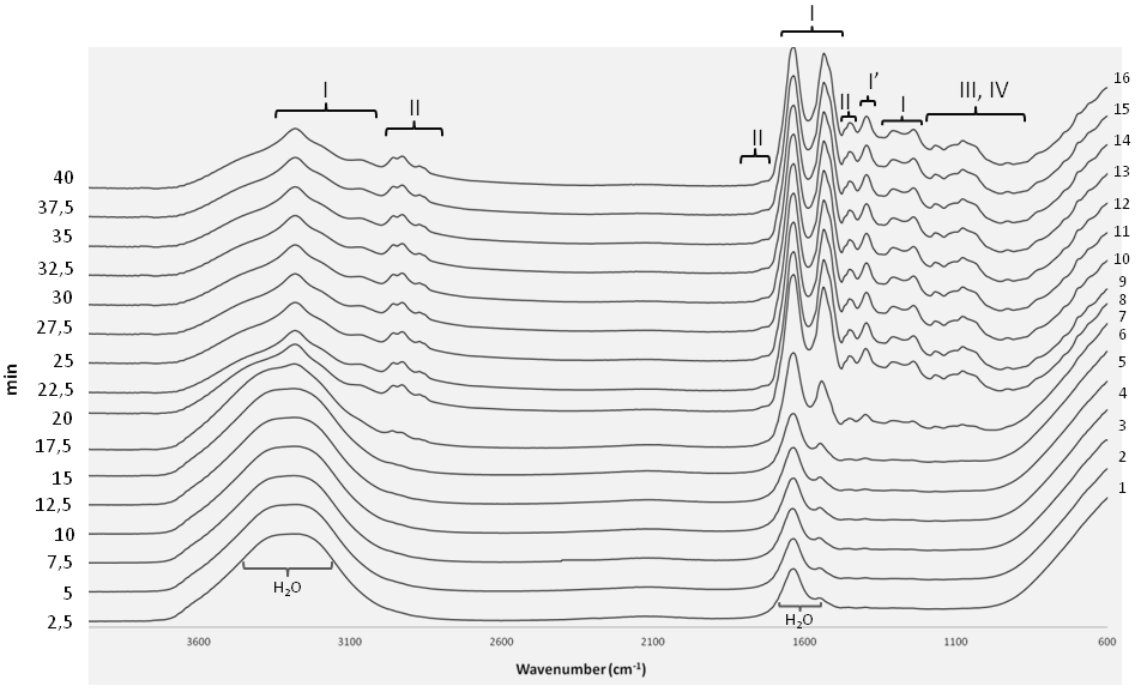

Figure 12. ATR spectra acquired during the drying process (film preparation) of a serum sample. Spectroscopic regions mainly associated with the presence of proteins (I) amino acids (I'), lipids (II), carbohydrates (III) and DNA/RNA (IV). Adapted from (110,134,135).

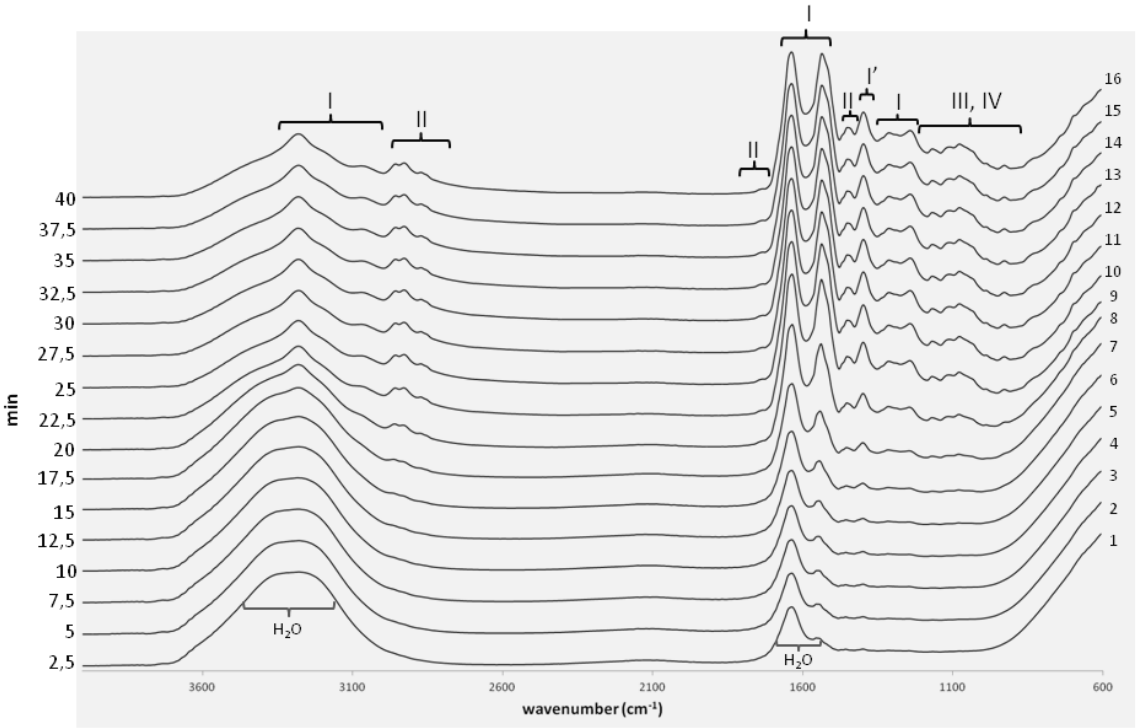

Figure 13. ATR spectra acquired during the drying process (film preparation) of a plasma sample. Spectroscopic regions mainly associated with the presence of proteins (I) amino acids (I'), lipids (II), carbohydrates (III) and DNA/RNA (IV). Adapted from (110,134,135).

For both serum and plasma samples, in the beginning (*spectra 1*), the spectra are dominated by the broad water absorption bands at 3400-3200 cm^{-1} and at 1700-1500 cm^{-1} due to O-H stretching and H-O-H bending respectively (121).

With the drying kinetics process (Figures 12 and 13) is possible observe bands that gradually become much sharper as the water evaporates, mainly in the ranges of broad water signals, corresponding to spectroscopic regions directly overlapped with H_2O vibrational modes. These spectral features correspond to vibrations of functional groups of specific solutes present in plasma/serum, mainly proteins (I) and lipids (II). There are other compounds (carbohydrates (III) and DNA/RNA (IV)) whose spectroscopic signals are not directly hidden with water signals but can be detected after the drying process (110). This is due to increase of concentration of these solutes that naturally occurs when water evaporates.

Thus, for each sample, after 40 minutes of drying process, it was possible to obtain a spectrum with more spectroscopic information and enhanced SNR whose peaks can be assigned, enabling a qualitative analysis of the sample. The dried spectra shows apparent contributions of proteins in the frequencies range of 3400-3030 cm^{-1} (135), 1720-1480 cm^{-1} (110,135) and 1301-1229 cm^{-1} (136); lipids in the range of 3020-2819 cm^{-1} (110), 1750-1725 cm^{-1} (134) and 1480-1430 cm^{-1} (110); carbohydrates and nucleic acids (DNA/RNA) in the frequencies range of 1200-900 cm^{-1}. In the latter region are also detected vibrations of some functional groups of proteins and lipids (110,134).

As showed in the Figures 12 and 13, both samples of plasma and serum give rise to a final spectrum with practically the same spectral information. However it is also perceptible that their drying patterns differ slightly. For the same atmospheric conditions (temperature and humidity), the drying of serum sample proved to be faster than the plasma sample. This can be seen in the passage of spectrum 6 to 7 of Figure 12, which contrasts with the more gradual drying of plasma sample (Figure 13). Comparing the spectra 7 of both samples, it is possible to observe that the peaks in the plasma sample are less defined, which in this case reflect a sample less dry. This small difference in the pattern of drying may be due to the fact that plasma be slightly more viscous than serum, due to presence of fibrinogen and other compounds absent in serum (137). This higher viscosity can be associated with higher intermolecular forces that slow down water evaporation.

Applying principal component analysis (PCA) to compare the 16 spectra of the same sample it is possible to ensure that drying was complete and, to identify the identical spectra (Figure 14).

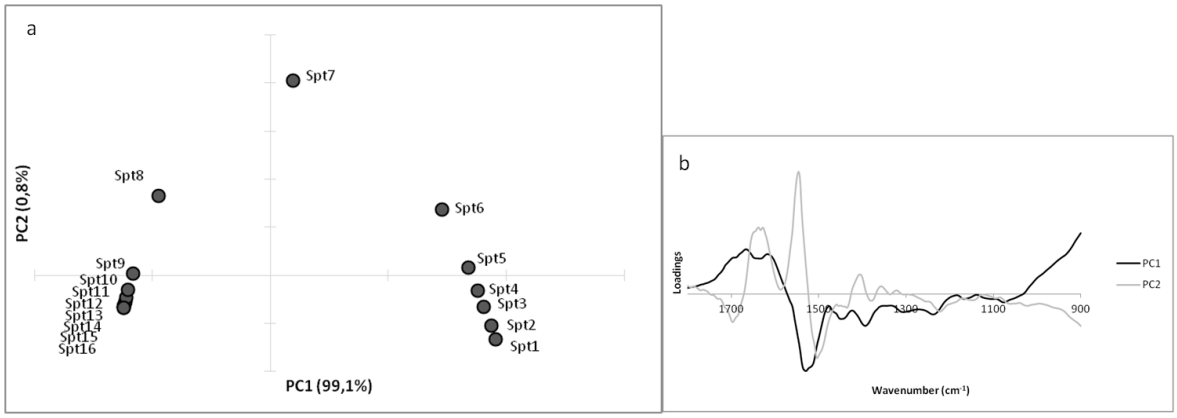

Figure 14. PCA scores (a) and loadings (b) of 16 spectra of one sample obtained by dry kinetics. Spt: Spectrum

The distribution of samples in PCA enables visualize that the last spectra are very close to each other. This allows confirming that little, or none, differences occur between them, and thus it is reached the maxim stability of samples. The last three spectra (*spectra 14, 15* and *16*) were completely dry and do not compromise the reproducibility. These will be selected to be later used in multivariate analysis at Chapter 3.

3.2. Comparison of different methods to minimized water signals of plasma and serum samples

Figures 15 and 16 show ATR MIR spectra of serum and plasma, respectively, obtained by three possible ways of minimizing water contribution. The first method consists in the arithmetic subtraction of water to sample spectrum (*spectrum 3)*, the second method uses pure water in the acquisition of the background single beam which is later used to make the ratio with sample single beam (*spectrum 2*), and the third process is based in obtained after drying kinetics of a drop of sample (*spectrum 1*).

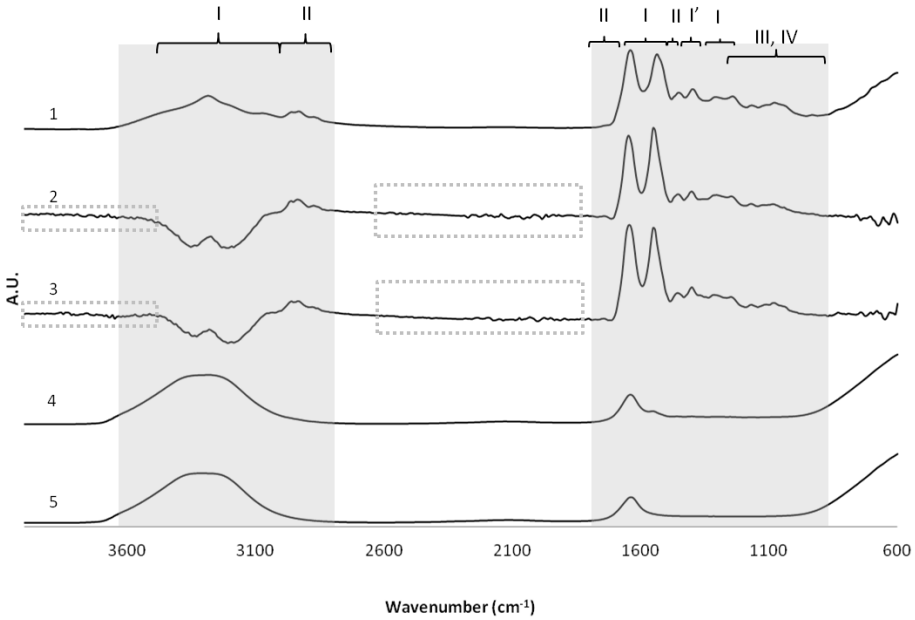

Figure 15. Comparison of the effect of 3 different methods to minimize water signals of a serum sample. 5) Water spectra; 4) Row serum spectrum; 3) Spectrum resulting from the arithmetic subtraction of the water spectrum (5) to serum spectrum (4); 2) Spectrum obtained after the acquisition of background single beam with water; 1) Typical serum spectrum after drying kinetics. Shaded regions contain spectral information of interest, and dashes indicate regions with noise. Regions mainly associated with the presence of proteins (I), amino acids (I'), lipids (II), carbohydrates (III) and DNA/RNA (IV); A.U – Arbitrary units. Adapted from (110,134,135).

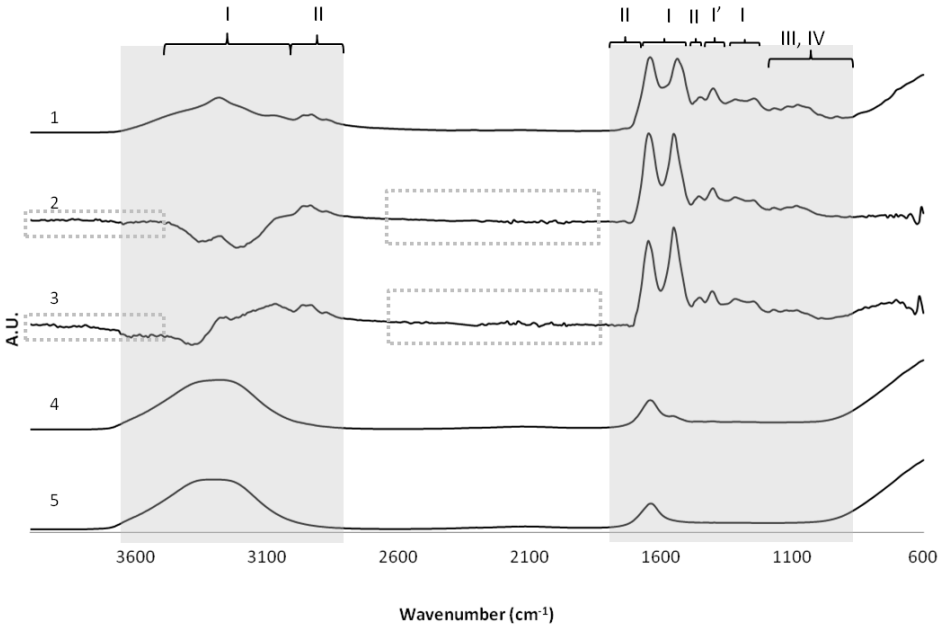

Figure 16. Comparison of the effect of 3 different methods to minimize water signals of a plasma sample. 5) Water spectra; 4) Row plasma spectrum; 3) Spectrum resulting from the arithmetic subtraction of the water spectrum (5) to plasma spectrum (4); 2) Spectrum obtained after the acquisition of background single beam with water; 1) Typical plasma spectrum after drying kinetics. Shaded regions contain spectral information of interest, and dashes indicate regions with noise. Regions mainly associated with the presence of proteins (I), amino acids (I'), lipids (II), carbohydrates (III) and DNA/RNA (IV); A.U – Arbitrary units. Adapted from (110,134,135).

In the Figures 15 and 16, it was possible observe that water (*spectra 5*) clearly dominates the overall spectra of plasma/serum samples (*spectra 4*). This justifies the need to eliminate the water signal for further spectral interpretation.

With all of the 3 methods tested, after water removal, several bands that are absent in the *spectra 4* of both samples became visible. After water peaks elimination it is possible to identify typical peaks of the major component groups (proteins (I), lipids (II), carbohydrates (III) and DNA/RNA (IV)) present in plasma and serum samples. Although it has been shown that *spectra 1*, *2* and *3* have almost equivalent information, *spectra 1* was the unique spectra that has spectroscopic information in all spectral range (4000 – 600 cm^{-1}) and has most intense and defined peaks in region of 1800 – 900 cm^{-1}.

Moreover, the quality of baseline found in the *spectra 1*, is not observed in the *spectra 2* and *3.* In fact these spectra are noisier than *spectra 1* as it can be observed in the regions of 4000-3400 cm^{-1} and 2300-1800 cm^{-1}, highlighted by dashed rectangles in the Figures 15 and 16.

In the regions between 3500 and 3000 cm^{-1} in *spectra 2* and *3* are observable negative peaks due to the excessive subtraction factor used, showing the subjectivity of these methods in the removal of the water contribution.

Apart from the apparent less subjectivity, the drying kinetics method, even time consuming, requires less computational manipulations and the obtained spectra present better SNR than the obtained from the methods 2 and 3 that at the first glance would be more desirable because they are faster to acquire.

4. Conclusion

With drying kinetics it was found a methodology to eliminate the spectral contribution of water, maintaining a reasonable signal-to-noise ratio.

This methodology allows the optimization of the experimental design. That is, by simply allowing water to evaporate from the sample, whereas spectra are being acquired, it is possible observe changes in spectroscopic signals over time, ensuring that the last spectrum obtained reached a constant drying stage. This information is not possible to obtain with the acquisition of a single spectrum of the film at the end of the drying process.

Indeed, the process based in the drying kinetics of a drop of sample proved to be better to minimize water contribution in all MIR spectral range than methods of subtraction of water from

a direct sample spectrum. For this reason, this was the chosen method for the acquisition of the spectra analyzed in Chapter 3.

Chapter 3

I. Methods of study

1. Study group

Inclusion criteria for the study group were: age between 50-90 years, resident in the Aveiro region, with complaints including objective memory impairment or other cognitive complains. The exclusion criteria were if individuals undergoing chemotherapy or radiotherapy, psychiatric illness such as bipolar disorder, schizophrenia, and the use illicit drugs.

The cognitive evaluation of individuals was carried out at several Centers for Primary Health Care in the Aveiro region. The project was approved by the ethics committee of the Regional Health Center - Coimbra, protocol number 012 804 of April 4, 2012.

The Clinical Dementia Rating scale (CDR) (138,139), the Mini-Mental State Examination (MMSE) (140), and the Geriatric Depression Scale (GDS) (141,142) were the cognitive testes applied to the study group.

The CDR scale: 0 indicates normal function; 0.5 indicates a transition level (termed questionable dementia); 1.0 indicates significant loss (almost always a clear correlation with dementia); 2.0 indicates loss of moderate cognitive function; 3.0 indicates severe loss. For this study cognitive dysfunction was considered when CDR ≥ 0.5.

The MMSE test permits patient stratification according to the education level: cutoff of 22 for 0-2 years schoolarship; 24 for 3-6 years; and 27 for more than 7 years (143). Additionally, clinical routine questions were included to address other possible neurological pathologies.

All depressed individuals were excluded using the GDS scale. The GDS (141,142) consists of 15 questions, to survey for symptoms suggestive of depression, in which individuals with 0-5 positive questions were considered normal.

According to the cognitive evaluation, 17 individuals were subdivided in 3 groups (Table 5): the age and sex matched control group (negative for the 3 tests); the putative AD group (positive for CDR and MMSE scales, negative for GDS and other neuropathologies) and the other neuropathologies group (which includes two individuals with other pathologies or mixed disease and therefore also positive for CDR and MMSE scales).

Table 5. Characterization of study subjects according to MMSE and CDR scores.

Sex	Age	COD	MMSE (score)	Cognitive impairment		Condition
				MMSE	CDR	
F	49	C3	30	-	-	Control
F	72	C5	30	-	-	Control
F	72	C7	30	-	-	Control
F	75	C8	29	-	-	Control
F	75	C2	24	-	-	Control
F	78	C4	28	-	-	Control
M	74	C9	30	-	-	Control
M	82	C1	30	-	-	Control
F	49	D3	23	+	+	Putative AD
F	72	D7	23	+	+	Putative AD
F	74	D5	17	+	+	Putative AD
F	74	D8	21	+	+	Putative AD
F	80	D4	24	+	+	Putative AD
M	74	D9	14	+	+	Putative AD
M	83	D1	24	+	+	Putative AD
F	76	D6	14	+	+	Other neuropathology
F	76	D2	20	+	+	Other neuropathology

2. Blood samples collection and preparation

The serum and plasma preparation followed the same procedure stated in Chapter 2 (pg. 43-44).

3. Biospectroscopy procedure

After sample preparation, the spectra were obtained by mid infrared spectroscopy. Then, data underwent multivariate analysis to its classification (infer discrimination between putative AD and controls) and interpretation (identification of relevant spectroscopic regions and corresponding assignments to chemical functional groups).

3.1. MIR spectral acquisition

Each spectral acquisition was performed by drying kinetics as stated in Chapter 2 (pg 44). For each sample, a total of three independent aliquots (replicates) were recorded. Between determinations, the crystal was carefully cleaned with water.

The temperature and humidity were always controlled and, when it recorded inappropriate conditions, the spectra were not acquired. In addition, replicas with discrepant values were

removed from the analysis, which led to the final analysis of only a replica. Thus the acquisition of three replicates increased the confidence of results, ensuring every eventuality uncontrollable.

3.2. Data multivariate analysis

Multivariate analysis methods were used in order to extract information from spectra, and to assist in biomedical interpretation. Chemometric methods are diverse and offer different approaches to gather specific information from the measured data (Figure 17).

Multivariate methods can be divided into techniques of multivariate classification (or pattern recognition techniques) and of multivariate regression. Techniques of multivariate classification can be divided in unsupervised and supervised learning procedures. In unsupervised pattern recognition techniques such as principal-component analysis (PCA) and cluster analysis (CA), no *a priori* knowledge about the training set samples (spectra) is required. These methods are used to look at the "natural" differences and similarities between spectra. By contrast, supervised pattern recognition techniques such as linear discriminant analysis (LDA) and artificial neural networks (ANNS) require some *a priori* knowledge, e.g. clearly identifying samples from disease cases versus samples from healthy cases. In this way, supervised procedures allow for a more precise classification within the class boundaries, whilst unsupervised methods are useful for an exploratory analysis of data (83,144).

On the other hand, multivariate regression techniques (or multivariate calibration methods), are frequently applied to analyze one or multiple constituents in a complex sample that are subject to significantly overlapping analytical signals. Among these techniques are principal components regression (PCR) and partial least squares regression (PLS) (Figure 1)(145).

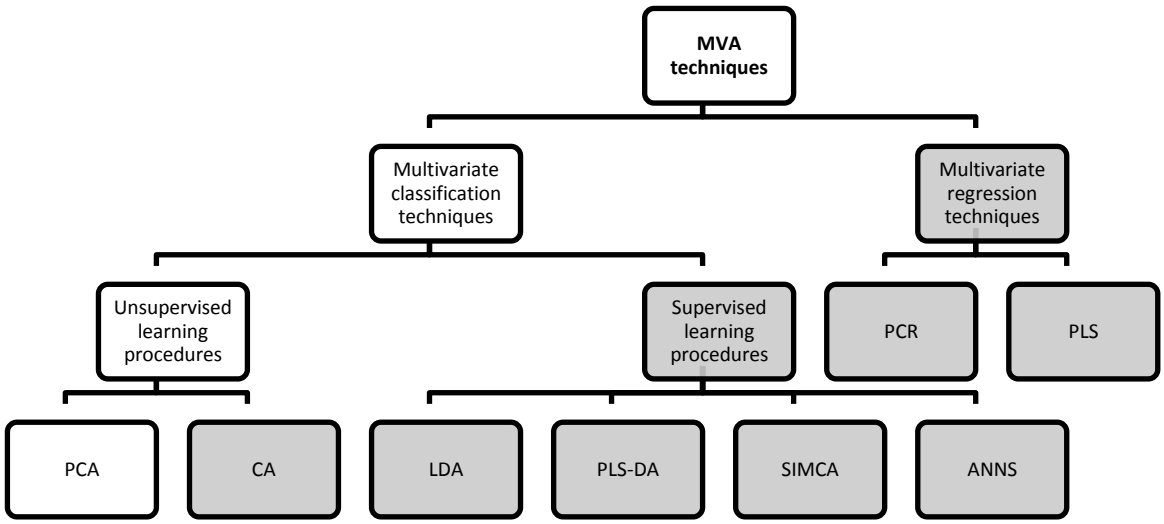

Figure 17. Most frequently applied multivariate data-analysis techniques in combination with MIR spectroscopic methods. MVA: Multivariate data analysis; PCR: Principal component regression; PLS: Partial least-squares regression; PCA: Principal-component analysis; CA: Cluster analysis; LDA: Linear discriminant analysis; PLS-DA: Partial least-squares discriminant analysis; SIMCA: Soft independent modeling of class analogy; ANNS: Artificial neural networks. Adapted from (144).

In this work, PCA is applied to the FTIR-ATR spectra, to find out if the spectral profile of AD group has some differences to the spectral profile of control group. In addition, some differences and similarities between plasma and serum samples will be discussed.

3.2.1. PCA analysis

Previously to multivariate analysis, as stated in Chapter 2, the three last spectra of one replicate of each sample were selected and were transferred through JCAMP-DX format into the data analysis software developed in the Institut National Agronomique Paris-Grignon in collaboration with the University of Aveiro (146).

Principal Component Analysis (PCA) was applied to the mid-infrared spectra of plasma and serum samples in order to extract the main sources of variability. PCA was applied to several spectral regions according to some metabolic characteristics related with Alzheimer's pathology that are possible identify with FTIR spectroscopy (Table 6), at ranges of 3600–3000, 1800–900 and 1200–900 cm^{-1}. The region at 875-820 cm^{-1} was not analyzed, since at this specific region the spectra were noisy and results would not be credible. Standard Normal Variate (SNV) was the pre-treatment applied to all spectral regions; the data set was auto-scaled, to put all of the spectra to the same scale (standardize) and increase the differences between they (divided by the standard

deviation). In this work was not used derivative processing since makes loadings interpretation difficult and may undermines the confidence of results.

Table 6. **Spectral regions according to some metabolic characteristics related with Alzheimer's pathology.**

Studied regions (cm^{-1})		Specific bands (cm^{-1})	Assignment	Metabolic characteristics of AD	Refs
3600-3000		**3600-3100**	O–H stretching of hydroperoxyl groups	Lipid oxidation	(147)
		3100-3000	C=C-H indicative of unsaturation (olefinic band)	Lipid oxidation	(148)
1800–900		**1750-1725**	C=O stretching absorption band	Lipid oxidation (aldehydes, ketons and carboxylic acids)	(147)
		1700-1600	Amide I band	Amyloid β-sheet structures (changes in the amide I band)	(74)
	1200-900	**1300-1151**	Asymmetric PO_2^- stretching vibrations	Signaling alteration Phosphorylation of carbohydrates and proteins	(149)
		1149-980	Symmetric PO_2^- stretching vibrations		
		1000-800	C-O stretching of nucleic acids sugars	DNA/RNA oxidation Changes in the DNA/RNA backbone	(150)
		980-950	C-C stretching of DNA backbone		
		875-820	DNA S-type sugar puckering modes	Epigenetic alterations DNA methylation (in cytosines)	(151)

II. Results and discussion

1. Spectral analysis

1.1. Results

Figures 18 and 19 show spectra of all samples of serum and plasma, respectively.

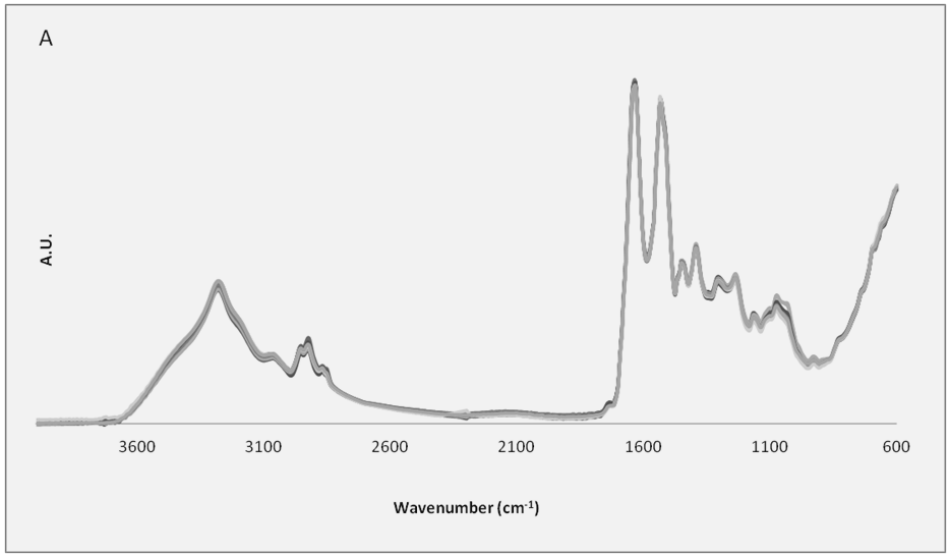

Figure 18. Spectra of all serum samples of putative AD patients and controls, obtained after drying kinetics. A.U – Arbitrary units

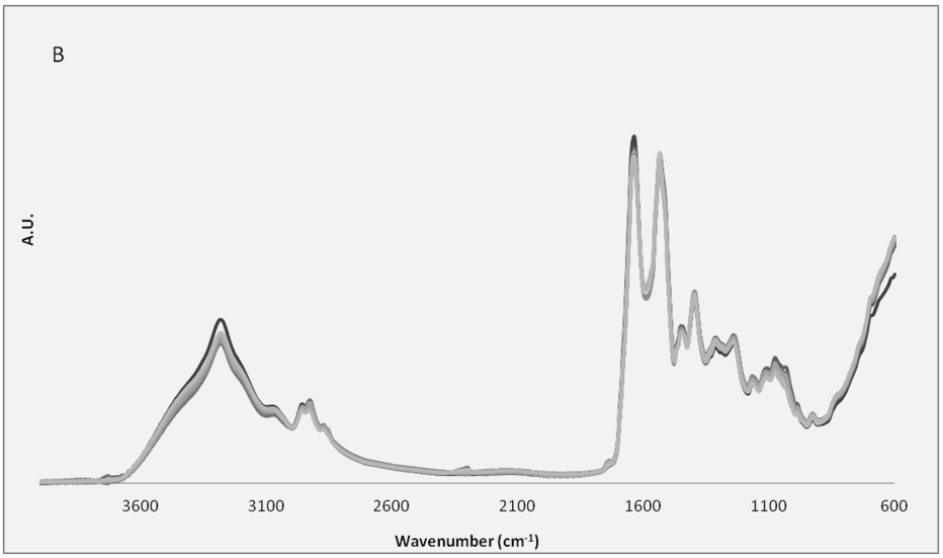

Figure 19. Spectra of all plasma samples of putative AD patients and controls, obtained after drying kinetics. A.U – Arbitrary units

At first glance the spectra appear to be very similar, where it is possible to verify that all spectra overlap, without revealing major differences.

Figure 20 shows four representative spectra obtained after drying kinetics: two spectra of serum – one is of a control subject and the other is of a putative AD patient (*spectrum 1* and *2*, respectively); and two spectra of plasma – one is of a control subject and the other is of a putative AD patient (*spectrum 3* and *4*, respectively). The region at range of 1800-800 cm^{-1} of the spectra was expanded in order to better assign the bands of this region rich in information.

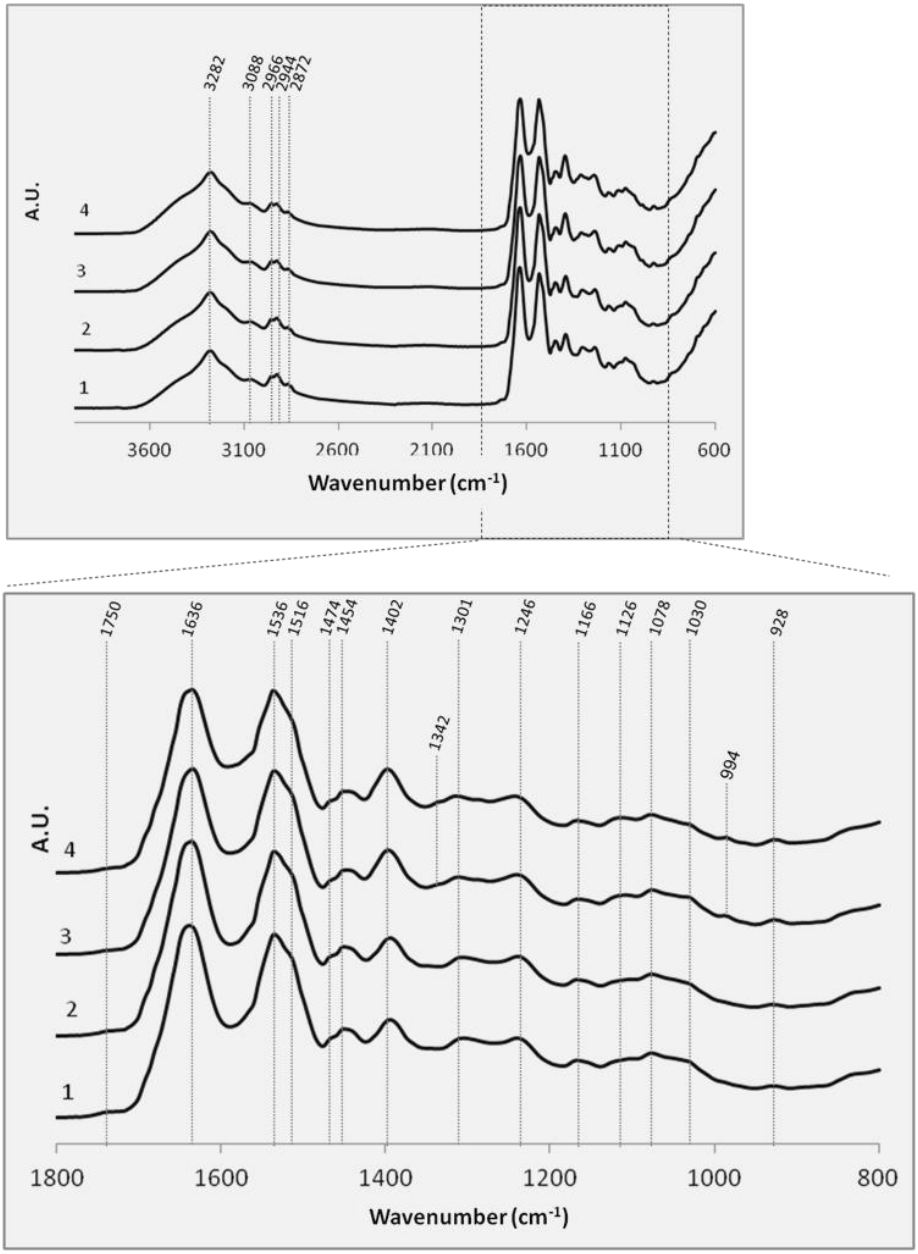

Figure 20. 4000-600 and 1800-800 cm^{-1} regions of the FTIR spectra of serum and plasma samples. Serum spectrum of a control subject (spectrum 1); Serum spectrum of a putative AD patient (spectrum 2); Plasma spectrum of a control subject (spectrum 3); Plasma spectrum of a putative AD patient (spectrum 4). A.U. – Arbitrary units.

The four spectra represented at Figure 20 are very similar amongst them, being impractical infer about differences between the control sample and putative AD sample. However it is possible try to do the assignments of peaks related with several contents of the serum/plasma. Furthermore, in the figure it is possible verify two peaks in both plasma spectra (~1342 and ~994 cm^{-1}) that are not present in serum spectra.

1.2. Discussion

Overall spectra appearance: Since the samples are complex mixtures of several compounds with multiple functional groups, the overall spectra appearance shows to be complex. This complexity often results in several possible assignments of functional groups to the same peak, hindering the unequivocal interpretation of spectra. The assignments of bands of Figure 20 were made resorting to some group frequency tables (110,120,121,134,152,153). The major content assignments for serum and plasma FTIR spectra absorption bands are indicated in Table 7, wherein the possible assignments of functional groups are displayed.

Table 7. Spectral assignments of plasma and serum samples.

Bands (cm^{-1}) of spectra of plasma and serum	Major assignments for plasma and serum contents	
	Assignments	Contents
~ 3282	N-H stretching	Proteins (Amide A)
~ 3088	N-H stretching	Proteins (Amide B)
~ 2966	C-H asymmetric stretching of CH_3 group	Lipids (cholesterol esters, triglycerides)
~ 2944	C-H asymmetric stretching of CH_2 group	Lipids (long chain fatty acids, phospholipids)
~ 2872	C-H symmetric stretching of CH_3 group	Lipids (long chain fatty acids, phospholipids)
~ 1750	C=O symmetric stretching	Lipids (cholesterol esters, triglycerides)
~ 1636	C=O stretching and N-H in plane bending	Proteins (Amide I)
~ 1536 and ~ 1516	N-H in plane bending and C-N stretching	Proteins (Amide II)
~1474 and ~1454	C-H asymmetric bending of CH_3 group / C-H bending of CH_2 group	Lipids (fatty acids,phospholipids, triglycerides)
~1402	COO^- stretching	Amino acids side chains
~1342*	CH_2 wagging	Collagen
~ 1301 and ~ 1246	N-H bending and C-N stretching	Proteins (Amide III)
1200-900	C-O-C, C-O, C-C, C-O-P, P-O-P vibrations	DNA, RNA, carbohydrates, lipids and proteins
~ 994*	C-O ribose, C-C	Ribose

** only present in plasma*

Amide vibrations of proteins: The protein backbone shows nine vibrational modes, which result in nine fundamental absorption bands specific for proteins, including amide I, II, III, IV, V , VI and VII, amide A, and amide B modes (136). The amide IV-VII bands have very low intensities in MIR and are not of importance in MIR analyses.

The two very strong prominent amide absorptions one at ~1636 cm^{-1} essentially due to C=O stretching coupled with little in plane N-H bending (less than 20%), and another at ~1536 cm^{-1}

due to in plane N-H bending (40-60% of the potential energy) and C-N stretching (18-40%), corresponds to Amide I and Amide II bands, respectively (136). These two characteristics vibrational modes of proteins are only determined by the secondary structure adopted by the polypeptide chain, reflecting the backbone conformation and hydrogen-bonding pattern. The amide I band frequency at ~1636 cm^{-1} is assigned to β-sheet conformation of proteins. The correlation between secondary structure and frequency of amide II is less simple than for the amide I vibration. The slight peak at ~1516 cm^{-1} is also due to Amide II of proteins that have other conformation than those with vibrations at ~1536 cm^{-1} (136). Secondary structure is also difficult assign to amide III perceptible at peaks of ~1301 and ~1246 cm^{-1} attributed to N-H bending and C-N stretching (135,136).

After water evaporation, hydrogen-bonded amino groups can dominate the region between 3400 and 3250 cm^{-1}, wherein the NH stretching vibration gives rise to the amide A band at ~ 3282 cm^{-1}. The weaker band at ~3088 cm^{-1} from apparent amide B (3100-3030 cm^{-1}) is commonly reported as being either an overtone of amide II (NH bend) or a combination mode of amide I and amide II that interacts with the strong NH, acquiring enough intensity to be observable through a Fermi resonance (FR), resulting in two bands (amide A and amide B) (120,154).

CH_2 and CH_3 vibrations: The presence of lipid compounds is suggested by the peaks at ~2966 and ~2872 cm^{-1} due to CH asymmetric and symmetric stretching of methyl group respectively, and peak at ~2944 cm^{-1} assigned to CH asymmetric stretching of methylene group. Moreover, the bending vibrations of the same hydrocarbons groups are visible at ~1474 and ~1454 cm^{-1}, also supporting the mainly presence of lipids (110,152,153).

C=O vibrations: The weak band at ~1750 cm^{-1} is most likely related with carbonyl compounds absorptions (1750–1725 cm^{-1}) and is probably related with a simple carbonyl compound, such as a ketone, an aldehyde, an ester, or a carboxylic acid of lipids (110,152).

COO^- vibrations: The band at ~1402 cm^{-1} is attributable to COO^- stretching and also suggests the presence of amino acids in plasma and serum (110,155).

***"Fingerprint region"(1200-900 cm^{-1})*:** Bands at region of 1200-900 cm^{-1} are due to C-O-C, C-O, C-C, C-O-P, P-O-P vibrations of DNA, RNA, carbohydrates, lipids and proteins (156). Some substances at this region present some specific signatures that enable its rapid identification, so it is also called fingerprint region. In complex mixtures such as serum/plasma these features are

very difficult to observe, and the undoubted assignment of bands is often impractical, occurring by deduction.

In all spectra is possible to visualize the probable contributions of lipids, proteins, amino acids, carbohydrates and small molecules of low abundance present in plasma and serum samples. Moreover, it is observable slight differences between plasma and serum spectra at ~1342 and ~994 cm^{-1}. These bands are only observable in plasma samples. The weak band at ~1342 cm^{-1} is maybe due to CH_2 wagging of collagen (134). Collagen is an abundant protein present in endothelial layer of blood vessels and, when vessels are damaged for example due to needle prick during blood collection, collagen is exposed to flowing blood. Collagen is thought to function as a substrate for the adhesion and activation of platelets and also initiates the clotting process by activating Hageman factor (factor XII of coagulation). Both the activation of platelets and the activation of factor XII lead to thrombin generation, which converts fibrinogen into fibrin and that constitute the blood clot (157). Since that serum is the fraction of blood collected after the clotting factors being allowed to act, it has no collagen and other proteins because they are removed in clot. The band at ~994 cm^{-1} in plasma spectra (*3* and *4*) is probably due to ring vibrations of ribose of RNA (134). RNA that is released when tissue is damage is thought to promote blood clotting. Further, it was shown large concentrations of RNA retained in the clot (128). These findings may justifies the presence of band at ~994 cm^{-1} in *spectra 3* and *4*, suggesting higher concentrations of RNA in the plasma than in serum. However, it can also be due to D-ribose vibration that is a monosaccharide essential to obtain energy, suggesting that the plasma concentrations of this monosaccharide is greater than the serum.

Although visual interpretation of the spectra allows some distinction between serum and plasma samples, it proved insufficient to distinguish between the spectrum of the control sample and the spectrum of the putative AD patient. Therefore, taken into account its ability to withdraw more information of the data, multivariate analysis was used to highlight differences between the study groups (putative AD vs control) in both samples of serum and plasma.

2. Multivariate analysis

FTIR experiments consist of the results of observations of many variables for a number of samples. Each variable may be regarded as constituting a different dimension, such that if there are *n* variables each object may be said to reside at a unique position in an abstract entity

referred to as *n*-dimensional hyperspace. This hyperspace is difficult to visualize, and the multivariate data analysis (MVA) allows reduce the data dimensionality, being possible to have a better perception of the data, with the least possible loss of information (83). PCA is probably the most widespread multivariate chemometric technique that most significantly changed the chemist's examination of spectroscopic data.

2.1. Results

The purpose of PCA analysis is verify if there are a short number of new variables – principal components (PCs) – that explain a high percentage of total variation associated with the original set, without sacrificing information relevant. This is performed through a transformation of the original data matrix with each wavenumber (variable) being a column and each spectrum (sample) a row. This transformation gives rise to two types of diagrams: diagram of factorial coordinates (scores) and diagram of factorial contributions (loadings). Scores contain information on how the spectrum relate to each other. Loadings contain information on how the wavenumbers relate to each other and, thus, justify the sample distribution along the scores diagram (116). PCs are ordered so that PC1 exhibits the greatest amount of variation, PC2 the second greatest amount of variation and so on. In this way, PCA allows as much as possible of the variance in the data set to be described by the first significant PCs, while all subsequent PCs are so low as to be virtually negligible (158).

The average spectra from each group to remove the peaks which distinguish them may mask important spectral values, which characterize certain samples. When using the PCA, this trend is eliminated because the information contained in the PCA loadings gives spectral information that allows distinguishing groups with the least possible loss of information, taking into account all samples.

PCA was applied to the spectral regions of 3600-3000, 1800–900 and 1200-900 cm^{-1}. The region at 3600-3000 cm^{-1} that could give the information related to lipid peroxidation (Table 6), showed no discrimination capable to be explained in accordance with the assumption initial. The samples are shuffled and loadings are too noisy (Figures 21 and 22).

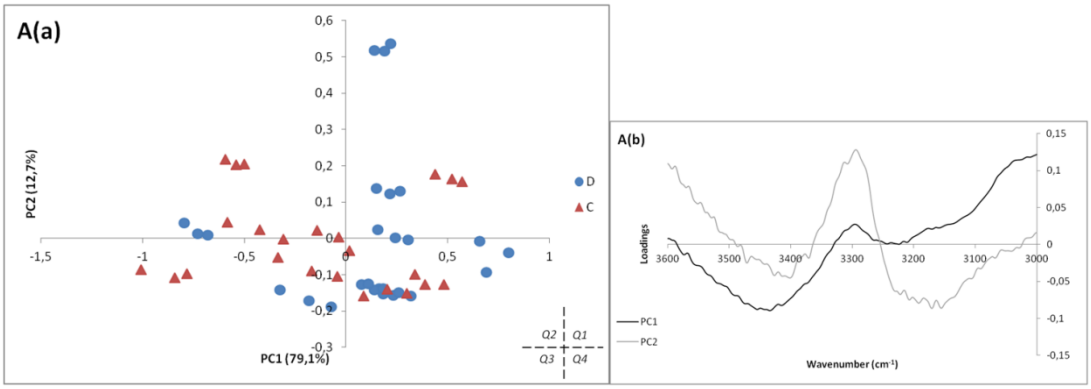

Figure 21. PCA scores (Aa) and loadings (Ab) of serum samples (3600-3000 cm^{-1} range).

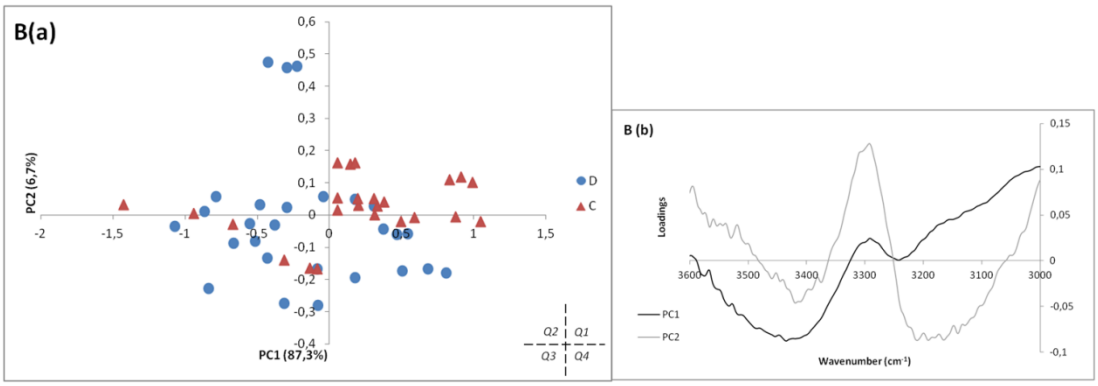

Figure 22. PCA scores (Ba) and loadings (Bb) of plasma samples (3600-3000 cm^{-1} range).

The region at 1800-900 cm^{-1} could also give relevant information (Table 6), mainly about lipid oxidation and amyloid β-sheet structures (1700-1600 cm^{-1}), as well as alterations in the backbone of DNA/RNA and nucleic acids, and phosphorylation of carbohydrates and proteins (1300-900 cm^{-1}). Figures 23 and 24 show PCA of the spectral region between 1800 and 900 cm^{-1}.

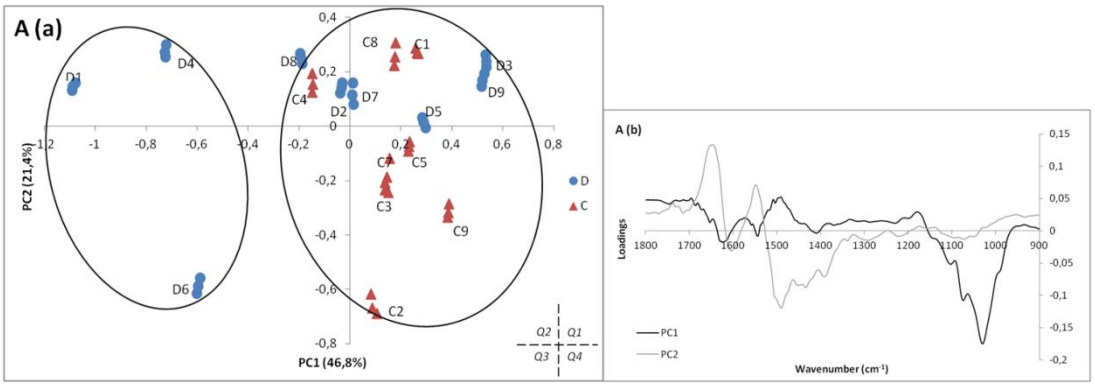

Figure 23. PCA scores (Aa) and loadings (Ab) of serum samples (1800-900 cm^{-1} range).

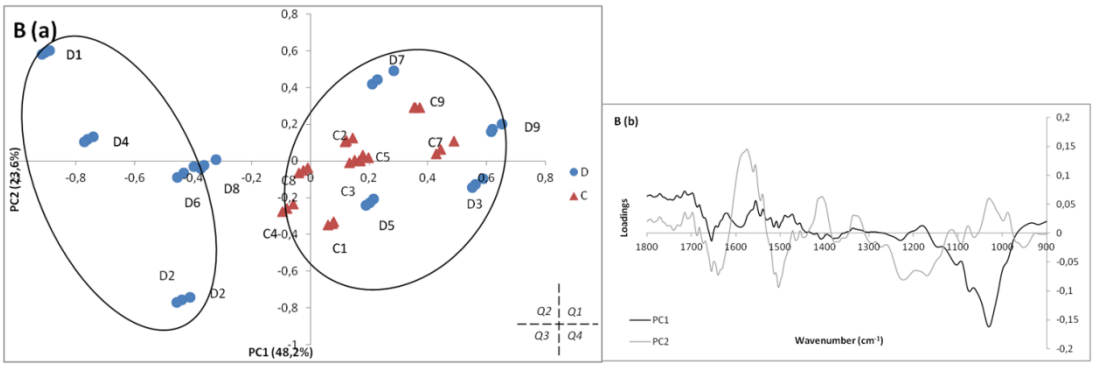

Figure 24. **PCA scores (Ba) and loadings (Bb) of plasma samples (1800-900 cm^{-1} range).**

The region at 1800-900 cm^{-1} is very information rich and shows some tendency to form two main groups, one mainly explained by the negative side of PC1 and another mainly explained by the positive side of PC1. However, the corresponding loadings profile diagram proved to be noisy (mainly in plasma samples) and complex to interpret at range of 1800-1400 cm^{-1}. In addition, the separation of groups could be better, seeming to reveal little information to the aim of the study. Therefore, it was necessary to reduce the spectral region in order to find the one that best fit with the study propose. As shown in PCA loadings, the region between 1400 and 1200 cm^{-1} has little spectroscopic information (Figure 23 Ab and 24 Bb). To the contrary, 1200 and 900 cm^{-1} region is rich in spectral information (Figure 23 Ab and 24 Bb) that can be related with carbohydrates structures, phosphate groups, and various vibrations of amino acids, which in turn can be related with some pathologic processes of Alzheimer's disease (Table 6). This specific region was also analyzed through PCA (Figure 25 and 26).

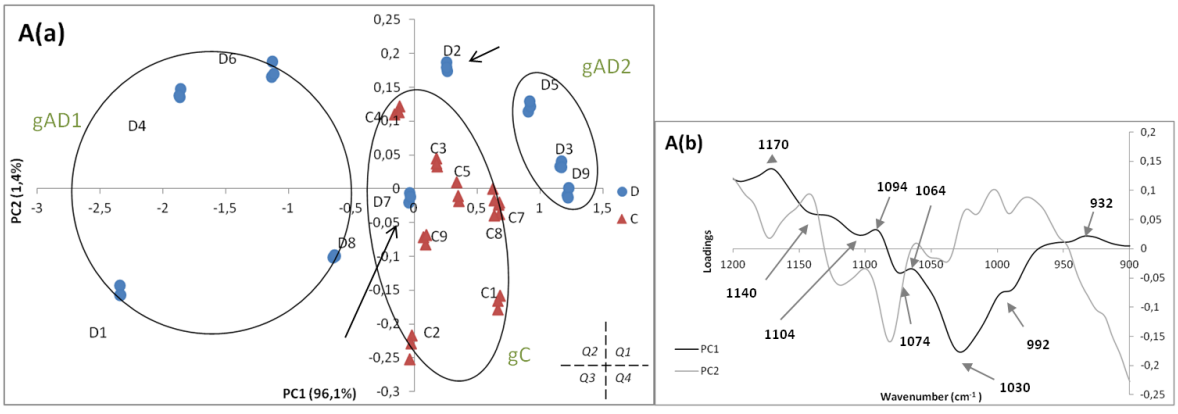

Figure 25. PCA Scores (Aa) and loadings (Ab) of serum samples (1200-900 cm^{-1} range).

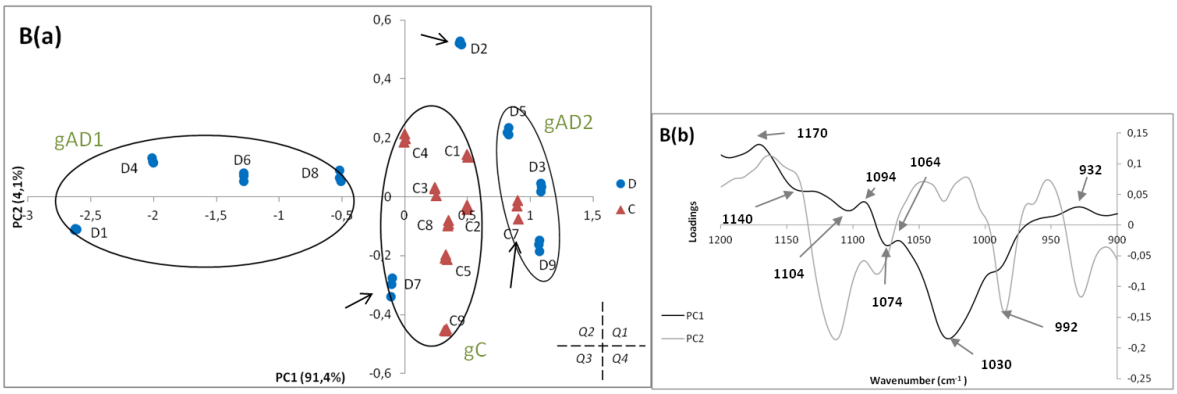

Figure 26. PCA Scores (Ba) and loadings (Bb) of plasma samples (1200-900 cm^{-1} range).

Three groups may be suggested based on the distribution of samples along PC1 that explains most the variability, and PC2, which conveys the second most important factor of the remaining analysis. Serum and plasma have practically the same information, but serum has a better discrimination.

In both serum and plasma (Figure 25Aa e 26Ba) it can be observed that one group of putative AD patients – gAD1 – is mainly distributed in Q2 and Q3 and is constituted by D1, D4, D6 and D8; another group of patients – gAD2 – is mainly distributed in the Q1 and Q4 and include D5, D3 and D9. The patient D2 seems to be an outlier, based on the analysis of both samples of serum and plasma, because it is not close to any study group. The patient D7 is located very close to controls.

The group of controls – gC – is distributed close to zero of both PCs, as a result is slightly less affected by the peaks identified in PCA loadings. Group gC is constituted by C1, C2, C3, C4, C5, C7, C8 and C9. In plasma (Figure 26Aa), the control C7 seems to be influenced by any plasma characteristics that somehow prevent its position in gC, as clearly occur in serum (Figure 25Ba).

The examination of the loadings is useful to understand the basis of the observed separation of the samples. Table 8 shows the possible assignments of the peaks selected in the PCA loadings (Figure 25Ab and 26Bb) that reflect the peculiarities of the sugar-phosphate skeleton of nucleic acids and carbohydrates.

Table 8. MIR bands between 1200 and 900 cm^{-1} range identified in PCA loadings.

Serum bands (cm^{-1})	Plasma bands (cm^{-1})	Assignments	AD group
1170	**1170**	C-OH stretching of amino acids (serine, threonine, and tyrosine)	gAD2
1140	**1140**	C-OH bonds in oligosaccharides	gAD1
1104	**1104**	C-O stretching of glucose	gAD1
1094	**1094**	Symmetric stretching of PO_2^- of phosphodiesters	gAD2
1074	**1074**	Symmetric stretching of PO_2^- of phosphodiesters	gAD1
1064	**1064**	C-O stretching of ribose	gAD2
1030	**1030**	C-O stretching of glucose	gAD1
992	**992**	C-O ribose, C-C	gAD1
932	**932**	C-O/ C-C stretching of deoxyribose	gAD2

2.2. Discussion

Group gAD1: possible coexistence of Alzheimer's disease and vascular pathology

The analysis of PCA scores shows that patient D1, D4, D6 and D8 are very close to each other. This proximity is justified by peaks at 1104 and 1030 cm^{-1} that was related with glucose vibrations (159) and peak at 1140 cm^{-1} due to C-OH bonds in oligosaccharides (160). Peak at 1074 cm^{-1} is may be due to symmetric stretching of PO_2^- (134). The other peak common to patients of this group is at 992 cm^{-1} due to ring vibrations of ribose.

Vibrations of carbohydrates suggest that they are altered in patients of gAD1 group and high levels of carbohydrates are hallmarks of DM (161). DM 2 type and AD are considered age-related diseases, and several studies report that patients with diabetes have an increased risk of developing AD (two to five times) compared with healthy individuals (40,41). Elderly patients with diabetes develop more extensive vascular pathology, which together with AD hallmarks, results in increased dementia risk (36,162). Patients D1, D4 and D6 suffer from DM, and the whole group report hypertension, which, together with advanced aging and DM, are vascular risk factors to develop degeneration in cerebral capillaries (35). This vascular damage can converge to create a cerebral hypoperfusion state – CATCH – that impairs optimal delivery of glucose needed for normal brain cell function. The outcome of this defect generates a cascade of events leading to the progressive evolution of brain metabolic, cognitive and tissue pathology that characterize Alzheimer's disease (42).

Moreover, brain insulin resistance that promotes neuro-inflammation and increased expression of Aβ, can be caused by peripheral insulin resistance due to DM 2 type, which in turn is

also correlated with increase tau hyperphosphorylation, NTFs and subsequent neurodegeneration (39). This suggests a closely relation between DM 2 type and AD.

Hyperglicemia promotes protein glycation and the gradual accumulation of AGEs (40). A glycated protein loses its function, is more susceptible to oxidative damage, and is more resistant to degradation and removal. Glycation and oxidation of Aβ convert it into an oligomeric complex with reduced susceptibility to degradation by the lysosomes. This resistance of Aβ to degradation invokes the rapid ROS generation within lysosomes leading to a lysosomal general dysfunction, which progress to mitochondrial dysfunction and subsequent neuronal death (40).

The vibrations of carbohydrates at 1140, 1104 and 1030 cm^{-1} may be due to high levels of 'free' sugars in plasma/serum, AGEs, and/or glycoxidation. The vibrations of ribose ring at 992 cm^{-1} can be due to 'free' D-ribose, an monossacaride essential to production of energy, that also participates in the proteins glycation (also called ribosylation) producing AGEs, that may be involved in cell dysfunction and subsequent cognitive impairments (163).

Oxidative stress is prominent in the onset of AD (164) due to several dysfunctional mechanisms (41). The subsequent outcome is the damage of cellular biomolecules such as lipids, proteins, nucleic acids, and sugars, leading to posterior cellular dysfunction and death (40). Structural alteration of nucleic acids affects the vibrational dynamics of these molecules. ROS, and particularly hydroxyl radical, can react with all components of the DNA molecule, causing different kinds of damage. Free radicals can directly attack phosphodiester-deoxyribose moiety, abstracting a hydrogen atom from the sugar component and yield a wide variety of products (165). Ribose vibration at 992 cm^{-1} can also be due to alterations of ribose of RNA as consequence of oxidative damage. Strand breaks and loss of phosphoric acid are also causes of ROS attack (165) and increase the degrees of freedom of the molecule (150). The vibrations of phosphate groups suggested by peak at 1074 cm^{-1} may be due to breaks in DNA/RNA backbones.

Patient D6 of gAD1 group reveals visual hallucinations at clinical evaluation suggesting the presence of dementia with Lewy Bodies. However, hallucinations are also common after mini-stocks due to vascular pathology. Indeed, its metabolic proximity to putative AD patients suggests a mixed dementia for AD and DLB or AD and vascular pathology that are both common conditions (1).

Having said this, it was shown that gAD1 have a metabolic profile consistent with clinical information, neuropsychologic tests and pathogenesis of AD that suggest a possible coexistence of AD and vascular pathology. Glycation is suggested by peaks at 1140, 1104, 1030 and 992 cm^{-1} and oxidative damage is suggested by peaks at 1074 and 992 cm^{-1}. According to our knowledge,

the absorptions related with carbohydrates in relation with AD are presented here for the first time.

Group gAD2: possible pure Alzheimer's disease

Analysis of scores demonstrated that the group gAD2 and gC are both in positive side of PC1. However, gAD2 is farther from the center axis of the PCA than group gC, so it is more strongly affected by variables that justify the disposition of samples in the positive side of PC1. Distribution of the gAD2 group is strongly justified by four peaks: 1170 cm^{-1} due to C-OH stretching of amino acids such as serine, threonine, and tyrosine (134); 1094 cm^{-1}, due to symmetric PO^{2-} stretching of DNA/RNA backbone (134); 1064 cm^{-1} due to ribose vibration (C-O/C-C) (134); and 932 cm^{-1} due to deoxyribose vibration (C-O/C-C) (134).

Among several interveners that contribute to neuronal loss and progression of damage and cognitive decline in AD, oxidative stress and signaling pathways alteration such as protein hyper-phosphorylation have received great attention by researchers (31,33,34,166,167).

The peak at 1170 cm^{-1} suggests that there are certain alterations in proteins that somehow alter their conformation, affecting the exhibitions of amino acids such as serine, threonine, and tyrosine. This conformational alteration may be due to oxidative damage of proteins or phosphorylation of proteins. A variety of AD associated proteins (APP, BACE, PS and tau) are shown to be phosphorylated (33), wherein tau has been shown to be abnormally hyper-phosphorylated at several serine/threonine residues in AD (166), and phosphorylation of serine residues in β-sheet conformation of Aβ was also proved (166). In turn, all of amino acids can be attacked by ROS, but aromatic amino acids such as threonine are highly susceptible (31). Therefore, oxidation of amino acids can be other cause of protein alteration suggested by peak at 1170 cm^{-1}.

Damage of structural backbone of DNA/RNA probably induced by ROS is suggested by peaks at 1094, 1064 and 932 cm^{-1}. Peaks at 1064 and 932 cm^{-1} may represent the alteration of sugar of nucleic acids and peak at 1094 cm^{-1} due to symmetric PO_2^- stretching may be due to strand breaks and loss of phosphoric acid.

In sum, it was shown that gAD2 have also a metabolic profile consistent with clinical information, neuropsychologic tests and pathogenesis of AD, suggesting a dementia only due to AD. The gAD2 group is highly justified by spectroscopic findings at 1094, 1064 and 932 cm^{-1} related with oxidative damage, as verified in other similar study (113), and by peak at 1170 cm^{-1}

related with protein alteration (maybe by phosphorylation or oxidation) that seems to be related with AD for the first time.

Common points of the two AD groups

Oxidative damages are suggested in both gAD1 and gAD2, which suggest that both of them are related with metabolic profiles that present oxidative stress and allow their distinction from control group.

ROS are also reactive with nucleotide bases, but vibrations of these structures are not seen in this spectral region, but between 1750 and 1300 cm^{-1} (165). The breaks of DNA can give rise to oxidized DNA bases such as 8-hydroxy-2'-deoxyguanosine (8-OHdG) (31). The high levels of 8-OHdG were found in AD plasma samples and were also related with similar spectroscopic results to those obtained here (113). In turn, RNA is more vulnerable to oxidation than DNA and levels of 8-hydroxyguanosine (8-OHG) was associated as a marker of oxidative damage to RNA (31). Indeed, significant levels of 8-OHdG and 8-OHG were found in patients with MCI (168,169), indicating that oxidative damages of DNA and RNA are early events in the pathogenesis of AD, and that in turn the FTIR may be useful to detect this early events.

Complementary analysis

Alzheimer's disease is a multifactorial disease with multiple biochemical consequences, and certain vibrations that characterize disease samples can be masked by others vibrations, thus can approximate it to the control group.

Since gAD1 disposition is affected mainly by alterations of carbohydrates and D1, D4 and D6 are diabetics, one possibility is that metabolic profile of these patients can mask some characteristics of D7, which prevents that it deviates from the control group. Thus, to test this possibility, diabetic patients (D1, D4 and D6) were removed to attenuate its interference (Figure 27 and 28).

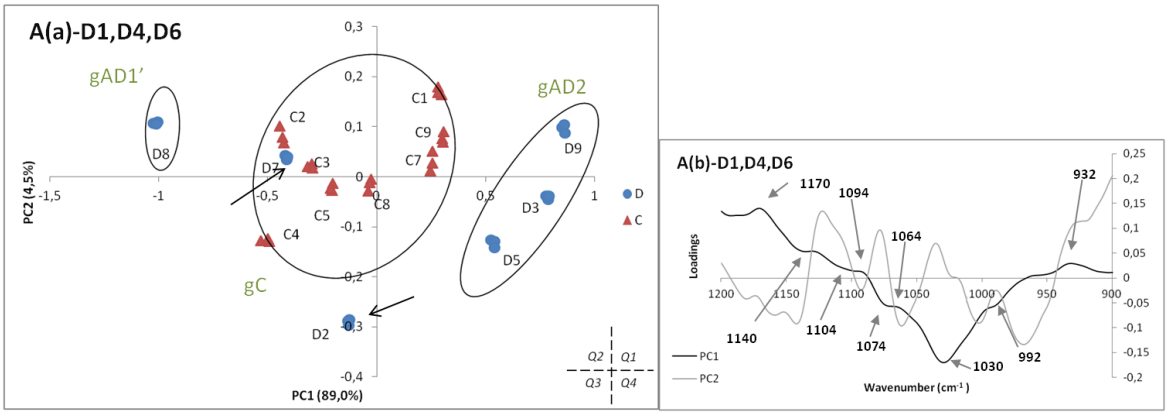

Figure 27. PCA scores (Aa) and loadings (Ab) of serum samples, without D1, D4 and D6 (1200-900 cm^{-1} range).

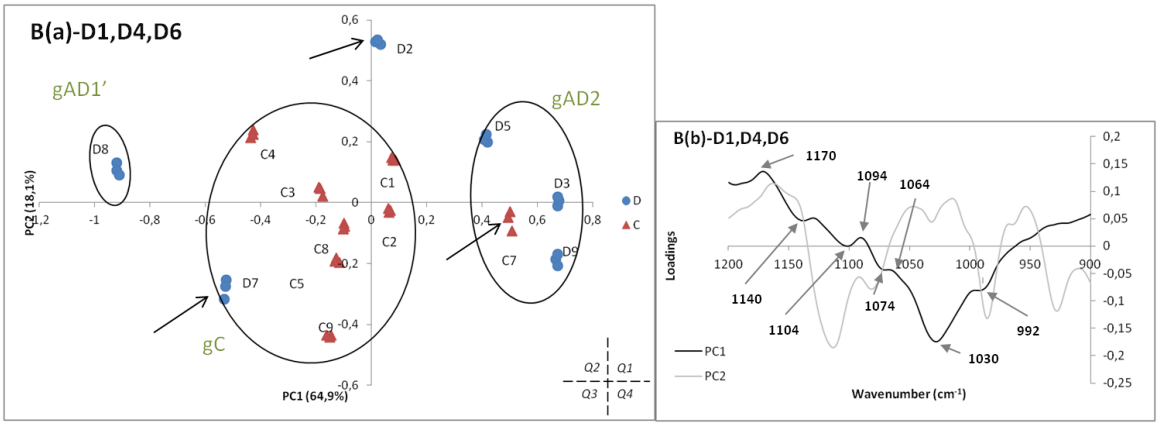

Figure 28. PCA scores (Ba) and loadings (Bb) of plasma samples, without D1, D4 and D6 (1200-900 cm^{-1} range).

With this new analysis is possible observe that three initial proposal groups and loadings profile remain the same. The disposition of patient D8 (gAD1') in PCA scores is highly justified by the same peaks of the initial gAD1 group (1140, 1074, 1030 and 992 cm^{-1}). This also suggests that these peaks highly characterize gAD1, which is associated to glycation and oxidative stress that also occurring in AD patients that are non-diabetics but have alterations in carbohydrates.

One of two things, either patient D8 (*i*) may have recent ingestion of food compared to all other subjects in study, or (*ii*) can be a pre-diabetic. First situation suggest that carbohydrates profile can mask peaks that justify AD presence in gAD1 and only signals of carbohydrates due to its high concentration are present. This hypothesis has to be considered, since it was not possible to have biochemical information and volunteers are not necessarily fasting. However it is very remote, since it is unlikely that only the patient D8 has high carbohydrate levels due to recent ingestion of food. The last situation supports the possibility of a relation between AD, DM and hypertention – coexistence of AD with vascular pathology – because D8 is a putative AD with hypertension and is close to diabetic patients.

An obvious distinction between gAD2 and control group is also shown in Figure 27, this distribution is justified by the same peaks (1170, 1094, 1064 and 932 cm^{-1}) indicating that this group is highly affected by oxidative stress and/or protein phosphorylation.

Moreover, given its permanent proximity to controls, the patient D7 is either a putative AD patient influenced by other wavenumber profile or a probable false positive to AD. Finally, this new analysis allows seeing that patient D2 is clearly an outlier.

Regarding to D2, it is suggested to be a probable patient with PDD or DLB, since he reveals Parkinsonism and hallucinations at the clinical evaluation. In addition, its spectral information is not close to any group. This evidence suggests that this patient is characterized by other peaks other than those characterizing the groups of putative AD. In order to test little influence of D2 in results, he was removed to the study (Figure 29 and 30).

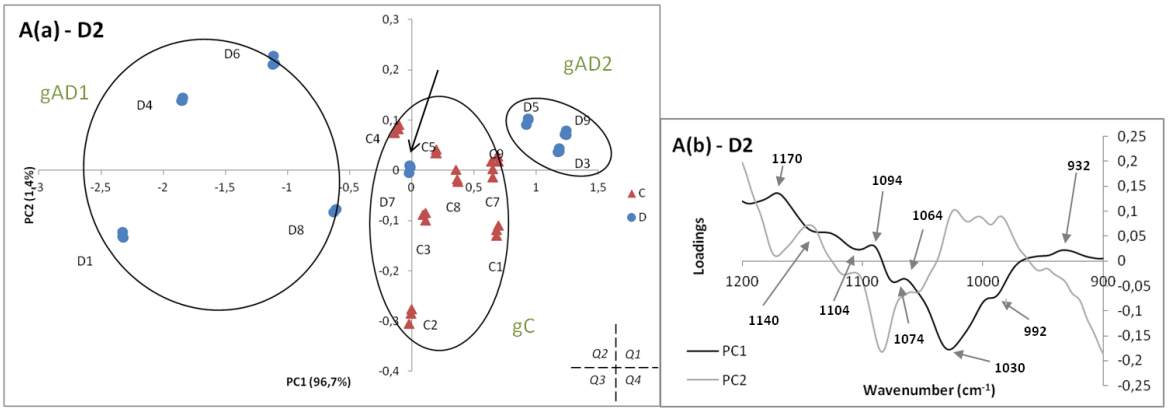

Figure 29. PCA Scores (Aa) and loadings (Ab) of serum samples, without D2 (1200-900 cm^{-1} range).

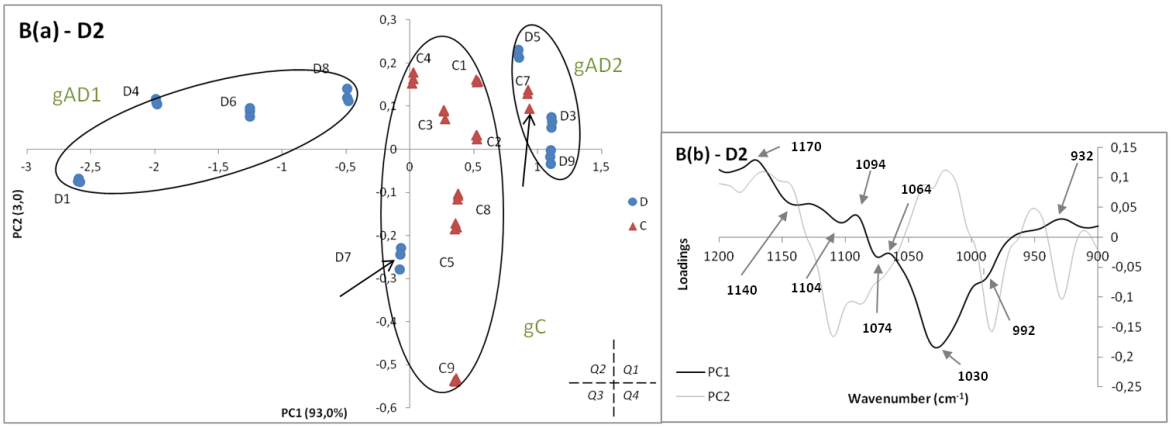

Figure 30. PCA Scores (Ba) and loadings (Bb) of plasma samples, without D2 (1200-900 cm^{-1} range).

Comparing this new analysis with Figures 25 and 26, it is possible to show that, in both plasma and serum, gAD2 has now less intra-class variability, which suggests that D2 adds a little variability to the gAD2. However, in general, the D2 not hides nor the loadings or the scores, so the peaks that justify each AD group are the same.

III. Conclusion

It was established conditions of analysis for serum and plasma samples. Using FTIR spectrometer at resolution of 8 cm^{-1} with 64 co-added scans to the spectral acquisition and resorting to drying kinetics to the water removal it was possible obtain spectra with reasonable SNRs, which allowed good spectral interpretation and subsequent multivariate approach. The drying time was achieved after 40 minutes with little amount of sample (8 µL), in atmospheric controlled conditions.

With direct analysis of spectra it was possible identify the main bands of spectra of serum and plasma between 4000-600 cm^{-1}. Although this analysis allows some distinction between serum and plasma samples, proved to be insufficient to distinguish the spectra of the control samples of the spectra of putative AD patients. This is due to intrinsic complexity of biological samples that result in several overlaps of absorptions of the main biomolecules, in IR spectra. Therefore, to draw out the significant and nonredundant information contained in these highly dimensional data is required the support of an appropriate multivariate analysis approach.

Multivariate analysis of data highlights differences between putative AD patients and controls matched by age and sex. In fact, with both serum and plasma, three groups were suggested by PCA scores analysis in range of 1200-900 cm^{-1}. PCA loadings profile revealed biochemical modifications in serum/plasma of putative AD patients probably related to oxidative stress according to other similar studies, protein alteration maybe by phosphorylation or oxidation and glycation that seems be suggested for the first time. In addition, results also suggest that other neuropathological conditions, either in a mixed condition with AD (gAD1) or not (D2), may have different profiles than pure AD (gAD2). With effect, the results showed that identification of functional groups maybe associated to biomarkers is only suitable with a combination of spectroscopy and of multivariate analysis.

The information obtained from plasma and serum is quite similar, with no large differences both in scores and in loadings. Serum scores scatter plot provide better discrimination between

putative AD and control samples and loadings profile plasma does not provide additional spectroscopic information that may lead to the identification of biomarkers. Serum proved to be more suitable for a further study.

Although the small sample size has limited the biological relevance of the results, this qualitative data served effectively as a first step to more intensive and targeted confirmatory experiments in the future.

This pilot study showed that dry serum/plasma samples, with posterior IR spectroscopic analysis and PCA are an interesting routine of methods for AD evaluation. In turn, IR spectroscopy reveals to be a potential multi-biomarker technique to a rapid diagnosis of AD, even in early states of cognitive impairment. It was proved to be very convenient because is reagent free, requires small amount of samples, is cost effective, simple to perform, provides real time results and, with proper customization, do not need of highly qualified technician.

IV. Limitations and future remarks

This pilot study, with such as promising results, needs to be continued. It is imperative to increase the data set and to build a robust AD classification model that should be validated with an independent and unequivocally classified data set.

Given the intrinsic complexity of biological systems, some overlaps of absorptions occur, masking relevant information. In order to deep understand the AD pathology and to further identify AD related biomarkers, purifications of specific molecules could be a close approach, specifically to analyze evidence of damage of nucleic acids and protein phosphorylation. It would also be an upcoming challenge, supplement the results obtained with a more specific metabolomic techniques, such as Mass Spectrometry or Nuclear Magnetic Resonance.

Apart from a good characterization of the volunteers, that proved to be essential to obtained consistent results, other information of patient samples would be useful to correlate with FTIR data, including biochemical analysis of glucose, cholesterol and markers of oxidation and antioxidation. To eliminate external variables related to the intake of carbohydrates that affects the 1200-900 cm^{-1} profile, it would be advisable to collect blood from patients after an overnight fast.

Bibliography

1. Association A. 2012 Alzheimer's disease Facts and Figures. 2012.

2. Hogg L, Watt A. Overcoming the stigma of dementia World Alzheimer Report 2012. 2012.

3. Paulson HL, Igo I. Genetics of dementia. Seminars in neurology. 2011 Nov;31(5):449–60.

4. Portugal AA. Alzheimer Portugal [Internet]. 2013. Available from: http://www.alzheimerportugal.org

5. Alzheimer Europe [Internet]. 2013. Available from: http://www.alzheimer-europe.org/

6. Portugal A. Plano Nacional de Intervenção Alzheimer. 2009.

7. Jack CR, Albert MS, Knopman DS, McKhann GM, Sperling RA, Carrillo MC, et al. Introduction to the recommendations from the National Institute on Aging-Alzheimer's Association workgroups on diagnostic guidelines for Alzheimer's disease. Alzheimer's & dementia. 2011 May 1;7(3):257–62.

8. Serrano-Pozo A, Frosch MP, Masliah E, Hyman BT. Neuropathological alterations in Alzheimer disease. Cold Spring Harbor Perspectives in Medicine. 2011 Sep;1(1):a006189.

9. Swerdlow RH. Brain aging, Alzheimer's disease, and mitochondria. Biochimica et biophysica acta. 2011 Dec;1812(12):1630–9.

10. Monte SD La. Alzheimer's disease pathogenesis-core concepts, shifting paradigms and therapeutic targets. Monte SD La, editor. InTech; 2011. p. 1–20.

11. Rosenmann H, Blum D, Kayed R, Ittner LM. Tau protein: function and pathology. International journal of Alzheimer's disease. 2012 Jan;2012:707482.

12. Braak H, Braak E. Neuropathological stageing of Alzheimer-related changes. Acta neuropathologica. 1991;239–59.

13. Iæ DC. Neuropathological hallmarks of Alzheimer's disease. 2001;9(3):195–9.

14. Thal DR, Rüb U, Orantes M, Braak H. Phases of Aβ-deposition in the human brain and its relevance for the development of AD. Neurology. 2002;58:1791–800.

15. Jack CR, Lowe VJ, Weigand SD, Wiste HJ, Senjem ML, Knopman DS, et al. Serial PIB and MRI in normal, mild cognitive impairment and Alzheimer's disease: implications for sequence of pathological events in Alzheimer's disease. Brain: a journal of neurology. 2009 May;132(Pt 5):1355–65.

16. Perl DP. Neuropathology of Alzheimer's Disease. 2010;32–42.

17. Rocchi A, Pellegrini S, Siciliano G, Murri L. Causative and susceptibility genes for Alzheimer's disease: a review. Brain Research Bulletin. 2003 Jun;61(1):1–24.

18. Bird TD. Genetic Aspects of Alzheimer Disease. Genet Med. 2008;10(4):231–9.

19. Turner PR, O'Connor K, Tate WP, Abraham WC. Roles of amyloid precursor protein and its fragments in regulating neural activity, plasticity and memory. Progress in Neurobiology. 2003 May;70(1):1–32.

20. Priller C, Bauer T, Mitteregger G, Krebs B, Kretzschmar H, Herms J. Synapse formation and function is modulated by the amyloid precursor protein. The Journal of Neuroscience. 2006 Jul 5;26(27):7212–21.

21. Duce JA, Tsatsanis A, Cater MA, James SA, Robb E, Wikhe K, et al. Iron-Export Ferroxidase Activity of β-Amyloid Precursor Protein Is Inhibited by Zinc in Alzheimer's Disease. Cell. 2010 Sep 17;142(6):857–67.

22. Di Carlo M, Giacomazza D, San Biagio P. Alzheimer's disease: biological aspects, therapeutic perspectives and diagnostic tools. Journal of physics. Condensed Matter. 2012 Jun 20;24(24):244102.

23. Liu C-C, Kanekiyo T, Xu H, Bu G. Apolipoprotein E and Alzheimer disease: risk, mechanisms and therapy. Nature reviews. Neurology. 2013 Feb;9(2):106–18.

24. Karran E, Mercken M, De Strooper B. The amyloid cascade hypothesis for Alzheimer's disease: an appraisal for the development of therapeutics. Nature reviews. Drug discovery. 2011 Sep;10(9):698–712.

25. Mohandas E, Rajmohan V, Raghunath B. Neurobiology of Alzheimer's disease. Indian J Psychiatry. 2009;51(1):55–61.

26. LaFerla FM. Intracellular amyloid-[beta] in Alzheimer's disease. Nat Rev Neurosci. 2007;8(7).

27. Hortschansky P, Schroeckh V, Christopeit T, Zandomeneghi G, Fa M. The aggregation kinetics of Alzheimer's b-amyloid peptide is controlled by stochastic nucleation. Protein Science. 2005;14:1753–9.

28. Crews L, Masliah E. Molecular mechanisms of neurodegeneration in Alzheimer's disease. Human molecular genetics. 2010 Apr 15;19(1):R12–R20.

29. Floyd RA. Antioxidants, oxidative stress, and degenerative neurological disorders. Proceedings of the Society for Experimental Biology and Medicine. Society for Experimental Biology and Medicine (New York, NY). Royal Society of Medicine; 1999. p. 236–45.

30. Zhang L, Sheng R, Qin Z. The lysosome and neurodegenerative diseases Structure and Function of Lysosomes. Acta Biochim Biophys Syn. 2009;41(6):437–45.

31. Ferreiro E, Baldeiras I, Ferreira IL, Costa RO, Rego AC, Pereira CF, et al. Mitochondrial- and endoplasmic reticulum-associated oxidative stress in Alzheimer's disease: from pathogenesis to biomarkers. International journal of cell biology. 2012 Jan;2012(735206):23.

32. Mattson MP. Apoptosis in neurodegenerative disorders. Nature reviews. Molecular cell biology. 2000 Nov;1(2):120–9.

33. Kumar S, Walter J. Phosphorylation of amyloid beta (Aβ) peptides – A trigger for formation of toxic aggregates in Alzheimer's disease. AGING. 2011;3(8):1–10.

34. Oliveira JM de. Abnormal protein phosphorylation in Alzheimer's disease. Master Thesis, Universidade de Aveiro, Portugal; 2011.

35. De la Torre JC. Cardiovascular risk factors promote brain hypoperfusion leading to cognitive decline and dementia. Cardiovascular Psychiatry and Neurology. 2012 Jan;2012(367516):15.

36. Messier C. Diabetes, Alzheimer's disease and apolipoprotein genotype. Experimental Gerontology. 2003 Sep 1;38:941–6.

37. Wellington CL. Cholesterol at the crossroads: Alzheimer's disease and lipid metabolism. Clinical Genetics. 2004 Jul 1;66(1):1–16.

38. Kálmán J JZ. Cholesterol and Alzheimer's disease. Orv Hetil. 2005;146(37):1903–11.

39. M. de la Monte S. Brain Insulin Resistance and Deficiency as Therapeutic Targets in Alzheimers Disease. Current Alzheimer Research. 2012 Jan 1;9(1):35–66.

40. Seneff S, Wainwright G, Mascitelli L. Nutrition and Alzheimer's disease: the detrimental role of a high carbohydrate diet. European Journal of Internal Medicine. 2011 Apr;22(2):134–40.

41. Carlo M Di, Picone P, Carrotta R, Giacomazza D, Biagio PLS. Topics in the prevention, treatment and complications of Type 2 Diabetes. 1st ed. Zimering MB, editor. 2010. p. 29–52.

42. De la Torre J. Critically attained threshold of cerebral hypoperfusion: the CATCH hypothesis of Alzheimer's pathogenesis. Neurobiology of Aging. 2000 Mar;21:331–42.

43. George M. Norma n^{o} 053/2011 de 27/12/2011 - Abordagem Terapêutica das Alterações Cognitivas. 2011.

44. Services H. Alzheimer's Disease Medications [Internet]. 2010. Available from: http://www.nia.nih.gov/Alzheimers

45. Butterfield DA, Pocernich CB. The Glutamatergic System and Alzheimer ' s Disease Therapeutic Implications. CNS Drugs. 2003;17(9):641–52.

46. Kihara T, Shimohama S. Alzheimer's disease and acetylcholine receptors. Acta Neurobiol Exp. 2004;64:99–105.

47. Tabet N. Acetylcholinesterase inhibitors for Alzheimer's disease: anti-inflammatories in acetylcholine clothing! Age and ageing. 2006 Jul;35:336–8.

48. McKhann G, Drachman D, Folstein M, Katzman R, Price D, Stadlan EM. Clinical diagnosis of Alzheimer's disease: Report of the NINCDS-ADRDA Work Group* under the auspices of Department of Health and Human Services Task Force on Alzheimer's Disease. Neurology. 1984 Jul 1;34(7):939–939.

49. McKhann GM. The diagnosis of dementia due to Alzheimer's disease: Recommendations from the National Institute on AgingAlzheimer's Association workgroups on diagnostic guidelines for Alzheimer's disease. Alzheimers Dement. 2011;7(3):263–9.

50. Tartaglia MC, Rosen HJ, Miller BL. Neuroimaging in dementia. Neurotherapeutics. 2011;8(1):82–92.

51. Macijauskienė J, Lesauskaitė V. Dementia with Lewy bodies: the Principles of Diagnostics, treatment, and Management. Medicina (Kaunas). 2012;48(1):1–8.

52. Geser F, Wenning GK, Poewe W, McKeith I. How to diagnose dementia with Lewy bodies: state of the art. Movement disorders. 2005;20(S12):S11–S20.

53. Dodel R. Dementia in Parkinson's disease. Orphanet Encyclopedia. 2004. p. 1–5.

54. Association A. Alzheimer's Association [Internet]. 2013. Available from: http://www.alz.org/

55. Sieben A, Van Langenhove T, Engelborghs S, Martin J-J, Boon P, Cras P, et al. The genetics and neuropathology of frontotemporal lobar degeneration. Acta neuropathologica. 2012;124(3):353–72.

56. Chow N, Aarsland D, Honarpisheh H, Beyer MK, Somme JH, Elashoff D, et al. Comparing hippocampal atrophy in Alzheimer's dementia and dementia with Lewy bodies. Dementia and Geriatric Cognitive Disorders. 2012;34(1):44–50.

57. Jellinger KA, Attems J. Neuropathological evaluation of mixed dementia. Journal of the neurological sciences. 2007;257(1):80–7.

58. Galvin JE, Sadowsky CH. Practical guidelines for the recognition and diagnosis of dementia. Journal of the American Board of Family Medicine: JABFM. 2012;25(3):367–82.

59. Monte SD La. The clinical spectrum of Alzheimer ' s disease – the charge toward comprehensive diagnostic and therapeutic strategies. Monte SD La, editor. InTech; 2011. p. 362.

60. Nasreddine Z. The Montreal Cognitive Assessment - MoCA© [Internet]. 2013. Available from: http://www.mocatest.org/

61. Burns A. Rating scales in old age psychiatry. The British Journal of Psychiatry. 2002 Feb 1;180(2):161–7.

62. Muliyala KP, Varghese M. The complex relationship between depression and dementia. Annals of Indian Academy of Neurology. 2010;13(Suppl2):S69.

63. Oksengard A-R. Dementia Diagnostics Made Evidence-Based: A Critical Evaluation of Cognitive Assessment Tools in Clinical Dementia Diagnostics [Internet]. Current Opinion in Psychiatry. 2005. p. 439–42. Available from: http://www.medscape.org/

64. Petrella JR, Coleman RE, Doraiswamy PM. State of the Art Radiology Neuroimaging and Early Diagnosis of Alzheimer Disease : A Look to the Future 1. 2003;315–36.

65. Klunk WE, Engler H, Nordberg A, Wang Y, Blomqvist G, Holt DP, et al. Imaging brain amyloid in Alzheimer's disease with Pittsburgh Compound-B. Annals of neurology. 2004;55(3):306–19.

66. Vitali P, Migliaccio R, Agosta F, Rosen HJ, Geschwind MD. Neuroimaging in Dementia. Seminars in Neurology. 2008;28(4):467–83.

67. Jain KK. The handbook of biomarkers. Press H, editor. Springer; 2010.

68. Trojanowski JQ, Vandeerstichele H, Korecka M, Clark CM, Aisen PS, Petersen RC, et al. Update on the biomarker core of the Alzheimer's Disease Neuroimaging Initiative subjects. Alzheimer's & dementia: the journal of the Alzheimer's Association. 2010;6(3):230.

69. Schoonenboom NSM, Van der Flier WM, Blankenstein MA, Bouwman FH, Van Kamp GJ, Barkhof F, et al. CSF and MRI markers independently contribute to the diagnosis of Alzheimer's disease. Neurobiology of aging. 2008;29(5):669–75.

70. Blennow K, Zetterberg H, Fagan AM. Fluid biomarkers in Alzheimer disease. Cold Spring Harbor Perspectives in Medicine. 2012;2(9).

71. Anoop A, Singh PK, Jacob RS, Maji SK. CSF biomarkers for Alzheimer's disease diagnosis. International journal of Alzheimer's disease. 2010;2010:12.

72. Baldeiras I, Santana I, Garrucho MH, Pascoal R, Lemos R, Santiago B, et al. CSF biomarkers for the early diagnosis of Alzheimer's disease in a routine clinical setting – the first Portuguese study. Sinapse. 2012;12(2):15–22.

73. Irizarry MC. Biomarkers of Alzheimer disease in plasma. NeuroRx. 2004;1(2):226–34.

74. Carmona P, Molina M, Calero M, Bermejo-Pareja F, Martínez-Martín P, Alvarez I, et al. Infrared spectroscopic analysis of mononuclear leukocytes in peripheral blood from Alzheimer's disease patients. Analytical and bioanalytical chemistry. 2012;402(6):2015–21.

75. Ray S, Britschgi M, Herbert C, Takeda-Uchimura Y, Boxer A, Blennow K, et al. Classification and prediction of clinical Alzheimer's diagnosis based on plasma signaling proteins. Nature medicine. 2007;13(11):1359–62.

76. Bermejo-Pareja F, Antequera D, Vargas T, Molina J, Carro E. Saliva levels of Abeta1-42 as potential biomarker of Alzheimer's disease: a pilot study. BMC neurology. 2010;10(1):108.

77. Dunckley T, Coon KD, Stephan DA. Discovery and development of biomarkers of neurological disease. Drug discovery today. 2005 Mar 1;10(5):326–34.

78. Ikehara K. Advances in the study of genetic disorders. Ikehara K, editor. InTech; 2011.

79. Shulaev V. Metabolomics technology and bioinformatics. Briefings in Bioinformatics. 2006;7(2):128–39.

80. Field R, Goss R, Kemsley K, Brun N Le, Gall G Le, Martin C, et al. Metabolomics on the Norwich Research Park [Internet]. 2011. Available from: http://www.metabolomics-nrp.org.uk

81. Smith BC. Fundamentals of Fourier Transform Infrared Spectroscopy. Second. Press C, editor. 2011.

82. Crupi V, Venuti V, Majolino D. FT-IR Spectroscopy: An Advanced Tool for Studying Biomedical Problems. Spectroscopy. 2004;19(7):22–30.

83. Ellis DI, Goodacre R. Metabolic fingerprinting in disease diagnosis: biomedical applications of infrared and Raman spectroscopy. The Analyst. 2006;131(8):875–85.

84. Petrich W. Mid-infrared and Raman spectroscopy for medical diagnostics. Applied Spectroscopy Reviews. 2001;36(2-3):181–237.

85. Naumann D. FT-infrared and FT-Raman spectroscopy in biomedical research. Applied Spectroscopy Reviews. 2001;36(2-3):239–98.

86. Bellisola G, Sorio C. Infrared spectroscopy and microscopy in cancer research and diagnosis. American journal of cancer research. 2012;2(1):1.

87. Sahu RK, Mordechai S. Fourier transform infrared spectroscopy in cancer detection. Future Oncology. 2005;1(5):635–47.

88. Kendall C, Isabelle M, Bazant-Hegemark F, Hutchings J, Orr L, Babrah J, et al. Vibrational spectroscopy: a clinical tool for cancer diagnostics. The Analyst. 2009;134(6):1029–45.

89. Wong PT, Wong RK, Caputo TA, Godwin TA, Rigas B. Infrared spectroscopy of exfoliated human cervical cells: evidence of extensive structural changes during carcinogenesis. Proceedings of the National Academy of Sciences. 1991;88(24):10988–92.

90. Rigas B, Morgello S, Goldman IS, Wong PT. Human colorectal cancers display abnormal Fourier-transform infrared spectra. Proceedings of the National Academy of Sciences. 1990;87(20):8140–4.

91. Chiriboga L, Yee H, Diem M. Infrared spectroscopy of human cells and tissue. Part VI: a comparative study of histopathology and infrared microspectroscopy of normal, cirrhotic, and cancerous liver tissue. Applied Spectroscopy. 2000;54(1):1–8.

92. Mackanos MA, Contag CH. FTIR microspectroscopy for improved prostate cancer diagnosis. Trends in biotechnology. 2009;27(12):661–3.

93. Baker MJ, Gazi E, Brown MD, Shanks JH, Gardner P, Clarke NW. FTIR-based spectroscopic analysis in the identification of clinically aggressive prostate cancer. British journal of cancer. 2008;99(11):1859–66.

94. Meurens M, Wallon J, Tong J, Noel H, Haot J. Breast cancer detection by Fourier transform infrared spectrometry. Vibrational spectroscopy. 1996;10(2):341–6.

95. Schultz CP, Liu KZ, Johnston JB, Mantsch HH. Differentiation of leukemic from normal human lymphocytes by FT-IR spectroscopy and cluster analysis. Leukemia Res. 1996;20:649–55.

96. Liu K-Z, Jia L, Kelsey SM, Newland AC, Mantsch HH. Quantitative determination of apoptosis on leukemia cells by infrared spectroscopy. Apoptosis. 2001;6(4):269–78.

97. Eysel HH, Jackson M, Nikulin A, Somorjai RL, Thomson GTD, Mantsch HH. A novel diagnostic test for arthritis: multivariate analysis of infrared spectra of synovial fluid. Biospectroscopy. 1997;3(2):161–7.

98. Staib A, Dolenko B, Fink DJ, Früh J, Nikulin AE, Otto M, et al. Disease pattern recognition testing for rheumatoid arthritis using infrared spectra of human serum. Clinica chimica acta. 2001;308(1):79–89.

99. Estepa L, Daudon M. Contribution of Fourier transform infrared spectroscopy to the identification of urinary stones and kidney crystal deposits. Biospectroscopy. 1997;3(5):347–69.

100. Carmona P, Bellanato J, Escolar E. Infrared and Raman spectroscopy of urinary calculi: A review. Biospectroscopy. 1997;3(5):331–46.

101. Naumann D. Infrared spectroscopy in microbiology. In: Meyers RA, editor. Encyclopedia of Analytical Chemistry. John Wiley & Sons, Ltd; 2006. p. 102–31.

102. Maquelin K, Kirschner C, Choo-Smith L-P, Van den Braak N, Endtz HP, Naumann D, et al. Identification of medically relevant microorganisms by vibrational spectroscopy. Journal of microbiological methods. 2002;51(3):255–71.

103. Kodali DR, Small DM, Powell J, Krishnan K. Infrared micro-imaging of atherosclerotic arteries. Applied spectroscopy. 1991;45(8):1310–7.

104. Li C, Ebenstein D, Xu C, Chapman J, Saloner D, Rapp J, et al. Biochemical characterization of atherosclerotic plaque constituents using FTIR spectroscopy and histology. Journal of Biomedical Materials Research Part A. 2003;64(2):197–206.

105. Petrich W, Dolenko B, Früh J, Ganz M, Greger H, Jacob S, et al. Disease pattern recognition in infrared spectra of human sera with diabetes mellitus as an example. Applied optics. 2000;39(19):3372–9.

106. Budinova G, Salva J, Volka K. Application of molecular spectroscopy in the mid-infrared region to the determination of glucose and cholesterol in whole blood and in blood serum. Applied spectroscopy. 1997;51(5):631–5.

107. Kostrewa S, Paarmann C, Goemann W, Heise HM. Multivariate determination of hematocrit in whole blood by attenuated total reflection infrared spectroscopy. AIP Conference Proceedings. 1998. p. 271.

108. Heise HM, Marbach R, Koschinsky T, Gries FA. Multicomponent assay for blood substrates in human plasma by mid-infrared spectroscopy and its evaluation for clinical analysis. Applied spectroscopy. 1994;48(1):85–95.

109. Hoşafçı G, Klein O, Oremek G, Mäntele W. Clinical chemistry without reagents? An infrared spectroscopic technique for determination of clinically relevant constituents of body fluids. Analytical and bioanalytical chemistry. 2007;387(5):1815–22.

110. Deleris G, Petibois C. Applications of FT-IR spectrometry to plasma contents analysis and monitoring. Vibrational Spectroscopy. 2003;32(1):129–36.

111. Fabian H, Choo L-P, Szendrei GI, Jackson M, Halliday WC, Otvos L, et al. Infrared spectroscopic characterization of Alzheimer plaques. Applied spectroscopy. 1993;47(9):1513–8.

112. Griebe M, Daffertshofer M, Stroick M, Syren M, Ahmad-Nejad P, Neumaier M, et al. Infrared spectroscopy: a new diagnostic tool in Alzheimer disease. Neuroscience letters. 2007;420(1):29–33.

113. Peuchant E, Richard-Harston S, Bourdel-Marchasson I, Dartigues J-F, Letenneur L, Barberger-Gateau P, et al. Infrared spectroscopy: a reagent-free method to distinguish Alzheimer's disease patients from normal-aging subjects. Translational Research. 2008;152(3):103–12.

114. Gauthier SG. Alzheimer's disease: the benefits of early treatment. European Journal of Neurology. Wiley Online Library; 2005;12(s3):11–6.

115. Trushina E, Dutta T, Persson X-MT, Mielke MM, Petersen RC. Identification of Altered Metabolic Pathways in Plasma and CSF in Mild Cognitive Impairment and Alzheimer's Disease Using Metabolomics. PloS one. 2013 Jan;8(5):e63644.

116. Kelly JG, Trevisan J, Scott AD, Carmichael PL, Pollock HM, Martin-Hirsch PL, et al. Biospectroscopy to metabolically profile biomolecular structure: a multistage approach linking computational analysis with biomarkers. Journal of proteome research. 2011;10(4):1437–48.

117. Committee ES. Statistical Significance and Biological Relevance 1. EFSA Journal. 2011;9(9):1–17.

118. Jackson M. Introductory Lecture From biomolecules to biodiagnostics: Spectroscopy does it all. Faraday discussions. 2004;126:1–18.

119. Finkenthal D, Rodecker S, Lee RL, Schaffer MJ, Schissel DP. Introduction to the Electromagnetic Spectrum. General Atomics. 1996.

120. Larkin P. Infrared and Raman Spectroscopy: Principles and Interpretation. Elsevier; 2011.

121. Stuart BH. Infrared spectroscopy: fundamentals and applications. Wiley; 2004.

122. Nicolet T. FT-IR versus Dispersive Infrared [Internet]. 1960. Available from: http://www.thermoscientific.com/

123. PerkinElmer. FT-IR Spectroscopy Attenuated Total Reflectance (ATR) [Internet]. 2005. Available from: http://www.perkinelmer.com/

124. Specac. Golden Gate ATR [Internet]. Available from: www.specac.com

125. Shaw RA. Multianalyte serum analysis using mid-infrared spectroscopy. Ann Clin Biochem. 1998;35(Pt 5):624–32.

126. Graça G, Moreira AS, Correia AJV, Goodfellow BJ, Barros AS, Duarte IF, et al. Mid-infrared (MIR) metabolic fingerprinting of amniotic fluid: A possible avenue for early diagnosis of prenatal disorders? Analytica chimica acta. 2013;764:24–31.

127. Boyanton BL, Blick KE. Stability studies of twenty-four analytes in human plasma and serum. Clinical chemistry. 2002 Dec;48(12):2242–7.

128. Kannemeier C, Shibamiya A, Nakazawa F, Trusheim H, Ruppert C, Markart P, et al. Extracellular RNA constitutes a natural procoagulant cofactor in blood coagulation. Proceedings of the National Academy of Sciences of the United States of America. 2007 Apr 10;104(15):6388–93.

129. Lundblad RL. Considerations for the Use of Blood Plasma and Serum for Proteomic Analysis [Internet]. The Internet Journal of Genomics and Proteomics. 2005. Available from: http://archive.ispub.com/journal/the-internet-journal-of-genomics-and-proteomics/volume-1-number-2/considerations-for-the-use-of-blood-plasma-and-serum-for-proteomic-analysis.html#sthash.lURJ6Lnr.dpuf

130. Dunn WB, Broadhurst D, Begley P, Zelena E, Francis-McIntyre S, Anderson N, et al. Procedures for large-scale metabolic profiling of serum and plasma using gas chromatography and liquid chromatography coupled to mass spectrometry. Nature protocols. 2011 Jul;6(7):1060–83.

131. Corp. MS& D. The Merck Manuals [Internet]. Available from: http://www.merckmanuals.com/

132. Lian CYF. Comparison of Heparinized Plasma and Serum Samples for Measurement of Ordinary Chemistry Analytes. Journal of Practical Medical Techniques. 2007;33:8.

133. Liu L, Aa J, Wang G, Yan B, Zhang Y, Wang X, et al. Differences in metabolite profile between blood plasma and serum. Analytical biochemistry. 2010 Nov 15;406(2):105–12.

134. Movasaghi Z, Rehman S, ur Rehman DI. Fourier Transform Infrared (FTIR) Spectroscopy of Biological Tissues. Applied Spectroscopy Reviews. 2008 Feb;43(2):134–79.

135. Barth A, Zscherp C. What vibrations tell about proteins. Quarterly Reviews of Biophysics. 2002 Nov;35(4):369–430.

136. Kong J, Yu S. Fourier Transform Infrared Spectroscopic Analysis of Protein Secondary Structures. Acta Biochimica Biophysica Sinica. 2007;39(8):549–59.

137. Lane DW, l'Anson S. Viscosimetric effect of fibrinogen. Journal of clinical pathology. 1994 Nov;47(11):1004–5.

138. Hughes CP, Berg L, Danziger WL, Coben LA, Martin RL. A new clinical scale for the staging of dementia. The British Journal of Psychiatry. 1982;140(6):566–72.

139. Marshall GA, Rentz DM, Frey MT, Locascio JJ, Johnson KA, Sperling RA. Executive function and instrumental activities of daily living in mild cognitive impairment and Alzheimer's disease. Alzheimer's and Dementia. 2011;7(3):300–8.

140. Folstein MF, Folstein SE, McHugh PR. Mini-Mental State: a practical method for grading the cognitive state of patients for the clinician. Journal of psychiatric research. 1975;12(3):189–98.

141. Mitchell AJ, Bird V, Rizzo M, Meader N. Diagnostic validity and added value of the Geriatric Depression Scale for depression in primary care: a meta-analysis of GDS30 and GDS15. Journal of affective disorders. 2010;125(1-3):10–7.

142. Mendonça A, Guerreiro M. Escalas e Testes na Demência. Grupo de Estudos de Envelhecimento Cerebral e Demência. 2ª ed. GEECD, editor. Lisboa; 2008.

143. Morgado J, Rocha CS, Maruta C, Guerreiro M, Martins IP. Novos Valores Normativos do Mini-Mental State Examination New Normative Values of Mini-Mental State Examination. Sinapse®. 10.

144. Wang L, Mizaikoff B. Application of multivariate data-analysis techniques to biomedical diagnostics based on mid-infrared spectroscopy. Analytical and bioanalytical chemistry. 2008;391(5):1641–54.

145. Wentzell PD, Vega Montoto L. Comparison of principal components regression and partial least squares regression through generic simulations of complex mixtures. Chemometrics and Intelligent Laboratory Systems. 2003 Feb;65(2):257–79.

146. Barros A. Contribution à la sélection et la comparaison de variables caractéristiques. PhD Thesis, Institute National Agronomique Paris-Grignon, France.; 1999.

147. Armstrong D. Oxidative stress biomarkers and antioxidant protocols. Armstrong D, editor. Springer; 2004.

148. Severcan F, Gorgulu G, Gorgulu ST, Guray T. Rapid monitoring of diabetes-induced lipid peroxidation by Fourier transform infrared spectroscopy: evidence from rat liver microsomal membranes. Analytical biochemistry. 2005 May 1;339(1):36–40.

149. Kneipp J, Lasch P, Baldauf E, Beekes M, Naumann D. Detection of pathological molecular alterations in scrapie-infected hamster brain by Fourier transform infrared (FT-IR) spectroscopy. Biochimica et biophysica acta. 2000 Jun 15;1501(2-3):189–99.

150. Lipiec E, Kowalska J, Lekki J, Wiecheć A, Kwiatek WM. FTIR Microspectroscopy in Studies of DNA Damage Induced by Proton Microbeam in Single PC-3 Cells. Acta physica polonica. 2012;121(2):506–9.

151. Ami D, Mereghetti P, Doglia SM. Multivariate Analysis for Fourier Transform Infrared Spectra of Complex Biological Systems and Processes. Multivariate Analysis in Management, Engineering and the Sciences. InTech; 2012. p. 189–220.

152. Coates J. Interpretation of Infrared Spectra, A Practical Approach Interpretation of Infrared Spectra. In: Meyers RA, editor. Encyclopedia of Analytical Chemistry. John Wiley & Sons Ltd; 2000. p. 10815–37.

153. Thirunavukkarasu M. Ftir and uv-visible spectral study on normal blood samples. IJPBS. 2011;1(2).

154. Lee S, Mirkin NG. A quantitative anharmonic analysis of the amide A band in α-helical poly(L-alanine). Biopolymers. 1999;49(3):195–207.

155. Davis R, Mauer LJ. Fourier tansform infrared (FT-IR) spectroscopy : A rapid tool for detection and analysis of foodborne pathogenic bacteria. 2010;(1):1582–94.

156. Caine S, Heraud P, Tobin MJ, McNaughton D, Bernard CC a. The application of Fourier transform infrared microspectroscopy for the study of diseased central nervous system tissue. NeuroImage. 2012 Feb 15;59(4):3624–40.

157. Van der Meijden PEJ, Munnix IC a, Auger JM, Govers-Riemslag JWP, Cosemans JMEM, Kuijpers MJE, et al. Dual role of collagen in factor XII-dependent thrombus formation. Blood. 2009 Jul 23;114(4):881–90.

158. Krafft C, Steiner G, Beleites C, Salzer R. Disease recognition by infrared and Raman spectroscopy. Journal of biophotonics. 2009 Feb;2(1-2):13–28.

159. Petibois C, Rigalleau V, Melin a M, Perromat a, Cazorla G, Gin H, et al. Determination of glucose in dried serum samples by Fourier-transform infrared spectroscopy. Clinical chemistry. 1999 Sep;45(9):1530–5.

160. Yoshida S, Miyazaki M, Sakai K, Takeshita M, Yuasa S, Sato A, et al. Fourier transform infrared spectroscopic analysis of rat brain microsomal membranes modified by dietary fatty acids: possible correlation with altered learning behavior. Biospectroscopy. 1997;3(4):281–90.

161. Sone H, Shimano H, Ebinuma H, Takahashi A, Yano Y, Iida KT, et al. Physiological changes in circulating mannose levels in normal, glucose-intolerant, and diabetic subjects. Metabolism. 2003;52(8):1019–27.

162. Ahtiluoto S, Polvikoski T, Peltonen M, Solomon A, Tuomilehto J, Winblad B, et al. Diabetes, Alzheimer disease, and vascular dementia A population-based neuropathologic study. Neurology. 2010;75(13):1195–202.

163. Wei Y, Han CS, Zhou J, Liu Y, Chen L, He RQ. D-ribose in glycation and protein aggregation. Biochimica et biophysica acta. 2012 Apr;1820(4):488–94.

164. Chauhan V, Chauhan A. Oxidative stress in Alzheimer's disease. Pathophysiology. 2006 Aug;13(3):195–208.

165. Kondepati VR, Heise HM, Oszinda T, Mueller R, Keese M, Backhaus J. Detection of structural disorders in colorectal cancer DNA with Fourier-transform infrared spectroscopy. Vibrational Spectroscopy. 2008 Mar;46(2):150–7.

166. Augustinack J, Schneider A, Mandelkow E-M, Hyman B. Specific tau phosphorylation sites correlate with severity of neuronal cytopathology in Alzheimer's disease. Acta Neuropathologica. 2002 Jan 1;103(1):26–35.

167. Neal ML, Lamb BT. The Role of Oxidative Stress in the Pathophysiology of Cerebrovascular Lesions in Alzheimer's Disease. Brain Pathol. 2002;12:21–35.

168. Migliore L, Fontana I, Trippi F, Colognato R, Coppede F, Tognoni G, et al. Oxidative DNA damage in peripheral leukocytes of mild cognitive impairment and AD patients. Neurobiology of aging. 2005;26(5):567–73.

169. Lovell MA, Markesbery WR. Oxidatively modified RNA in mild cognitive impairment. Neurobiology of disease. 2008;29(2):169–75.